STRUCTURAL FIRE MODELING

By

HYEONG-JIN KIM

Bachelor of Engineering
Chonbuk National University
Chonju, Korea
1993

Master of Engineering
Chonbuk National University
Chonju, Korea
1995

Submitted to the Faculty of the
Graduate College of the
Oklahoma State University
in partial fulfillment of
the requirements for
the Degree of
DOCTOR OF PHILOSOPHY
August, 2001

STRUCTURAL FIRE MODELING

Thesis Approved:

Thesis Adviser

Dean of the Graduate College

ACKNOWLEDGMENTS

I wish to express my sincere appreciation to my major advisor, Dr. David G. Lilley for his intelligent supervision, constructive guidance, inspiration and friendship. I could not thank him enough. My sincere appreciation extends to my other committee members Dr. Afshin J. Ghajar, Dr. Jeffrey D. Spitler, and Dr. Arland H. Johannes, whose guidance, assistance, encouragement, and friendship are also invaluable. I would like to thank Dr. David G. Lilley and the School of Mechanical and Aerospace Engineering for providing me with this research opportunity and their generous financial support.

Moreover, I wish to express my sincere gratitude to those who provided suggestions and assistance for this study: Dr. Ashwani K. Gupta, Dr. Bock Choon Pak, Dr. Byung Joon Baek, Dr. Byung Soo Cho, Dr. Gil Han Park, Dr. Ronald L. Dougherty, Dr. Young Chang, Mr. Jae-Yong Kim, Mr. Seung Won An, and Mr. Yoesbar Sofyan.

I would also like to give my special appreciation to my beloved wife, Gyeong-He, for her understandings and deep love throughout this whole process, and especially for her strong encouragement at times of difficulty. I deeply appreciate the spiritual encouragement and support given by my parents, Mr. Gyung-Joo Kim and Mrs. Suk-Hyun Kim. Thanks also go to my brothers, a sister, and children for their inspirations.

Finally, I would like to thank our Lord and Korean Catholic Community of Stillwater for the spiritual support during the five years of study.

TABLE OF CONTENTS

Chapter Page

Chapter Page

LIST OF TABLES

Table Page

LIST OF FIGURES

Figure Page

Figure Page

NOMENCLATURE

A	cross-sectional area (m)
A_o	area of ventilation opening (m^2)
A_W	wall area (m^2)
A_T	total area of the compartment surfaces (m^2)
c	specific heat (kJ/kgK)
c_c	specific heat of the compartment surface (kJ/kgK)
C_d	flow coefficient
c_f	fuel specific heat (kJ/kgK)
c_p	specific heat of air at constant pressure (kJ/kgK)
c_v	specific heat of air at constant volume (kJ/kgK)
CV_i	control volume of i^{th} layer
d	separation between the item on fire and the exposed item (m)
E	internal energy (J)
g	gravitational constant (m/s^2)
h_k	effective heat transfer coefficient (kW/mK)
	= $(k\rho c/t)^{1/2}$ for $t \le t_p$
	= k/δ for $t < t_p$
ΔH_{eff}	effective heat of combustion (kJ/kg)
Δh_c	effective heat of combustion of the fuel (kJ/kg)
h_i	maximum height (above and below the neutral plane) (m)
H_o	height of ventilation opening (m)
m	mass of the layer (kg)

$\dot{m}$	mass flow rate (kg/s)
$\dot{m}_a$	mass flow rate of air (kg/s)
$\dot{m}_{b,f}$	mass burning rate of fuel (kg/s)
$\dot{m}_e$	mass flow rate of cold entrainment into the fire plume (kg/s)
$\dot{m}_f$	mass flow rate of fuel (kg/s)
$\dot{m}_g$	mass flow rate out of the door (kg/s)
$\dot{m}_{i,loss}$	losses due to surface deposition or settling of particulates (kg/s)
$\dot{m}_p$	mass flow rate in the plume at the hot layer interface (kg/s)
$\dot{m}_{react}$	mass rate of gaseous fuel supplied (kg/s)
$\dot{m}_{st}$	stoichiometric mass loss rate (kg/s)
P	global pressure in control volume (Pa or N/m^2)
P_∞	outside pressure (Pa or N/m^2)
P_r	total radiative power of the flame (kW)
R	gas constant for air (J/kgK)
$\dot{Q}$	heat (energy) release rate of the fire (kW)
$\dot{Q}_{ig}$	heat (energy) level required for ignition (kW)
$\dot{Q}_{fo}$	heat (energy) level required for flashover (kW)
$\dot{q}_0^{"}$	incident radiation on the target (kW/m^2)
$\dot{q}$	rate of heat supplied (kW)
$\dot{q}_{loss}$	rate of heat transfer lost at the boundary (kW)
R_o	distance (radius) to target fuel (m)
r_s	stoichiometric air/fuel mass ratio
r	stoichiometric fuel to oxygen mass ratio
R	flame radius (m)
$\dot{s}_i$	enthalpy flow to i^{th} layer (J/s)
t	time (s)

t_0	length of the incubation period (s).
t_p	thermal penetration time (s) : $(\rho c / k)(\delta / 2)^2$
T_i	temperature in i^{th} layer (C or K)
T_a	air temperature (C or K)
T_{ig}	ignition temperature (C or K)
T_g	gas temperature (C or K)
T_s	fuel temperature beyond the range of the flame's heat (C or K)
T_u	upper (smoke) layer temperature (C or K)
V	volume of the control volume (m^3)
V_i	volume of the i^{th} layer (m^3)
v	velocity (m/s)
v_{spread}	flame spread velocity (m/s)
v_n	velocity normal to the surface of control volume (m/s)
W	width of opening (m)
x_p	position at the ignition temperature, T_{ig}
x_r	radiative fraction
y_i	mass yield of species i produced per mass rate of fuel supplied
y_{ox}	ratio of oxygen to other gases in a volume
$y_{ox,low}$	low limit on the ratio of oxygen to other gases
z	height (above and below the neutral plane) (m)

Greek Symbols

α_d	fire-decay coefficients (kW/s^2),
α_g	fire-growth coefficients (kW/s^2)

δ	ceiling/wall thickness (m)
ρ	density (kg/m^3)
ρ_a	air density (kg/m^3) = 1.2 kg/m^3 = ρ_∞
ρ_c	compartment surface density (kg/m^3)
ρ_f	fuel density (kg/m^3)
ρ_∞	air density (kg/m^3) = 1.2 kg/m^3 = ρ_a
γ	ratio of c_p / c_v
k	thermal conductivity of ceiling/wall material (kW/mK)

Subscripts (i =)

1	upper layer (hot layer, smoke layer)
2	lower layer (cold layer)
a	cold air
g	hot gas (smoke)
l	lower layer (cold layer)
u	upper layer (hot layer, smoke layer)

CHAPTER I

INTRODUCTION

The study of uncontrolled fire is motivated by risks to society. Approximately 2.5 million fires are reported in the United States each year, and roughly 5,000 deaths occur each year (see Quintiere, 1994). United States Fire Administration (USFA, 1999) reported that there are more than 2,800 fatal residential home fires in the United States each year between 1994 and 1996. These fires resulted in approximately 3,700 deaths per year. During the past 150 years, the science of fires has been rapidly developed. The development of the fire analytical modeling also has accelerated over the last 30 years. As a result, fire modeling can often be used to appraise the effectiveness of the protective measures proposed when one designs a building.

Fire behavior is extremely important in fire protection engineering and building design engineering, see Combustion Institution (1979), NFPA (1991), SFPE (1995), and Lilley (1995a). The references given provide a good cross-section of experimental and theoretical studies related to the understanding of real-life fires. These also provide useful test data for the development and application of the theory of fires.

The ultimate goal of my study is to improve scientific and technical understanding of fire behavior leading to flashover in structural fires. Burning rates, radiant ignition, fire spread rates, ventilation limit imposed by size of openings,

flashover, and fire modeling are all topics of immense concern to achieve this goal. Main outcomes of this study are: (a) Improved mathematical simulations via fire specifications and environment during fire events so as to improve the accuracy of theoretical calculation. (b) Extension of the range of knowledge and modeling capability that goes beyond the range of available experimental data.

1.1 The Phenomenon

Technical and scientific understandings are both important on the study of fire development. It will include chemistry, physics, fluid dynamics, combustion, and heat transfer topics. And also technical information about burning rate, fire spread, ventilation limit, flashover, and backdraft is relevant.

Chemistry is the science that deals with composition, structure, and properties of substance and the transformations that they undergo. Physics is the science that deals with matter and energy and their interactions in the fields of mechanics, acoustics, optics, heat electricity, magnetism, radiation, atomic structure, and nuclear phenomena. Thus, whereas chemistry deals with how things are put together and what their composition is, physics deals with how things work in both normal and abnormal conditions. Rates of chemical reaction are determined by laws of both chemistry and physics. Combustion is generally considered to be the science that deals with exothermic chemical reactions, particularly where a fuel is involved as one of the chemical components.

A fire is generally considered to be defined as the self-sustaining process of rapid oxidation of a fuel being reduced by an oxidizing agent with the evolution of heat and

light. Fire must maintain a very delicate balance to maintain combustion. There must be a number of things (oxygen, heat, and fuel) within the correct range of proportions. Lacking this, there will be no fire.

The structural fire progression is as follows:

1. All fires have a starting place (a point of origin) and require a source of heat (ignition source).
2. All fires result from an occurrence of "the coming together of heat, fuel, and oxygen". The oxygen may be limited by the openings of compartments in structural fires.
3. At the very start of a fire, the entire room is assumed to be at uniform ambient temperature, and a single item starts to burn.
4. Fire usually start small, but depending on influencing factors can accelerate rapidly, and spreads in the path of least resistance.
5. When in a confined area or room, fire will initially burn upward, then across the ceiling, and then down the wall.
6. Fire is communicated to uninvolved fuel supplies by conduction, convection, radiation or a combination of these contributing factors.
7. Approximately 65 to 75 % of the heat of combustion is transferred through convection (about 25 to 35 % for radiation and a few % for conduction).
    a. Convected air is buoyant from being heated and therefore rises.

b. As time progresses, this heat increases, thereby heating the fuel above the fire to its ignition temperature.

c. The fire grows.

8. Fire spreads up and out forming a "V" pattern mostly by convection.

9. Downward spread is primarily through radiation.

10. Fires produce a variety of combustion by-products that also affect normal fire progression.

11. As the fire progresses, the upper hot gas layer gets increasingly hotter and the layer extends progressively downward form the ceiling. This pre-flashover fire may be threatening to humans and important to the fire spreading problem, other items may be ignited via direct flame contact, flame spreading and/or radiation heat transfer levels becoming large enough to initiate burning.

12. As the upper layer temperature reaches between about 500 and 600 °C (932 and 1112 °F) flashover occurs – the entire room contents become involved in fire, see Drysdale (1986) for a review of the information. The upper hot layer is now down to near floor level, and the entire room is an inferno of flames. In extreme conditions, the occurrence of flashover has been observed even at temperature betweens in the wide range of 300 and 700 °C. The lower bound of the extreme condition is because of things like slow heating, small room, and well reflecting surfaces of the walls and ceiling.

13. Post-flashover fire is particularly important. The temperature history and fire spreading into other compartments after flashover is a prime importance in practice. Structural endurance of the building structure depends on the fire intensity after flashover. Most post-flashover fire are considered to be fully developed fire and limited by the size of opening. Backdraft may occur depending on the condition during this post-flashover fire.

Flashover is the most important even during fire, because no one can survive after the occurrence of flashover. Flashover is characterized by rapid transition in fire behavior from localized burning of fuel to the involvement of all combustibles in the enclosure. Flames and hot gases are much lighter than surrounding air, so fire burns upward. High radiation heat transfer levels from the original burning item, the flame and plume directly above it, and the hot smoke layer spreading across the ceiling are all considered to be responsible for the heating of the other items in the room, leading to their ignition.

Backdraft is considered to be an instantaneous explosion of smoke blasting back through a door or window (a combustion explosion). Backdrafts can occur when large quantities of carbon monoxide and other unburned gaseous fuels build up in the smoke layer due to incomplete combustion, and oxygen is then introduced.

1.2 The Problem

The development of structural fires can be understood more readily when technical knowledge puts the phenomena on a firm scientific footing. The theory assists in understanding and applying scientific information to real-world fire situations. Recent extensive study, research, experimentation, field observation and simulation have led to the need for critical evaluation of phenomena associated with fire dynamics, see Chapter II. The scientific topics of chemistry, physics, fluid dynamics, combustion, and heat transfer all play their part. Technical information about fuels, burning rates, fire spread, and flashover and backdraft phenomena is also relevant. Some of these topics and zone modeling are now addressed.

1.3 Objectives of the Present Study

The goal is to recommend methodologies and parameters for fire development calculations, including heat release rates, possible ignition of subsequent items, flashover determination, fire modeling. The objectives may be itemized as follows:

1. To present and illustrate simple empirical simulations of submodels associated with fire development
2. To determine parameter effects on the time to reach flashover
3. To compare and contrast different models of flashover theories
4. To characterize experimental heat release rate data in a uniform fashion

5. To calculate smoke temperature and layer height in multi-room structural fires with flashover, window breakout, and spread of fire to sequential rooms
6. To determine whether initiation of the next room's fire, at the instant of the previous room's flashover, provides a good methodology for multi-room fire development in a structural fire
7. To determine the validity of making calculations with a simple 3-room simulation

This thesis is very much application oriented and is in the field of fire dynamics, for which there is very little experimental data available, and modeling is in its infancy. Thus, this thesis presents preliminary modeling and calculations that are very helpful to understanding the dynamics of fire. This study is also useful for fire fighters, fire investigators, fire marshals, etc who would like to understand better the scientific and engineering aspects of fire dynamics. The results of calculations are not expected to be exactly the same as the experimental data. This is because even real-fires have large variance and uncertainty, and submodels have limitations. Thus the calculations should be considered as indication of what would happen in real-world situations.

1.4 Outline of the Thesis

After this brief introduction, extensive literature reviews are provided in Chapter II for subtopics of burning rates, radiant ignition, fire spread rates, ventilation limit

imposed by size of opening, flashover criteria, and modeling.

Theories related to fire development phenomena are discussed in Chapter III with appropriate equations including important empirical correlations. The limitation and accuracy of these are also presented in this chapter.

Chapter IV provides the governing equations and other background information about zone models. This chapter also includes history, governing equations, applications, and validations of the programs (CFAST and FASTLite) that used in this study.

The results and discussion of this study are presented in Chapter V, so as to meet the objectives of this study. This chapter includes parameter effect on the time to reach flashover conditions, comparison of flashover theories, Burning rates of typical items, and temperature and smoke prediction in a small and a large house fire.

Conclusions of my study are then summarized in Chapter VI.

CHAPTER II

LITERATURE REVIEW

Simple empirical simulations of submodels associated with fire development are important to understand better and to simulate structural fires better. Extensive background information is provided below for each submodel area and modeling of structural fires. Major references are NFPA Handbook (NFPA, 1991) and SFPE Handbook (SFPE, 1995).

2.1 Burning Rates

The "burning rate" is usually expressed either as a mass loss rate (kg/s) or as a heat release rate (kW) with the latter being more commonly used. Calculation procedures for fire effects in enclosures require knowledge of the energy release rate of the burning fuel. The term "energy release rate" is frequently used interchangeably with "heat release rate", and it is usually expressed in units of kilowatts (kW) and symbolized by $\dot{Q}$. Heat release rate (HRR) is used for later of this thesis.

The heat release rate from burning fuels cannot be predicted from basic measurements of material properties. It depends on the fire environment, the manner in which the fuel is volatilized and the efficiency of the combustion. Therefore, it must rely

on available laboratory test data. In addition, knowledge of the complete heat release rate history (HRR vs. time) may be required for many situations. This is particularly desirable where the fuel package exhibits unsteady burning. For those cases where only limiting conditions or worst-case analysis is required, it may be reasonable to assume that the fuel is burning at a constant rate, which simplifies the calculation considerably.

The most common method to measure energy release rate is known as oxygen consumption calorimetry. The basis of this method is that for most gases, liquids, and solids, a more or less constant amount of energy is released per unit mass of oxygen consumed, see Huggett (1980).

Babrauskas and Williamson (1979), and Pettersson et al (1976) introduce post-flashover fires in the case of a worst-case approach and a schematized approach receptively. Where an exact burning rate is not required, the worst-case approach can be applied. Also, the schematized approach can be used where all of the burning rate information is expressed solely as a fuel loading.

The rigorous treatment of energy release rates is available for selected material types such as wood cribs, wood and plastic slabs, and liquid pool fires where experimental correlations have been established. Section 3, Chapter 1, in the SFPE Handbook of Fire Protection Engineering, see SFPE (1995), provides a detailed discussion of the prediction of burning rates for liquid pool fires. Data on mass loss rates for selected fuel packages are available in several publications: Alpert and Ward (1983),, Babrauskas and Krasny (1985), Babrauskas et al (1982), and Lawson et al (1984). Also detailed discussions of heat release rates for specific fuels are available in publication by Babrauskas (1985), and Lawson and Quintiere (1985).

Budnick et al (1991) discuss simplified calculations for enclosure fires in their chapter in the NFPA Handbook (NFPA, 1991). They show the simple calculations for evaluating fire conditions in enclosures during the pre-flashover fire growth period. They include discussion about the maximum mass loss rate at ventilation-limited burning conditions.

Also Data are available for heat release rate vs. time for many items on Babrauskas and Grayson (1992). Janessens and Parker (1992) developed the principle of oxygen consumption calorimetry as a measurement technique.

Many more researchers have studied about burning rate. Babrauskas (1995), in his chapter in the SFPE Handbook (SFPE, 1995), summarizes burning rates categorizing a great deal of previous researchers' information into 13 sections dealing with:

1. Pools, liquid or thermoplastic
2. Cribs (regular arrays of sticks)
3. Wood pallets
4. Upholstered furniture
5. Mattresses
6. Pillows
7. Wardrobes
8. Television sets
9. Christmas trees
10. Curtains
11. Electric cable trays

12. Trash bags and containers

13. Stored commodities

The recent experimental data is available at National Institute of Standards and Technology (NIST) site with the pictures and movies, see http://fire.nist.gov/fire/fires.

The thermal radiation hazards from hydrocarbon spill fires depend on a number of parameters, including the composition of the hydrocarbon, the size and shape of the fire, the duration of the fire, its proximity to the object at risk, and the thermal characteristics of the object exposed to the fire. The state of the art of predicting the thermal environment of hydrocarbon spill fires consists essentially of semiempirical methods, some of which are based on experimental data from small- and medium-scale tests. Needless to say, such semiempirical methods are always subject to uncertainties when experimental data from small-scale fires are extrapolated to predict the thermal properties of very large-scale fires.

A systematic study of liquid hydrocarbon pool fires over the widest range of pool diameters was conducted by Blinov and Khudiakov (1957). Gasoline, tractor kerosene, diesel oil, and solar oil (and, to a limited extent, household kerosene and transformer oil) were burned in cylindrical pans (depth not indicated) of diameters 0.37 cm to 22.9 meters. Liquid burning rates and flame heights were measured, and visual and photographic observations of the flames were recorded.

Useful information about the rate of burning of pool fires is readily available in tables, see SFPE (1995) for example, via the mass consumed per unit area per unit time. From the energy per unit mass values also given, one can readily compute the heat

release rate $\dot{Q}$ in kW, or in Btu per hour since 100,000 Btu/hr = 29.31 kW. It may be noted that for pool diameters less than 1 meter, the burning rate expression is reduced because of a reduction in radiation feedback.

The heat release rates of furniture and bed are very important in the structural fires, because deaths due to furniture and bed fires rank as the top most category of fire losses. Krasny et al (2001) discuss these items in very detail including heat release rate, ignition, spread, toxic gases, test methods, etc.

2.2 Radiation Ignition

It is interest to estimate the radiation transmitted from a burning fuel array to a target fuel positioned some distance from the fire to determine if secondary ignitions are likely. The formulas for estimating the energy level required of a free burning fire to ignite a nearby item have been developed, on the basis that the exposed fuel item is not so close as to be in contact with the flame of the exposure fire, see section 3.2.

Modak (1977) computes and compares with experimental data an axisymmetric pool fire of specified flame shape and a gray flame absorption coefficient. His simple method of radiation to the surrounding can be approximated as isotropic, or as emanating from a point source. A more specific analysis of radiant heat flux to a target remote from a flame is developed by Dayan and Tien (1974). They consider the flame to be approximated as a homogenous cylinder of uniform temperature and other properties. The relationships expressed by this procedure were developed empirically from tests and reported by Babrauskas (1981b).

Budnick et al (1991) discuss the simple expression in their chapter in the NFPA Handbook (NFPA, 1991). Tewarson (1995) explains fire initiation (ignition) and shows experimental data in the view of concepts governing generation of heat and chemical compounds in fires in the SFPE Handbook (SFPE, 1995).

Flame spread tests are probably the best known fire performance tests. The most widely used of these are the Steiner Tunnel Test. These tests attempts to simulate the spread of fire across a plane surface and may include the imposition of a known external heat radiant flux, see Clarke (1991) and DeHaan (1991). For details about the test methods as an ASTM standard, see ASTM (1967 and 1969).

2.3 Fire Spread Rates

Fire spread applies to the growth of the combustion process including surface flame spread, smoldering growth, and the fireball in premixed flame propagation. In flame spread, and in fire growth generally, the rate of spread is highly dependent on the temperatures imposed by any hot smoke layer heating the unburned surface, but also gravitational and wind effect are important. The flows resulting from the fire's buoyancy or the natural wind of the atmosphere can assist (wind-aided) or oppose (opposed-flow) flame spread.

Quintiere and Harkleroad (1984) derive formulas and describe material properties involved in the lateral speed of a fire spreading in a direction other than that impinged by flame from the burning material; generally this means lateral or downward spread from a vertical flame.

Quintiere (1994) summarizes surface steady flame spread by following sections

1. Spread on Solid Surface
   a. Downward or Lateral Wall Spread
   b. Upward or Wind-Aided Spread
2. Spread though Porous Solid Arrays
3. Spread on Liquids

Some typical fire spread rates are given in Table 2. 1.

Table 2. 1 Typical Flame Spread Rates

Spread	Rate (cm/s)
Smoldering	0.001 to 0.01
Lateral or downward on thick solids	0.1
Wind driven spread through forest debris or bush	1.0 to 30.
Upward spread on thick solids	1.0 to 100.
Horizontal spread on liquids	1.0 to 100.
Premixed flames (Laminar)	10. To 100.
Premixed flames (Detonations)	about 10^5

Magee and McAlevy (1971) studied the rate of flame spread over strips of filter paper with different orientations (inclined angles), see Drysdale (1986) for discussion.

According to Campbell (1991b), fire spread rarely occurs by heat transfer through, or structural failure of, wall and floor-ceiling assemblies. The common mode of

fire spread in a compartmented building is through open doors, unenclosed stairways and shafts, unprotected penetrations of fire barriers, and nonfire-stopped combustible concealed spaces. Even in buildings of combustible construction, the common gypsum board or lath-on-plaster protecting wood stud walls or wood joist floors provides 25 to 30 min of resistance to a fully developed fire, as determined by a standard fire test (NBFU, 1956). When such barriers are properly constructed and maintained and have protected openings, they will normally contain fires of maximum expected severity in light-hazard occupancies. However, no fire barrier will reliably protect against fire spread if it is not properly constructed and maintained, and openings in the barrier are not protected.

Fire can spread horizontally and vertically beyond the room or area of origin and though compartments or spaces those do not contain combustibles. Heated unburned pyrolysis products from the fire will mix with fresh air and burn as they flow outward. This results in extended flame movement under noncombustible ceilings, up exterior walls, and through noncombustible vertical opening. This is a common way that fire spreads down corridors and up open stairways and shafts.

Campbell (1991b) explains fire spread and suggests fire protection in the following categories:

1. Concealed Spaces
2. Vertical Openings
3. Room or Suite Compartmentation
4. Protection of Corridors

5. Building Separation

6. Fire Plumes above Roofs

7. Structural Stability of Fire Walls.

Ramachandran (1995) shows stochastic models of fire growth governed by physical and chemical processes. Quintiere (1995) discusses flame spread applied to the phenomenon of a moving flame in close proximity to the source of its fuel originating from a condensed phase, i.e., solid or liquid. Details are in there chapters in SFPE Handbook (SFPE, 1995).

2.4 Ventilation Limit Imposed by Size of Opening

One of the enclosure effects is the availability of oxygen for combustion. If the air in the space, plus that drawn in through openings, plus that blown into the space by HVAC systems or other means is insufficient to burn all the combustible products driven from the fuel package, then only that amount of combustion supportable by the available oxygen can take place. This situation is referred to as ventilation-limited burning. When ventilation-limited burning occurs, the combustible products driven from the fuel package often burn outside of the room when they combine with air outside the room. This appears as flame extensions from the room. Also, ventilation-limited burning changes the mass loss rate of burn items.

Kawagoe and Sekine (1963) originally presented the idea that fire heat release rate within a compartment could be limited by ventilation geometry. This idea has been

followed, and many subsequent post-flashover experiments have been performed, see for examples Babrauskas (1979) and Fang and Breese (1980).

Heskestad (1991) covers venting practices as they would be applied to nonsprinklered buildings and Campbell (1991b) covers fire modeling in ventilation-limited fire in their chapters in the NFPA Handbook (NFPA, 1991).

Emmons (1995) shows equations for the measurement of velocity, volume flow, and mass flow for vent flows relating to orifice, nozzle and vent flows for buoyant and nonbuoyant flows. Quintiere (1995) reviews vent-limited effects on zone models. Walton and Thomas (1995) shows the simplified mass flow rate equation using the ventilation factor, see the SFPE Handbook (SFPE, 1995) for details.

2.5 Flashover Criteria

Flashover is characterized by the rapid transition in fire behavior from localized burning of fuel to the involvement of all combustibles in the enclosure, see Walton and Thomas (1995). High radiation heat transfer levels from the original burning item, the flame and plume directly above it, and the hot smoke layer spreading across the ceiling are all considered to be responsible for the heating of the other items in the room, leading to their ignition. Warning signs are heat build-up and "rollover" (small, sporadic flashes of flame that appear near ceiling level or at the top of open doorways or windows of smoke-filled rooms). Factors affecting flashover include room size, ceiling and wall conductivity and flammability, and heat and smoke producing quality of room contents. Water cooling and venting of heat and smoke are considered to be ways of delaying or

preventing flashover. Often the determination of whether or not flashover is expected is the single most important fire computation. This topic is addressed specifically in Thomas et al (1980) and Drysdale (1986). Three methods have been developed to estimate flashover, as described in the section 3.5, see Babrauskas (1980), Thomas (1981), and Macaffrey et al (1981).

2.6 Modeling

The effort of analyze fire to stop its hazard has been continually developed fire models. The physics and chemistry of fire are applied in computer models for simulating enclosure-fire environments. Analytical models for predicting fire behavior have been evolving since the late 1960's. Individuals have tried to describe in mathematical language the various phenomena which have been observed in fire growth and spread. These separate representations often describe only a small part of a fire experience. When combined, these separate pieces interact and form a complex computer code intended to give an estimate of the expected course of a fire based upon given input parameters. These complete analytical models have progressed to the point of providing predictions of fire behavior with an accuracy suitable for most engineering applications.

According to Friedman (1991) in his international survey, 36 actively supported models were identified. Of these, 20 predict the fire-generated environment (mainly temperature) and 19 predict smoke movement in some way. Six calculate fire growth rate, nine predict fire endurance, four address detector or sprinkler response, and two calculate evacuation times. Two different modeling techniques are commonly used in

fire modeling: field modeling (computational fluid dynamics technique) and zone modeling.

2.6.1 Field Models (Computational Fluid Dynamics Technique)

The most sophisticated deterministic models for simulating enclosure fires are termed "field models" or "CFD models." Field models of fire development in structures involve directly the fully 3-D time-dependent partial differential equations of the fundamental conservation laws, and are used in a wide range of engineering disciplines. Equations are solved for mass, momentum, energy and species at each of the many points of a fine grid covering the entire volume of the interior of the structure. In this way, values are permitted to vary from point to point within each room, and from room to room. Thus, these models have the capability of very accurate solution of the equations, and hence accurate simulation of the events. However, computational demands are very large, and correct simulation ultimately depends on the empirical-specification of things like ignition, burning rates, fire spread, ventilation-limitation, etc. At this time, field models are not well developed for the simulation of structural fires, and zone methods are currently preferred.

Jia et al (1997) introduce CED to calculate two simulations of two-dimensional compartment fire. They calculate the results of two scenarios, of fire in one room of a two room building showing differences between "open door throughout the simulation" and "open door that was initially closed".

Davis et al (1991) and Kerrison et al (1994) use a 3-D CFD computer code called FLOW3D to simulate and compare results with experimental data. Davis et al (1991)

find that the numerical results using this are in reasonable agreement with laboratory data for a small 100 kW fire in one and three room situations.

Kerrison et al (1994) calculate a one-room laboratory fire with various fire size (31.6 and 62.9 kW), fire location (center, corner, front, and back), and door width size (0.25 to 1 m). They find that mass flux predictions for the corner fires are within ±40 % of measured values, while most predicted quantities (including temperature and velocity at door) are within ±20 %.

2.6.2 Zone Models

Zone models solve the conservation equations for distinct regions. A number of zone models exist, varying to some degree in the detailed treatment of fire phenomena. The dominant characteristic of this class of model is that it divides the room(s) into hot upper layers and cold lower layers. The basic assumption of a zone model is that properties can be approximated throughout the zone by some uniform function. The uniform properties are temperature, smoke, and gas concentrations, which are assumed to be exactly same at every point in a zone. Experimental observations show that the uniform properties zone assumption yields good agreement (see Jones et al, 2000).

Zone modeling has proved to be a practical method for providing estimates of fire processes in enclosures. In this study, the computer calculation models used for the simulation are FASTLite and CFAST (Consolidated Model of Fire Growth and Smoke Transport). These codes are members of a class of models referred to as zone models. Evaluation of the accuracy of CFAST zone model including other researchers' calculations is described in section 4.2.3. Most previous researchers simulate one-

and/or three-room building fires with a fire only in one room. In my study, fire scenarios include fire spreading from one room to another and windows breaking out during the progress of the fire.

2.6.3 Simple Model Correlations

Equations are available, based principally on experimental correlations, which permit the user to make estimates of the results of a fire burning inside a given structure. Algebraic equations are available that correlate experimental data and results versus other parameters:

1. Room Model for Smoke Layer Depth and Temperature
2. Atrium Smoke Temperature
3. Buoyant Gas Head Pressure
4. Ceiling Jet Temperature
5. Ceiling Plume Temperature
6. Egress Time
7. Fire/Wind/Stack Forces on a Door
8. Mass Flow Through a Vent
9. Lateral Flame Spread
10. Law's Severity Correlation
11. Plume Filling Rate
12. Radiant Ignition of a Near Fuel
13. Smoke Flow Through an Opening

14. Sprinkler/Detector Response

15. Thomas' Flashover Correlation

16. Upper Layer Temperature

17. Ventilation Limit

The relevant equations are embodied in computer programs like FASTLite and HAZARD, so that making calculations of fire behavior becomes straightforward, provided one appreciates correctly the physics involved. Further details appear in Portier et al (1996) and Peacock et al (1991a, 1991b, and 1994), some of them are presented in the next chapter.

CHAPTER III

THEORY OF SUB-MODELS IN STRUCTURAL FIRE MODELING

This chapter summarizes important information in five topic areas: burning rates, radiant ignition, fire spread rates, ventilation limit imposed by size of opening, and flashover criteria. These are the main components related to the scientific understanding of the fire growth and flashover problem involved in real-world structural fires. Understanding and application of these topics are necessary to model the real-world structural fires better. Related calculations and graphical representations of these topics can be found in my recent papers (Kim and Lilley, 2000b and 2000c).

3.1 Burning Rates Theory

The energy generated by the fire is the primary influence on the temperature in a compartment fire, and much research has been conducted in characterizing the energy release rate of many fuels under a variety of conditions. The rate of energy release is equal to the mass loss rate of the fuel times the effective heat of combustion of the fuel (see Budnick et al, 1991).

$$\dot{Q} = \dot{m}_{b,f} \cdot \Delta h_{eff} \qquad (3.1)$$

where

$\dot{Q}$ = heat release rate of the fire (kW)

$\dot{m}_{b,f}$ = mass burning rate of the fuel (kg/s)

Δh_{eff} = effective heat of combustion of the fuel (kJ/kg)

The effective heat of combustion is the heat of combustion which would be expected in a fire where incomplete combustion takes place. This is less than the theoretical heat of combustion. The effective heat of combustion is often described as a fraction of the theoretical heat of combustion.

The most common method to measure heat release rate is known as oxygen consumption calorimetry. The basis of this method is that for most gases, liquids, and solids, a more or less constant amount of energy (heat) is released per unit mass of oxygen consumed. This constant has been found to be 13,100 kJ per kilogram oxygen consumed and is considered to be accurate with very few exceptions to about ±5 % for many hydrocarbon materials, see Huggett (1980). See also Babrauskas (1995) for the heat of combustions of various burning items.

In fuel-controlled fires, there is sufficient air to react with all the fuel within the compartment. In ventilation-controlled fires, there is insufficient air within the compartment, and some of the pyrolysis products will leave the compartment, possibly to react outside the compartment. For calculating the temperatures produced in compartment fires, the primary interest is in the energy released within the compartment.

The pyrolysis rate of the fuel depends on the fuel type, on its geometry, and on the fire-induced environment. The energy generated in the compartment by the burning pyrolysis products then depends on the conditions (temperature, oxygen concentration, etc.) within the compartment. While the processes involved are complex, and some are not well understood, there are two cases where some simplifying assumptions can lead to useful methods for approximation of the energy released by the fire:

1. Ventilation limited fires
2. Nonventilation limited fires

Experimentally, it has long been observed that (See Nilsson, 1971), unlike a pool fire, which can burn in a room in a highly fuel-rich manner, a wood crib does not burn more than approximately 30-40 percent fuel rich. Conditions more fuel rich than that are not sustained, presumably, because of the highly vitiated air being supplied to the crib under those conditions.

The following equation for stoichiometric fuel pyrolysis can be used to estimate the fuel mass loss rate at which ventilation-limited burning occurs, See Babrauskas (1981a).

$$\dot{m}_{st} = \frac{1}{r_s} \cdot 0.5 \cdot A_o \cdot \sqrt{H_o} \qquad (3.2)$$

where:

$\dot{m}_{st}$ = stoichiometric mass loss rate (kg/sec)

r_s = stoichiometric air/fuel mass ratio

A_o = area of ventilation opening (m^2)

H_o = height of ventilation opening (m)

Equation (3. 2) is applied to a compartment containing a single typical rectangular ventilation opening. This equation is primarily intended to be used in evaluating the fully developed fire, which mostly happened in the most post-flashover fire. The fully developed fire can be simplified with a condition of constant energy release rate. The approximate method produces estimates generally accurate to within ±5 % and typically ±3 %. However, this method is not recommended for accurate prediction of the initial start-up phase of pool fires in which the burning mixture is near stoichiometric.

A limit of approximately 37 percent fuel rich is reached when the maximum pyrolysis rate becomes the governing limit to the burning rate. Similar limits may possibly exist for other classes of combustibles, but experimental data are only available for wood cribs. For wood fuel, r_s=5.7. Values of r_s for other materials can be found in the Fire Protection Handbook, 17th Ed. NFPA (1991) (see Budnick et al, 1991).

Babrauskas (1995) also discusses the ability to predict burning rates of full-scale combustibles. It varies greatly with the combustible. In no case is it yet possible to predict the burning rates of practical combustibles simply on the basis of thermophysical and thermochemical data. Even in the "ideal" cases of a liquid pool, the relationships require actual test data.

The heat generate by the fire is the primary influence on the temperature in a compartment fire and heat release rate vs. time is an extremely import input to simulate a fire. Heat Release Rate can be characterized by t^2-fire growth model as NIST standardized and widely used for structural fire modeling. Slow, medium, fast and ultra-fast fire growths may be specified, where, after an initial incubation period,

$$\dot{Q} = \alpha_f (t - t_o)^2 \tag{3.3}$$

where α_f is a fire-growth coefficient (kW/s^2) and t_0 is the length of the incubation period (s). The coefficient α_f appears to lie in the range 10^{-3} kW/s^2 for very slowly developing fires to 1 kW/s^2 for very fast fire growth. The incubation period (t_0) will depend on the nature of the ignition source and its location, but data are now becoming available (see Babrauskas, 1984) on fire growth rates on single items of furniture (upholstered chairs, beds, etc.) that may be quantified in these terms. Suggested values for the coefficient α_f are also given in the formula section of Makefire - a subset of the FPETool and FASTLite Computer Programs. The specification of the fire-growth coefficient α_f (kW/s^2) is:

Table 3. 1 The Fire-Growth Coefficient

t^2-Fire Growth Model	Fire-Growth Coefficient α_f
Slow	0.002778 kW/s^2
Medium	0.011111 kW/s^2
Fast	0.044444 kW/s^2
Ultra-fast	0.177778 kW/s^2

3.2 Radiation Ignition Theory

The radiant heat flux received from a flame depends on a number of factors, including flame temperature and thickness, concentration of emitting species and the geometric relationship between the flame and the receiver. While considerable progress is being made towards developing a reliable method for calculating flame radiation, a high degree of accuracy is seldom required in real world fire engineering problems, such as estimating what level of radiant flux an item of plant might receive from a nearby fire in order that a water spray system might be designed to keep the item cool. Two approximate methods are now considered.

Considerations of inverse square distance lead to

$$\dot{q}_o'' = \frac{P_{rad}}{4\pi R_o^2} = \frac{x_r \dot{Q}}{4\pi R_o^2} \qquad (3.4)$$

where

$\dot{q}_o''$ = incident radiation on the target (kW/m^2)

R_o = distance (radius) to target fuel (m)

P_{rad} = total radiative power of the flame (kW)

x_r = radiative fraction

$\dot{Q}$ = total heat release rate (kJ/s) or (kW)

Usually x_r ranges from 20 to 60 percent, depending upon the fuel type. R_o should be measured from the center of the flame. Experimental measurements indicate that this equation has good accuracy for

$$R_o / R > 4 \qquad (3.5)$$

where R is the flame radius and the point-source nature of the heat from the flame is then a reasonable assumption. For radiation at

$$0.5 < R_o / R < 4 \qquad (3.6)$$

refer to SFPE (1995) for a more exact analysis.

In a second approximate method, the flame is approximated as a vertical rectangle and the radiant flux is calculated using "view factor" information. This takes into account the large size of the flame, with angles and orientations being accounted for appropriately. Flux levels close to the flame are then more accurately handled, see Drysdale (1986) and the FASTLite computer program (Portier et al, 1996).

This procedure applies to conditions where the exposed item is too close to the exposing fire for that source to be considered a point source. Rather the exposed item views the broad cross section of a fire typical of that produced by a free burning upholstered chair or couch.

Babrauskas (1981b) reported his results as three curves relating the energy level of a fire to the distance at which the incident radiation on an exposed target would be 10, 20, or 40 kW/m^2. These incident radiation are considered the approximate levels of incident radiation necessary for ignition of materials that are easily ignitable, normally ignitable, or difficultly ignitable, respectively. Simple correlations are shown, see Babrauskas (1981b) and Portier et al (1996).

Easily ignitable materials are those that respond rapidly to incident energy: ignites when it receives a radiant flux of 10 kW/m^2 or greater. Typical examples are thin curtains, loose newsprint, or draperies.

$$\dot{Q}_{ig} = 30.0 \times 10^{\frac{d+0.08}{0.89}} \tag{3.7}$$

Normally ignitable materials include those combustible that have increased resistance to heating: ignites when a radiant flux of 20 kW/m^2 or greater. These are typified by upholstered furniture and other materials with significant mass but small thermal inertia, $k\rho C_p$, are included.

$$\dot{Q}_{ig} = 30.0 \times (\frac{d+0.05}{0.019}) \tag{3.8}$$

Difficultly ignitable materials include those combustible that have greater resistance to heating: ignites when a radiant flux of 40 kW/m^2 or greater. Typical is a

half inch (0.013 m) or thicker materials with substantial thermal inertia $k\rho C_p$ like wood, and thermoset plastics.

$$\dot{Q}_{ig} = 30.0 \times (\frac{d + 0.02}{0.0092}) \qquad (3.9)$$

where

$\dot{Q}_{ig}$ = energy level required for ignition (kW)

d = separation between the item on fire and the exposed item (m)

= same as R_o in Equation (3.4)

These empirical equations are deduced from 11 data points ranged from 0.05 meters to 1.4 meters of d with about ±10 % error for difficult to ignite materials, and much greater accuracy for easily and normally ignitable materials.

3.3 Fire Spread Rates Theory

The concept of an ignition temperature is key to explaining flame spread in simple, but physically correct, terms. For flame spread, the pilot ignition temperature would apply because a pilot (the flame itself) is always present. We define the position x_p at the ignition temperature, T_{ig}. The temperature ahead of the flame, not affected by direct heating from the flame, is taken as T_s. In general, the flame can heat the region ahead of the flame in many ways. These depend on the mode of spread (orientation,

wind) and on the nature of the solid or liquid fuel. An observer riding on the flame front, at position x_p, sees the new fuel coming toward it at the flame spread velocity V_{spread} or the velocity the flame has in spreading along the fuel, which is at rest. The flame spread velocity formula states that the rate of energy supplied to this newly heated fuel, bringing to temperature T_{ig}, is equal to the net heat transfer rate from the burning region, $\dot{q}$. Using a balance for spread, the steady flame spread velocity is

$$v_{spread} = \frac{\dot{q}}{\rho_f c_f A(T_{ig} - T_s)} \tag{3. 10}$$

where

v_{spread} = flame spread velocity (m/s)

ρ_f = fuel density (kg/m^3)

c_f = fuel specific heat (kJ/kgK)

A = cross-sectional area (m^2)

$\dot{q}$ = rate of heat supplied (kW)

T_{ig} = ignition temperature (K)

T_s = fuel temperature beyond the range of the flame's heat (K)

Most specific cases of flame spread can be derived from this formula by more carefully describing of $\dot{q}$ and A, see Quintiere (1994).

These formulas should be considered as methods to make estimates, but not with accuracy under all conditions. Again, orientation, wind, and the nature of the fuel all make a difference.

3.4 Ventilation Limit Imposed by Size of Opening Theory

For fires nearing flashover and post-flashover fires the interface between the upper and lower layers is located near the floor, and smoke escapes through the top-part of an opening as fresh air enters through the bottom-part of the opening.. Rockett (1976) has shown that the temperature dependence of the flow becomes small above 150 °C, and the flow into the compartment can be approximated as a constant times the so-called ventilation factor

$$A_o\sqrt{H_o} \tag{3. 11}$$

Rockett (1976) calculated values for this constant was 0.40 to 0.61 kg/s·m$^{5/2}$, depending on the discharge coefficient of the opening. The value most commonly found in the literature is 0.5 kg/s·m$^{5/2}$ (Thomas and Heselden, 1972), taking the standard values of C_d=0.7, g=9.81m/s2, and ρ_∞=1.2kg/m^3, the constant in the above Equation (3. 11) becomes about 0.5. We therefore arrive at the very simple, useful, and well-known relationship for the mass flow into an opening:

$$\dot{m}_a = 0.5A_o\sqrt{H_o} \tag{3. 12}$$

$$\dot{Q} = 3000 \times \dot{m}_a \qquad (3.13)$$

where

$\dot{m}_a$ = mass flow rate of air (kg/s)

A_o = area of opening (m^2)

H_o = height of opening (m)

$\dot{Q}$ = heat release rate (kW)

The equations are deduced from more than 30 data points for $0.02 \leq A\sqrt{H} \leq 15$ with ±20 % error, see Babrauskas (1980) and Drysdale (1986). These equations are also used to drive other empirical correlations with even less error depending on the range of data.

We can now estimate the mass flow rate out through an opening by knowing only the area and the height of the vent. This equation gives an estimate of the mass flow rate for fires where the gas temperature is at least twice of the ambient temperature (measured in Kelvin) and where the enclosure temperature can be assumed to be uniformly distributed over the entire volume. In practice, this means that the gas temperature should be higher than 300 °C (≈573 K, which is slightly less than twice the ambient temperature of 293 K). The two conditions are most often met in post-flashover fires, where temperatures are in excess of 800 K and the enclosure is more or less filled with smoke of roughly uniform temperature. The equation has therefore been very useful in the analysis of post-flashover fires. According to Quintiere (1994), Large vents and

temperature well below 800 °C have lower flow rates than the theoretical maximum from Equation (3. 12).

The first use of this type of opening flow analysis for evaluating post-flashover fire-test data is attributed to Kawagoe (1958). See the Section 2-2 for stoichometric mass flow rate, and see Emmons (1995) for other calculations like velocity and volume flow.

3.5 Flashover Criteria Theory

According to Belles (1991) in his chapter in NFPA Handbook, NFPA (1991), it is a well-established fact that furnishings are frequently major contributors to fire growth. Recent developments make it possible to determine whether furnishings in a given environment are capable of producing sufficient energy to cause full room involvement. In this section, three simplified equations estimating the rate of heat release required for flashover to occur in a room is given. These contain a mathematical formula for estimating the amount of energy that must be present in a room or similar confined space to raise the upper level temperatures to a point likely to produce flashover.

3.5.1 Method of Babrauskas

According to Babrauskas (1980), at flashover about 50 percent of fire output goes to heat losses by radiation to the floor and by convection through ventilation, and the minimum fire heat release rate in kW is

$$\dot{Q}_{fo} = 750 A_o \sqrt{H_o} \qquad (3.14)$$

where

A_o = window or door ventilation area (m^2)

H_o = height of opening (m)

This correlation is driven from 33 test fires, which have energy release rates from 11 to 3820 kW and ventilation factor from 0.03 to 7.51. A gas temperature for flashover of 873 K, a specific heat of air of 1.0 kJ/KgK, emissivity of 0.5 are used to simplify.

3.5.2 Method of Thomas

From experimental data, Thomas (1981) developed an average for net radiative and convective heat transfer from the upper gas layer (kW), $\dot{q}_{loss}$, of $7.8A_T$ (Walton and Thomas 1995). Using upper layer temperature of 600 °C or a ΔT_g of 577 °C for flashover criterion and c_p = 1.26 kJ/kg·K, led the following expression for the minimum fire heat release rate in kW at flashover as

$$\dot{Q}_{fo} = 378 A_o \sqrt{H_o} + 7.8 A_T \qquad (3.15)$$

where

A_T = total area of the compartment-enclosing surfaces (m^2)

3.5.3 Method of McCaffrey, Quintiere, and Harkleroad

The method of McCaffrey et al (1981) for predicting compartment fire temperatures may be extended to predict the heat release rate of the fire required to result in flashover in the compartment. See Lawson and Quintiere (1985) and Walton and Thomas (1995) for further information. Simplifying the equation using an upper gas temperature of 522 °C and ambient temperature of 22 °C or ΔT_g = 500 °C for flashover, and substituting values for the gravitational constant (g = 9.8 m/s^2), the specific heat of air (c_p = 1.0 kJ/kg·K), and the density of air (ρ_∞ = 1.18 kg/m^3), and rounding 607.8 to 610 yields

$$\dot{Q}_{fo} = 610[h_k A_T A_o \sqrt{H_o}]^{1/2} \qquad (3.16)$$

where

h_k = effective heat transfer coefficient [(kW/m)/K]

= $(k\rho_c c_c / t)^{1/2}$ for $t \le t_p$

= k/δ for $t > t_p$

A_T = total area of the compartment surfaces (m^2)

A_o = area of opening (m^2)

H_o = height of opening from bottom to top (m)

k = thermal heat of the compartment surface material

δ = thickness of compartment surface

ρ_c = density of the compartment surface (kg/m^3)

c_c = specific heat of the compartment surface (kJ/kgK)

t = exposure time (s)

t_p = thermal penetration time (s) : $(\rho_c c_c / k)(\delta / 2)^2$

These three correlations are deduced from laboratory experimental data from small-scale to full-scale fires, and the estimated accuracy is ±30 % and typically ±10 %. Over the range of compartment sizes of most interest, all of the methods produce similar results.

In practice (including extreme conditions) it has been observed that flashover occurs when the upper room temperature of the smoke layer reaches between 300 and 700°C (572 and 1292°F). The lower bound of the extreme condition is like slow heating, small room, and well reflecting walls and ceiling. The occurrence of flashover depends on many factors, but a lower temperature should be used if one wishes to obtain a conservative safe estimate of the amount of time available before its occurrence. There is a need to assess which of the methods for predicting flashover is most appropriate.

Flashover is generally characterized by:

1. Temperatures reach approximately 500°C (932°F) to 600°C (1112°F) in the upper portions of the room.
2. Heat flux of from 20 to 25 kW/m^2 (6340 to 7925 Btu/hrft^2) occurs at floor level, with near-simultaneous ignition of combustibles not previously ignited.

3. The filling of almost the entire room volume with smoke and flames.

Generally, very high heat release rates occur after flashover, and (subject to oxygen availability) most ignitable items in the room burn, it gets very hot and the windows break and melt. The open window permits more oxygen to be made available and thereby increases the severity of the fire.

CHAPTER IV

THEORY OF CFAST AND FASTLite:
ZONE APPROACH FOR STRUCTURAL FIRE MODELING

The zone modeling approach to multi-room structural fire modeling is emphasized in this study and summarized in this chapter. This chapter summarizes the theory and methodology of the CFAST model and its simpler variant the FASTLite model which are zone type approach.

4.1 Zone Modeling

The zone model typically represents each area of the structure with two distinct compartment gas zones: an upper volume and a lower volume. These result from thermal stratification due to buoyancy. Conservation equations are applied to each zone and serve to embrace the various transport and combustion processes that apply. The fire is represented as a source of energy and mass, and manifests itself as a plume which acts as a pump of mass from the lower zone to the upper zone through a process called entrainment.

4.1.1 Conservation Equations

In the analysis of structural fires, the laws of conservation are applied in each control volume. They are conservation of mass, species, and energy. The assumptions and equations are given in the following analysis.

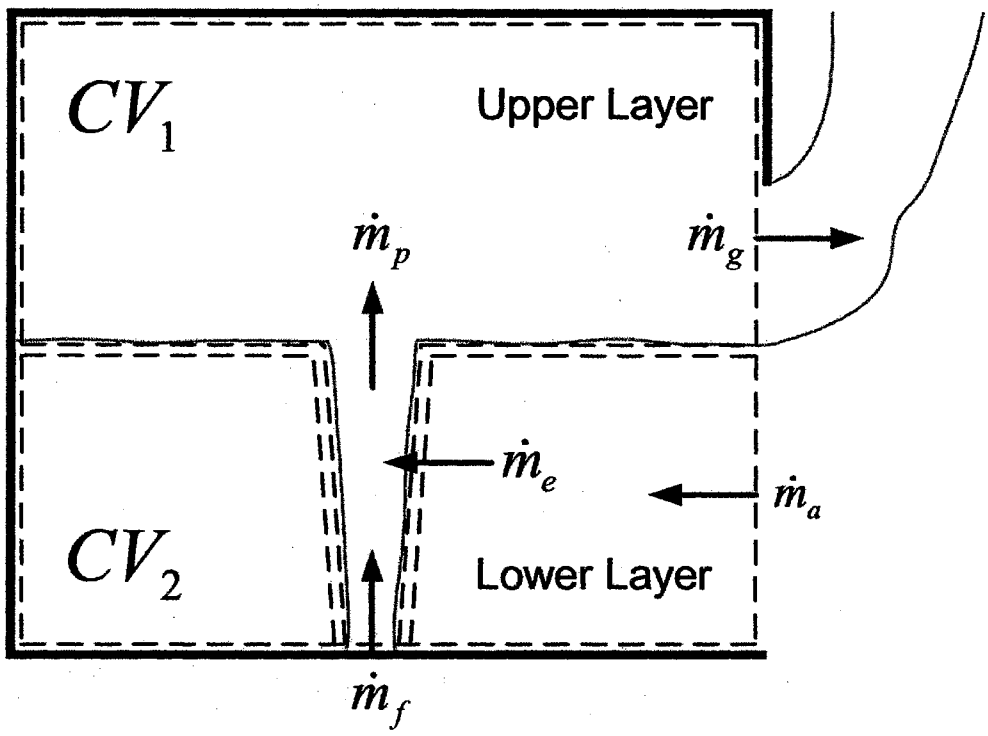

Figure 4. 1 Control Volumes Selected in Zone Modeling

4.1.1.1 Control Volume

The main part of the zone model is the conservation equation for the upper and lower gas zones. These are developed from the fundamental equations of energy and

mass transport, either in control volume as applied to the zones, or in the from of the differential equations representing the conservation laws, which are then integrated over the zones. The Figure 4. 1 illustrates a typical zone model representation of a compartment fire process. It shows a fire plume and a door vent. The hot combustion gases constitute the upper layer. A control volume (CV_1) is constructed to enclose the gas in this upper layer and the fire plume. The lower interface of the upper layer moves with the control volume such that no mass is transferred across this thermally stratified region.

4.1.1.2 Main Assumptions

The properties of a zone are treated to be spatially uniform but can vary with time. Therefore, temperature, T_g, and mass fraction of species i, Y_i, are properties associated with these ideal homogeneous gas layers. Other assumptions of typical zone models are followed below:

1. The gas is assumed to be an ideal gas with a constant molecular weight and constant specific heat, c_p and c_v.
2. Mass exchanges at free boundaries are caused by pressure differences or shear mixing effects. Typically natural or forced convection, or entrainment processes originate the mass exchange.
3. Unique source of mass and energy is combustion.
4. The plume instantly arrives at the ceiling.

5. Heat is assumed to be lost to the structure like wall, ceiling, and floor elements). Heat loss to room contents is ignored.
6. There is no pressure difference existed in a compartment, but hydrostatic variations account for pressure differences at free boundaries of the enclosure.
7. Cold airflow into the fire plume is due to turbulent entrainment. Entrainment is the process by which the surrounding gas flows into the fire plume as a result of buoyancy.

4.1.1.3 Conservation of Mass

In a zone (control volume), the rate of change of mass plus sum of net mass flow rates is zero, which applies the conservation of mass for a control volume. From Figure 4. 1, the conservation of mass can be expressed by

$$\frac{dm}{dt} + \sum_{j=1}^{n} \dot{m}_j = 0 \qquad (4.1)$$

The second term can be expressed

$$\sum_{j=1}^{3} \dot{m}_j = \dot{m}_g - \dot{m}_e - \dot{m}_f \qquad (4.2)$$

where

$\dot{m}_e$ = the mass flow rate of entrainment into the fire plume

$\dot{m}_g$ = the mass flow rate out of the door

$\dot{m}_f$ = the mass flow rate of gaseous fuel supplied.

The mass flow rate, $\dot{m}_p$, is the mass flow rate in the plume at the hot layer interface, and equal to $\dot{m}_e + \dot{m}_f$. The user of the zone model must in most cases specify the mass supply rate of fuel.

4.1.1.4 Conservation of species

The equation for conservation of species can be found by applying the conservation of mass for species i to a control volume. The equation of conservation for species is then given by

$$m\frac{dY_i}{dt} + \sum_{\substack{j=1 \\ net\ out}}^{n} \dot{m}_j (Y_{i,j} - Y_i) = y_i \dot{m}_f - \dot{m}_{i,loss} \qquad (4.3)$$

where

m = the mass of the layer

$\dot{m}_{i,loss}$ = the losses due to surface deposition or settling of particulates

$\dot{m}_{react}$ = the mass rate of gaseous fuel supplied

y_i = the mass yield of species i produced per mass rate of fuel

The production term ($y_i \dot{m}_f$) is dependent on the mass rate of fuel burning (kg/s), $\dot{m}_{react}$, which is related to the heat release rate (J/s) of the on-going fire and the heat of combustion of the fuel being burned (J/kg). However, for most practical applications the production term must be relied on experimental data. Experimentally, the yield of species i, y_i, is also measured in terms of $\dot{m}_f$ and not $\dot{m}_{react}$. Theoretically the production term can be described through knowledge of the chemical equation of the reaction or its particular stoichiometry. However this can be complicated and involves the stoichiometry of the chemical reaction and pyrolysis of solid fuels. For example, fuel gases can take many chemical forms as they emerge from the pyrolysis of solids. See Lilley (1989) for details.

4.1.1.5 Conservation of energy

The conservation of energy given by

$$\frac{d}{dt}\iiint_{CV} \rho u dV + \iint_{CV} \rho h v_n dS = \dot{Q} \tag{4. 4}$$

By substituting $h - P/\rho$ for u in the first term, assuming quasi-steady state for the control volume, and using the equation of state $P = \rho RT$, yields:

$$Vc_p \frac{dT_g}{dt} - V\frac{dP}{dt} + c_p \sum_{j=1}^{n} \dot{m}_j (T_j - T_g) = \dot{m}_{react} \Delta h_{eff} - \dot{q}_{loss} \tag{4. 5}$$

where

$\dot{m}_{react}$ = the rate at which fuel is reacted

P = the global pressure in the control volume

$\dot{q}_{loss}$ = the rate of heat transfer lost at the boundary

V = the volume of the control volume

Δh_{eff} = the effective heat of combustion

The change of internal energy within the control volume is represented in the first term on the left-hand side. In case the temperature is not changing rapidly with time, this term can be small, and its elimination gives rise to a quasi-steady approximation for growing fires that allows a more simple analysis.

The rate of work done by pressure as the gas layer expands or contracts caused by the motion of the thermal stratification interface is represented in the second of the left-hand side. In the equation (4. 5) of rearranging, this term now is expressed as rate of pressure increase for the compartment that essentially can be caused by net heat or mass additions to the compartment gases. Except for rapid accumulation of mass or energy, or for compartments with small openings to the surroundings, this pressure rise is small and the pressure nominally remains at nearly the ambient pressure.

In typical zone models it is assumed that all the fuel supplied can react if there is sufficient oxygen available. One assumption on the sufficiency of oxygen is to consider that all the fuel supplied reacts in that volume as long as the oxygen concentration in that volume is greater or equal to $Y_{ox,low}$ (0 to 21 %), i.e.,

$$\dot{m}_{react} = \dot{m}_f \qquad if \qquad Y_{ox} > Y_{ox,low} \tag{4.6}$$

When this condition is not met, unburned fuel can exist in the product of combustion, and can be transported into adjoining zones or control volumes. At the oxygen insufficiency condition, all of the oxygen supplied to the control volume is reacted in most zone models, so that as long as $Y_{ox} = Y_{ox,low}$,

$$\dot{m}_{react} = r \cdot (net\ mass\ rate\ of\ oxygen\ supplied\ through\ opeings) \tag{4.7}$$

where

r = stoichiometric fuel to oxygen mass ratio

Ventilation limit imposed by size of opening is taking place when $Y_{ox} = Y_{ox,low}$ in compartment fires. Significant changes take place in the nature of the chemical reaction with ventilation limit imposed by size of opening. Incomplete combustion is now more predominant for hydrocarbon fuels remarkably, leading to a significant increase in the yield of carbon monoxide and often soot. Therefore, care must be used in interpreting the results of zone models once ventilation-limited conditions arise, particularly with respect to the prediction of species concentrations and the extent of burning. However, This phenomenon is embodied in some of recent zone models like CFAST. In CFAST user can chose if ventilation limit applies in the calculation.

4.1.1.6 Summary

Two zones (the upper and lower gas layers) are applied in the common zone models for a compartment. The mass and energy equations comprise four equations that permit the determination of the two layer temperatures, one layer height, and the compartment pressure. The densities are found from the ideal gas equation of state, in which approximately ρT is constant.

Each of the source or transport terms in the equations must be given in terms of the above layer properties or auxiliary relationships must be included for each new variable introduced, in order to complete this solution process. The source terms are associated with the $\dot{m}_{react}$ and y_i terms, and the transport terms include the j mass flow rates and the boundary heat transfer rates.

4.1.2 Source Term Submodels

The most important submodel for source term is the burning rate of the fire, $\dot{m}_f$. In general,

$$\dot{m}_f = f(\textit{fuel properties, heat transfer}) \qquad (4.8)$$

in which the heat transfer to the fuel results from the flame configuration and the heated compartment. The mass burning rate (kg/s) generally depends on fuel properties, heat transfer, air availability, etc. For example, lack of air can reduce the fuel burning rate. Also, radiation feed back to the fire can enhance the fuel burning rate. The initial fire can be more often be prescribed from experimental data of burning rate versus time –

such data will be given in Section 5.3. Many items are included, making incorporation of a specific initial fire into any computer code very simple.

4.1.2.1 Mass Transport Submodels

Entrainment - The mass flow rate of entrainment relationship for the fire plume is an important feature of zone modeling. This permits the mechanism for flow between the lower and upper stratified gas layers. Considerable work has been performed to develop entrainment relationships for pool fires or axisymmetric gas burner fires.

Vent flows through openings in vertical partitions - It is a classical representation of fire in a room or building represents the structure with an opening such as a door or window to the ambient surroundings. When having a uniform gas temperature over its entire volume (well-mixed) as seen in Figure 4. 2, the maximum pressure difference at the top of the vent and at the bottom of the vent can be written as

$$\Delta P_{u,max} = (\rho_a - \rho_g) \cdot g \cdot h_u \tag{4. 9}$$

$$\Delta P_{l,max} = (\rho_a - \rho_g) \cdot g \cdot h_l \tag{4. 10}$$

where, h_u and h_l are both measured as positive entities from the neutral plane, and therefore $\Delta P_{u,max}$ is positive out of the vent and $\Delta P_{l,max}$ is positive into the vent.

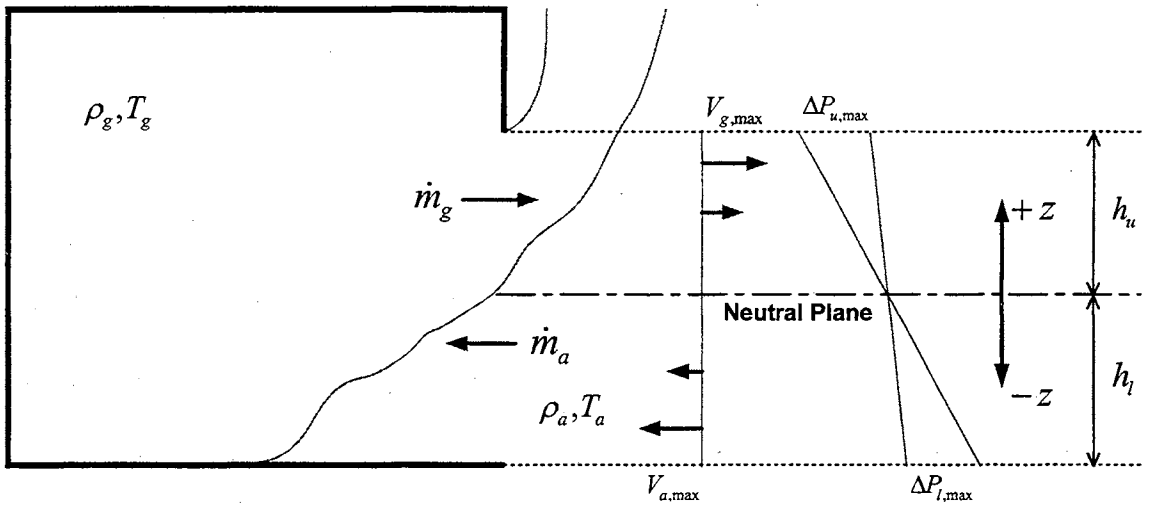

Figure 4. 2 Velocity and Mass flow Due to Pressure Difference in an Enclosure

Generally, the pressure difference as a function of height z (above and below the neutral plane) can be written as

$$\Delta P(z) = (\rho_a - \rho_g) \cdot g \cdot z \tag{4. 11}$$

with the same sign convention as above.

The theoretical basis of the computation is orifice flow utilizing Bernoulli's equation along a streamline of flow through an opening. The velocity above the neutral plane, v_g, and the velocity below the neutral plane, v_a, are given by

$$v_g(z) = \sqrt{\frac{2z(\rho_a - \rho_g)g}{\rho_g}} \tag{4. 12}$$

$$v_a(z) = \sqrt{\frac{2z(\rho_a - \rho_g)g}{\rho_a}} \tag{4. 13}$$

where the inside velocity of compartment assumed to be zero.

Finally, the mass flow rate of hot gases out of the vent and cold air in through the vent are then computed by integration over a flow area of width W and height z (above and below the neutral plane for each below equation) using equation below

$$\dot{m}_g = C_d \int_0^z W \rho_g v_g(z) dz \tag{4. 14}$$

$$\dot{m}_a = C_d \int_0^z W \rho_a v_a(z) dz \tag{4. 15}$$

where C_d is a flow coefficient. Emmons (1995) suggests that a value of 0.68 for C_d has an accuracy of ±10 % except at very low flow rates at the beginning at a fire.

Natural and forced vent flows can exists through an opening in a vertical partition. In both cases the above equations apply, but the pressure distribution must be described appropriately, because air may flow in and out. For example in the pure natural convection case, the pressure is determined by the static pressure with respect to the floor pressure, $P(0)$. Actually it is the floor pressure that applies in conservation of

energy equation and in the perfect gas equation of state. See Peacock et al (1993) and Jones et al (2000) for the similar analysis of vent flows between compartments, instead of from a compartment to the outside as given above.

Vent flows through openings in horizontal partitions - The flow through an opening in a horizontal partition can be considered in a manner similar to that for the vertical partition, provided the pressure difference is large enough. If there is only a single vent to the fire compartment through a horizontal partition, such as a ceilings, the flow must be oscillatory or bi-directional. The latter case implies a zero pressure difference with gravity solely determining the flow, see Epstein (1988) and Cooper (1990).

Mixing between the layers - The primary exchange of fluid between the lower and upper gas layers is due to the buoyant effect of the fire plume. Secondary, but significant, mixing processes can occur due to the other effects, which are

a. exchange due to a cold flow injected into the hot layer
b. exchange due to shear mixing associated with vent flows
c. exchange due to wall flows due to local buoyancy effects.

Although secondary mixing processes are important for improving the accuracy of a zone model, little work has been undertaken to establish their models with confidence or with full acceptance.

4.1.2.2 Heat Transport Submodels

Convective heat transfer to surfaces - In general, convective effects will vary along the ceiling, walls, and floor, and depend on the nature and position of the fire.

Radiative heat transfer - The theory is not sufficiently developed to predict flame radiation from first principles without very sophisticated modeling of the soot and temperature distributions. Hence, flame radiation is relegated to empirical practices. Radiation from a smoke to the layer is easier to deal with within the context of a uniform property gas layer for the zone model. One unresolved difficulty is the availability of property data to determine the contribution of smoke particulates to the layer radiation properties.

Conduction heat transfer - The radiation and convection heat transfer from the gas must be balanced by conduction heat transfer through the boundary surfaces. Usually zone models have considered only one-dimensional conduction, which should be adequate for most applications.

4.1.3 Unresolved Phenomena and Limitation

The zone model can be very versatile in accommodating new physics even if it appears inconsistent with the uniform property layer assumption. Some significant phenomena are absent from consideration by the zone modeling approach for fire. These include

1. vent flames
2. transient flow in corridors; and
3. shaft flows

Although the submodel of transient flow in corridors has been embodied in recent models like CFAST (version 4.0.1), it requires lots of assumptions of characteristic of corridor flows.

The zone modeling technique may not be suitable for some other geometries, such as smoke spread in rooms with a large length-to-width ratio or rooms where the horizontal length to vertical length ratio is very large or very small. The models are, however, often applied to such geometries, and the user must be acutely aware of the modeling limitations.

4.1.4 Zone models

The zone modeling approach emerged in the mid-1970s when the effort to study the developing fire in a compartment intensified. According to the survey of Friedman (1991), 12 zone models are in use around the world. Some important models related to this study are listed here.

ASMET (Atria Smoke Management Engineering Tools) consists of a set of equations and a zone fire model for analysis of smoke management systems for large spaces such as atria, shopping malls, arcades, sports arenas, exhibition halls and airplane

hangers. ASMET is written in C++ language. For program documentation and a description of the input data, see Klote (1994).

CCFM (Consolidated Compartment Fire Model version VENTS) is a two-layer zone-type compartment fire model computer code. It simulates conditions due to user-specified fires in a multi-room, multi-level facility. The required inputs are a description of room geometry and vent characteristics (up to 9 rooms, 20 vents), initial state of the inside and outside environment, and fire energy release rates as a function of time (up to 20 fires). If simulation of concentrations of products of combustion is desired, then product release rates must also be specified (up to three products). Vents can be simple openings between adjacent spaces (natural vents) or fan/duct forced ventilation systems between arbitrary pairs of spaces (forced vents). For forced vents, flow rates and direction can be user-specified or included in the simulation by accounting for user-specified fan and duct characteristics. Wind and stack effects can be taken into account. The program outputs for each room are pressure at the floor, layer interface height, upper/lower layer temperature and product concentrations, see Forney and Cooper (1990).

CFAST (Consolidated Model of Fire Growth and Smoke Transport) is a zone model that predicts the effect of a specified fire on temperatures, various gas concentrations and smoke layer heights in a multi-compartment structure. CFAST is based on solving a set of equations that predict the change in the enthalpy and mass over time. The equations are derived from the conservation equations for energy, mass,

momentum, and an equation of state, in this case, the ideal gas law. The conservation equations are fundamental to physical systems, and must hold in all cases. These equations are rearranged to form a set of predictive equations for the sensible variables in each compartment. CFAST is formulated as a set of ordinary differential equations. It was the first model of fire growth and smoke spread to cast the entire model in this form and was done because of the efficiency of solving the conservation equations this way. Bukowski (1996) used CFAST to reproduce the observed conditions and to support a theory of the accumulations of significant quantities of unburned fuel from a vitiated fire in a real apartment fire. More details are given in the section 4.2.

FAST (Fire Growth And Smoke Transport) is one of noteworthy multi-room zone-type computer programs. CFAST is embodied in the recent FAST as its actual calculation routine. It is a multi-compartment (up to 30 rooms for version 3.1.6) zone-type computer model to predict the temperature, heat transfer and smoke hazard development in each compartment of the compartments and the type and location of the fire, see Cooper (1982 and 1983), Jones (1985), Jones and Peacock (1989), and Walton et al. (1985) for details.

FASTLite is a collection of procedures that builds on the core routines of the earlier FIREFORM and a simplified version of the computer model CFAST to provide engineering calculations of fire phenomena for the building designer, code enforcer, fire protection engineer and fire-safety related practitioner. This program provides quantitative estimates of some of the likely consequences of a fire and the underlying

models have been subjected to a range of verification tests to assess the accuracy of the calculations. FASTLite is a small version of FAST (and/or CFAST), and can simulate up to 3 rooms through a graphical user interface (GUI). Kim and Lilley (1997 and 1998) have used FASTLite to study the time required to reach flashover conditions, and parameter effects on this time.

HAZARD I, see Bukowski et al. (1989), presents an advanced mathematical modeling approach to simulating fire development in a multi-room building complements the experimental approach and/or post-fire on-site investigations. HAZARD I is the first such fully-integrated modeling tool in the world. The HAZARD program initially used FAST as its solver, but the latest version uses CFAST (see Peacock et al, 1994). The latest microcomputer version of the code can handle buildings with up to 15 areas, multiple fires, HVAC connections, and ceiling, floor and wall venting. This code is a generalized version of the earlier program, with user-friendly input and output, and a useful database of experimental properties to be used in the calculations. The latest version (ver. 1.2) is described in Peacock et al (1994).

4.2 CFAST and FASTLite Computer Codes

Fire analytical models have been developing from the late 1960's. CFAST is a member of a class of models referred to as zone models, and it is the most popular zone model in use (see Karlsson and Quintiere, 2000). In zone element model, each room is divided into a small number of volumes (called zones), each of which is assumed to be

internally uniform. That is, the temperature and smoke and gas concentrations within each zone are assumed to be exactly same every point. In CFAST, each room is divided into two layers. Since these layers represent the upper and lower parts of the room, conditions within a room can only vary from floor to ceiling, and not horizontally. This assumption is based on experimental observation that in a fire, room conditions do stratify into two distinct layers. While we can measure variations in conditions within a layer, these are generally small compared to differences between the layers. This assumption places some limitations on the predictive capability that such a model can make. As modeling evolves over time, many of these assumptions are being lifted.

CFAST is based on solving a set of combined equations that simulate the change in the enthalpy and mass over time. The starting point is the set of conservation equations that are fundamental to physical systems, and hold in all cases. The equations are derived from the conservation equations for energy, mass, momentum. Subsidiary equations are the ideal gas law and definitions of density and internal energy. The resulting equations are rearranged to form a set of predictive equations for the calculation of sensible variables in each compartment. In CFAST the simulation is formulated as a set of ordinary differential equations.

Each formulation can be expressed by mass and enthalpy flow terms. These rates represent the exchange of mass and enthalpy between zones due to physical phenomena such as plumes, natural and forced ventilation, convective and radiative heat transfer, and so on. The formalism was used that the mass flow to the upper and lower is denoted $\dot{m}_u$ and $\dot{m}_l$ and the enthalpy flow to the upper and lower layers is denoted $\dot{s}_u$ and $\dot{s}_l$. It is tacitly assumed that these rates may be computed in terms of zone properties such as

temperature and density. These rates represent the net sum of all possible sources of mass and enthalpy due to phenomena.

4.2.1 History of CFAST and FASTLite Computer Codes

CFAST and FASTLite are distributed by Building and Fire Research Laboratory (BFRL) of National Institute of Standards and Technology (NIST). CFAST is the kernel of the zone fire models (FAST, FASTLite, FireCAD, and FireWalk) which are supported by BFRL. The version history of CFAST is as followed.

An amalgamation of FAST 18.5 and CCFM was developed as CFAST 1.0 in 1990. It was functionally equivalent to FAST 18.5 but more modules were added from CCFM. Multiple fires, multi-wall radiation, distributed mechanical ventilation ducts, ceiling jet and 3D positioning of fires, a more robust ODE solver (DASSL, see Brenan et al, 1989) were added later. The maximum number of compartments was increased to 15. In 1993, CFAST was updated to version 2.0 with adding of a new THERMAL.DF, a new conduction routine, and a new convection routine. The problems of flow through horizontal openings, very large fires in small rooms, interaction between fire size and plume entrainment, and optional ceiling jet calculation were fixed later. The comparison method and usage of different versions (1.4, 1.6.4, and 2.0.1) of CFAST can be found in Alvord (1995).

In 1996, version 3.0 was released with a new user interface for CEdit and a new phenomenon of ceiling/floor heat transfer for inter-compartment heat transfer. In November 1999, the last full Graphical User Interface (GUI) version (3.1.6) was released after some minor corrections and adding a new phenomenon of vertical heat flow.

Finally version 4.0.1 was released with adding of a new phenomenon of horizontal heat conduction, which runs an application under the Windows series of operating systems in March 2000. This version (up to 30 rooms and 30 ventilations) is the final version so far (June, 2001), and used in this study.

FASTLite is a smaller (lighter) version of CFAST. It is restricted to 3 rooms with a fire only in one of them. Some of my earlier work (one room calculations) was using FASTLite. I have verified that the results are the same for comparable situations. My later work has been done using CFAST, because of its increased capability like number of rooms and fire not been restricted to one room.

4.2.2 The Two-Layer Model in CFAST

A compartment is divide into two control volumes (called zones), a relatively hot upper layer and a relatively cold lower layer. The gas in each layer has attributes of mass, internal energy, density, temperature, and volume denoted m_i, E_i, ρ_i, T_i, and V_i where $i = l$ for the lower layer and $i = u$ for the upper layer. The compartment as a whole has the attribute of pressure P. These 11 variables are related by means of the following seven constraints.

$$\rho_i = \frac{m_i}{V_i} \qquad \text{(Density)} \qquad (4.16)$$

$$E_i = c_v m_i T_i \qquad \text{(Internal Energy)} \qquad (4.17)$$

$$P = R\rho_i T_i \qquad \text{(Ideal Gas Law)} \qquad (4.18)$$

$$V = V_l + V_u \qquad \text{(Total Volume)} \qquad (4.19)$$

Four required additional equations to complete the equation set obtained from conservation of mass and energy for each layer, and the first law of thermodynamics. The first law of thermodynamics represent that the rate of increase of internal energy plus the rate at which the layer does work by expansion is equal to the rate at which enthalpy is added to the gas.

$$\frac{dm_i}{dt} = \dot{m}_i \qquad \text{(Differential Equation for Mass)} \qquad (4.20)$$

$$\frac{dE_i}{dt} + P\frac{dV_i}{dt} = \dot{s}_i \qquad \text{(The First Law of Thermodynamics)} \qquad (4.21)$$

Many possible different equation formulations can be derived and selected from above equations. CFAST used the number of differential equation formulations that reduced by not mixing variable types between layers; that is, if upper layer mass is chosen as a solution variable, then lower layer mass must also be chosen. CFAST is set up to use the equations set for layer temperature, layer volume, and pressure as shown below.

$$P = P_\infty + \Delta P \qquad (4.22)$$

$$\frac{dP}{dt} = \frac{\gamma - 1}{V}(\dot{s}_l + \dot{s}_u) \qquad (4.23)$$

$$\frac{dV_u}{dt} = \frac{1}{\gamma P}\left((\gamma - 1)\dot{s}_u + V_u\frac{dP}{dt}\right) \qquad (4.24)$$

$$\frac{dT_u}{dt} = \frac{1}{c_p \rho_u V_u}\left((\dot{s}_u - c_p \dot{m}_u T_u) + V_u\frac{dP}{dt}\right) \qquad (4.25)$$

$$\frac{dT_l}{dt} = \frac{1}{c_p \rho_l V_l}\left((\dot{s}_l - c_p \dot{m}_l T_l) + V_l \frac{dP}{dt} \right) \qquad (4.26)$$

The differential equation for pressure can be derived by substituting summation of the upper and lower layer versions of the internal energy equation into the first law of the thermodynamics equation, taking constant c_v and $dV_u / dt = -dV_l / dt$. The differential equation for volume can be derived by substituting the differential form of internal energy into the first law of the thermodynamics equation. The differential equations for temperatures also can be derived from the differential equations for volumes by applying quotient rule to $d\rho_i / dt = d(m_i / V_i) / dt$ and $dT_i / dt = d(P / R\rho_i) / dt$.

This CFAST model can be split into distinct parts. There are routines for input, calculation, and output. The major routines of CFAST are depicted in Figure 4. 3. These physical interface routines link the CFAST model to the actual routines which calculate quantities such as mass or energy flow at one particular point in time for a given environment.

The major routines, which solves the equations, are SOLVE, RESID and DASSL. SOLVE is the control program that oversees the general solution of the problem. It invokes the differential equation solver DASSL (Brenan et al, 1989) that in turn calls RESID to solve the transport equations.

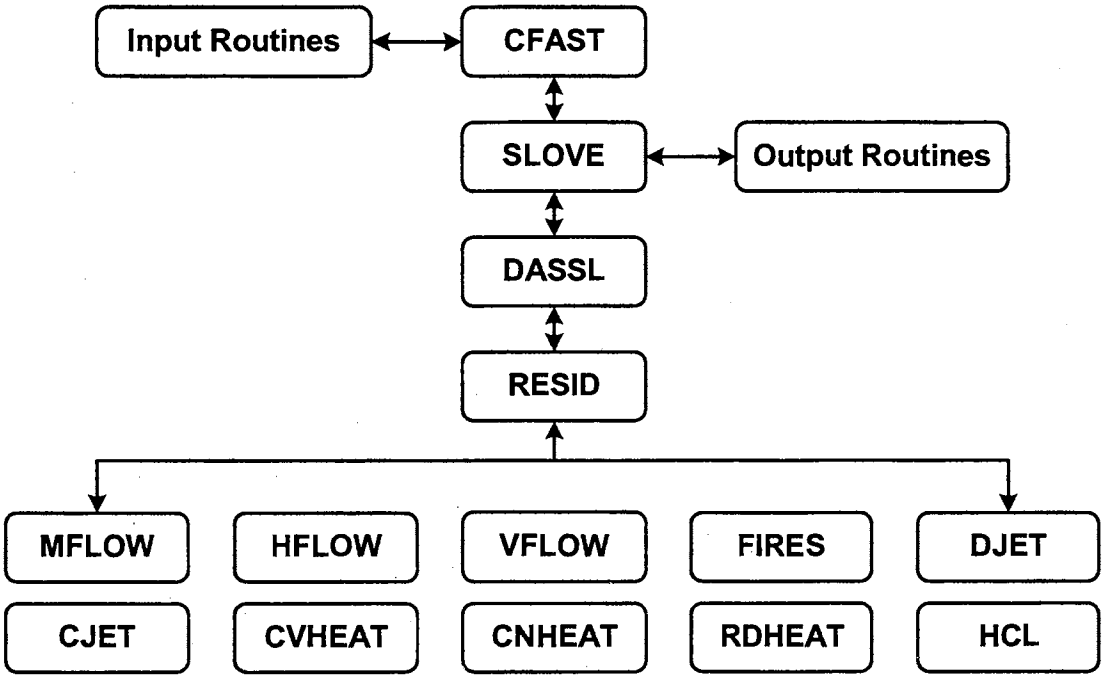

Figure 4. 3 Structure of CFAST Computer Code

Equations are solved by time-stepping methodology as follows. The solution at time $t + \Delta t$ is calculated from the given solution at time t. The differential equations are the form of

$$\frac{dy}{dt} = f(y,t) \tag{4. 27}$$

$$y(t_0) = y_0 \tag{4. 28}$$

where y is a vector representing pressure, volume, temperatures. f is a vector function that represents changes in these values with respect to time. The term y_0 is an initial

condition at the initial time t_0. The subroutine RESID computes the right hand side of Equation (4. 27) and returns a set of residuals of that calculation to be compared to the values expected by DASSL. DASSL then checks for convergence. Once DASSL reaches an error limit (defined as convergence of the equations) for the solution at $t + \Delta t$, SOLVE then advances the solution of species concentration, wall temperature profiles, and mechanical ventilation for the same time interval.

Note that there are several distinct time scales that are involved in the solution of this type of problem. The fastest will be chemical kinetics, which is assumed infinitely fast in this model. The next larger time scale is that associated with the flow field. Their equations are cast into the form of ordinary differential equations in the model. Then there is the time scale for mechanical ventilation, and finally, heat conduction through objects. By way of example, chemical kinetic times are typically on the order of milliseconds. The transport time scale will be on the order of 0.1 second. The mechanical ventilation and conduction time scales are typically several seconds, or even longer. CFAST (version 4.0.1) dynamically adjusts the time step over the entire simulation to a value that is appropriate for the solution of the currently defined equation set. In addition, very large time steps are possible if the problem being solved approaches steady-state.

The subroutines in the bottom of Figure 4. 3 (MFLOW, HFLOW, VFLOW, FIRES, DJET, CJET, CVHEAT, CNHEAT, RDHEAT, and HCL) are the subroutines for mechanical ventilation, horizontal flow, vertical flow, fire chemistry, door jet fires, ceiling jets, convection, conduction, radiation, and HCl deposition respectively.

4.2.3 Evaluation

The ASTM (1995a) guide for evaluating the predictive capability of fire models identifies four important areas for fire model evaluation.

1 model and scenario definition

2 theoretical basis and assumptions in the model

3 mathematical and numerical robustness of the model

4 quantifying the uncertainty and accuracy of the model

The first two of these areas of importance are largely documentation issues for the model developer. For the FASTLite and the CFAST model, a user's guides are available to direct model and scenario definition, see Portier et al (1996) and Jones et al (2000). This publication provides details of the theoretical basis and assumptions in the models. Additional guidance is available in the ASTM (1995b) guide for fire model documentation, and the models' user's guides are well satisfied the guidance. For the third area of importance, the work of Forney and Moss (1994) examines the numerical robustness of fire models using the CFAST model as an example. For the fourth area, sensitivity analysis and experimental comparisons have been done by previous researchers as now described.

A number of researchers have studied the level of agreement between computer fire models and real-scale fires. These comparisons fall into two broad categories: fire reconstruction and comparison with laboratory experiments. Both categories provide a level of verification for the models used. Fire reconstruction, although often more

qualitative, provides a higher degree of confidence for the user when the models successfully simulate real-life conditions. According to Milter (1985), predictions within 20 % of the experimental data have been considered reasonably good in view of many unresolved phenomena in fire science. Comparisons with laboratory experiments, however, can yield detailed comparisons that can point out weaknesses in the individual phenomena included in the models. The comparisons made to date are mostly qualitative in nature.

Nelson (1989) used simple computer fire models along with existing experimental data to develop an analysis of a large high-rise building fire. This analysis showed the value of available analytical calculations in reconstructing the events involved in a multiple-story fire. Bukowski (1990 and 1996), and Bukowski and Spetzler (1992) have applied the FAST and CFAST (HAZARD, FASTLite) models in several fatal fire reconstructions. Details of the fires including temperatures, vent flows, and gas concentrations were consistent with observed conditions and witness accounts.

Several studies comparing model predictions with experimental measurements are available. Deal (1990) reviewed four computer fire models (CCFM, FIRST, FPETOOL and FAST) to ascertain the relative performance of the models in simulating fire experiments in a small room. All the models simulated the experimental conditions including temperature, species generation, and vent flows, are "quite satisfactorily."

Duong (1990) studied the predictions of several computer fire models (CCFM, FAST, FIRST, and BRI), comparing the models with one another and with large gas-burner fires in an aircraft hanger. For a 4 MW fire size, he concluded that all the models are "reasonably accurate." At 36 MW, however, "none of the models did well."

Beard (1990) evaluated four fire models (ASET, FAST, FIRST, and JASMINE) by modeling three well-documented experimental fires, ranging in scope from single compartments to a large-department-store space with closed doors and windows. He provides both a qualitative and quantitative assessment of the models ability to predict temperature, smoke obscuration, CO concentration, and layer interface position (for the zone-based models).

Dembsey et al (1995) compared CFAST predictions to full-scale laboratory one-compartment fire experiments with 330, 630, and 980 kW heat release rates. He found that CFAST calculations show the average differences of upper temperature less than 10 %. More comparisons of one-room fires are available, see Klote and Forney (1993), Spearpoint et al (1999), and Reneke et al (2000).

Collier (1996) conducted a series of fire experiments in a three-bedroom dwelling, and compared to the predictions of the CFAST (HRR of 20, 250, and 1000 kW). He noted that user must apply a degree of judgment in selecting the input parameters in order to achieve a logical program output and gain the maximum benefit from the model.

Peacock et al (1993b and 1998) compared the CFAST model to a range of laboratory experimental fires (one- and three-room building). The model provided predictions of the magnitude and trends (time to critical conditions and general curve shape) for the experiments studied which range in quality from within a few % to a factor of two or three of the measured values. The general computational method is described in Peacock et al (1993a), where good agreement with experimental observations has been verified.

CHAPTER V

RESULTS AND DISCUSSION

Several applications of the computer code CFAST are now described. The time to reach flashover conditions is discussed in the first two sections. Burning rates of typical items are characterized in a consistent fashion for direct input into any computer modeling in the next section. They are applied to CFAST to simulate real house burns in the last two sections. A new and novel method of formulating a fire a scenario is used in the simulation of fire growth and spread in real house fires in last two sections.

5.1 Parameter Effects on the Time to Reach Flashover Conditions

The time to reach flashover is characterized by the criterion of the upper layer temperature reaching 600°C (1112°F) for my study. The FASTLite computer program (single room simulation) is used for calculations. Often the determination of whether or not flashover is expected is the single most important fire computation.

Figure 5. 1 shows the single room considered, with just one ventilation opening. Some geometric parameters are illustrated in the figure (numbers 1, 2, 3, 4, 5, 8 which are defined in the list below). There are 10 parameters of interest that affect the time

required to reach flashover conditions, which is calculated in this section. The parameters and their standard (default) values are:

1. Floor Area = 4m * 4m = $16m^2$
2. Vent Width = 2 m
3. Vent Height = 1 m (distance from bottom to top of the vent)
4. Vent Height above Floor = 1.5 m (distance from floor to mid-point of the vent)
5. Ceiling Height = 2.5 m
6. Fire Specification = Medium Fire
7. Fire Location = Fire in center of floor
8. Wall and Ceiling Material = 0.016 meter (5/8") thick Gypsum Board
9. Fire Radiation Fraction = 0.3 (radiation heat loss fraction from the flame)
10. Fire Maximum Heat Release Rate = 3 MW

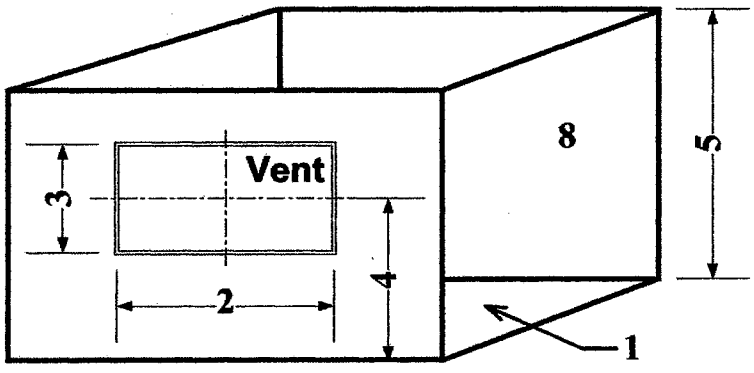

Figure 5. 1 Parameters investigated

Each of following sections show the calculated effect of varying one parameter only while keeping all other parameters at their standard default values. The standard values and the variation of each parameter are generally within the normal range of residential house fires.

5.1.1 Floor Area

Figure 5. 2 shows the effect of varying the floor area (Parameter Number 1) on the calculated time to reach flashover conditions. The floor area of the square room was varied through the range of 4, 9, 16, 25, and 36 m^2 with all other parameters retained at their default values.

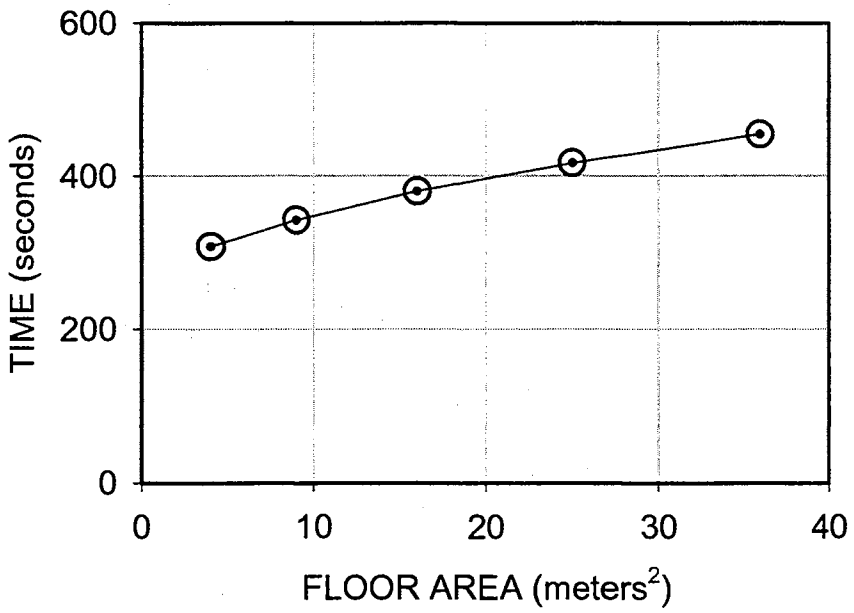

Figure 5. 2 Flashover Time vs. Floor Area

The calculations show that the time required to reach flashover relates to the floor area. In the case of the largest floor area (36 m^2), flashover occurs in about 450 seconds, as compared with the smallest floor area considered (4 m^2) taking about 300 seconds. This result is simply caused by the larger room needing a greater volume of combustion products to be generated in order to fill the larger horizontal space, and also that there is more mixing with cooler air as the smoke layer spreads out across the ceiling.

5.1.2 Vent Width and Height

The vent supplies air (oxidant) which is needed for combustion, so it is interesting to study the effect of vent size on the time to reach flashover conditions. The vent size was changed in two ways, its width and height (Parameter Numbers 2 and 3), while retaining all other parameters at their standard values. Figure 5. 3 and Figure 5. 4 respectively show the results.

The calculations (Figure 5. 3) were performed with the vent width varied over the range 1, 1.5, 2, 3, and 4 m with all other parameters held at their standard values. The vent height was 1 meter (its standard value) in these calculations of the width effect. The other calculation (Figure 5. 4) was performed with a range of different vent heights, varied over 0.5, 1.0, 1.5, and 2.0 m in height, while retaining all other parameters at their standard value, including for example the vent width retained at 2 meters.

These single room calculations of FASTLite conform to the general trends and expectations, which can be obtained directly from the more simplistic empirical equations given in the Babrauskas and Thomas criteria for flashover.

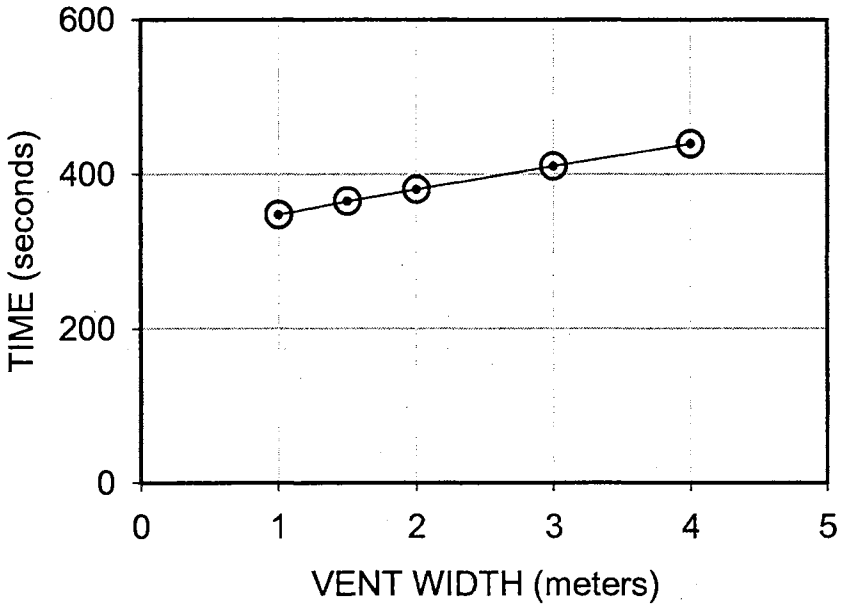

Figure 5. 3 Flashover Time vs. Vent Width

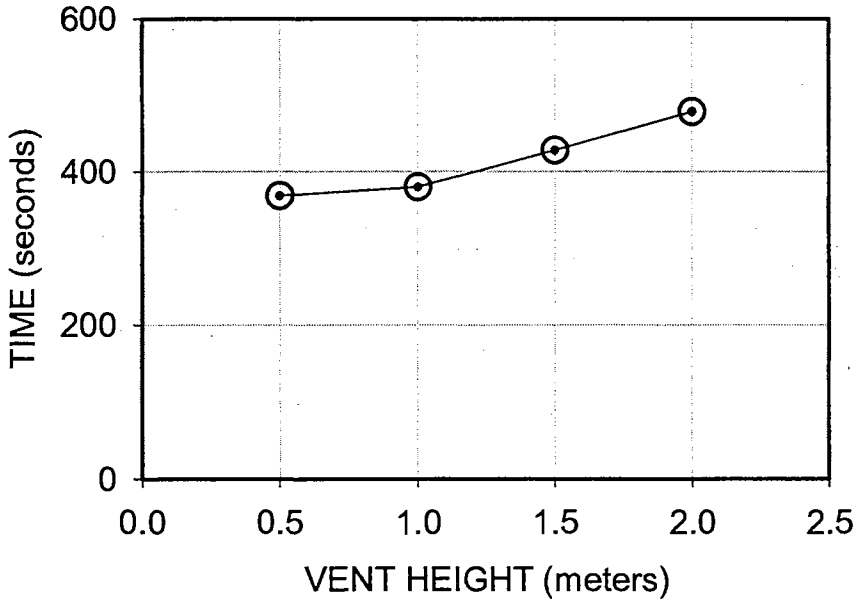

Figure 5. 4 Flashover Time vs. Vent Height

The Babrauskas and Thomas approaches use only information about the vent width, vent height and internal room surface area (in the case of Babrauskas only the first two of these). The trends are that a greater amount of time is required to reach flashover when a larger vent is involved. Almost a linear variation with width and height over the range of values calculated, for the particular standard values of the other parameters defining the problem. Air flowing in and smoke flowing out of vents in walls are also addressed in other parts of the FASTLite computer program.

5.1.3 Vent Height Above Floor

The effect of the vent height above the floor (distance from floor to the mid-point of the vent) is now considered (Parameter Number 4). Varying this distance from 0.5 to 2.0 m in steps of 0.5 meters considers vents, corresponds to vents which range from those touching the floor to those touching the ceiling. Results are plotted in Figure 5. 5, illustrating that the vent height above floor has no effect on the time required to reach flashover conditions (within the confines of the standard values given to other parameters used in the calculations).

5.1.4 Ceiling Height

The effect of the ceiling height (Parameter Number 5), changed from 2.0 to 3.5 m in steps of 0.5 m, with other parameters at their standard values, is shown in Figure 5. 6. Ceiling height is hereby demonstrated to affect only slightly the time to reach flashover.

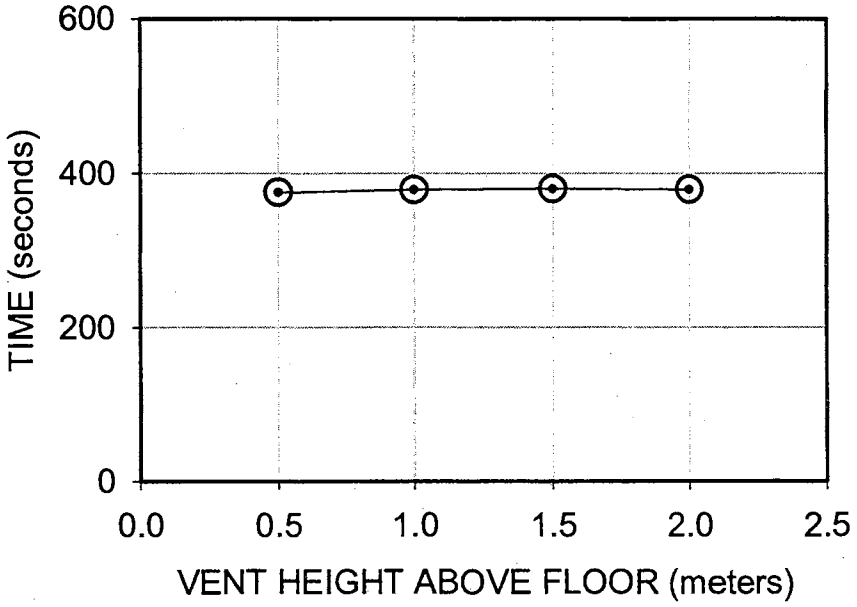

Figure 5. 5 Flashover Time vs. Vent Height above Floor

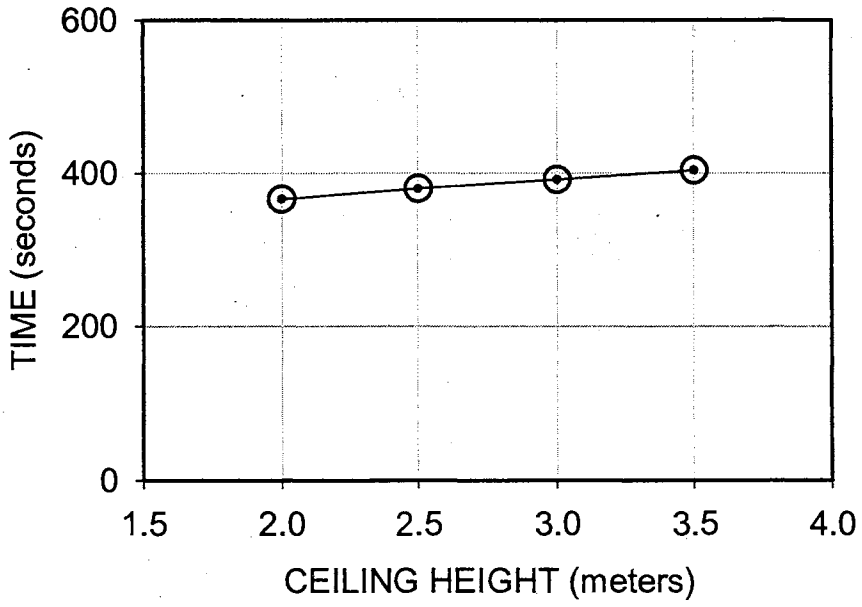

Figure 5. 6 Flashover Time vs. Ceiling Height

5.1.5 Fire Specification

The relationship between the time to reach flashover and the rate of growth of the fire is extremely significant as expected. Slow, medium, fast, and ultra-fast t^2-fire models range over a wide range of fires of practical importance (Parameter Number 6). Medium growth fires are typical of accidental fires (ex, cigarette ignition); fast and ultra-fast fires are typical of accelerated fires and fires involving modern polyurethane-filled furniture. The dramatic effect of fire growth rate is seen in Figure 5. 7. The time to reach flashover for the case of the slow fire growth model is off the scale at about 700 seconds. It is extremely important for reaching flashover how quickly the fire grows. This dramatic effect of fire growth rate on time to reach flashover is seen not only in the calculations given here for the particular values of the other parameters, but also for different values of the other parameters.

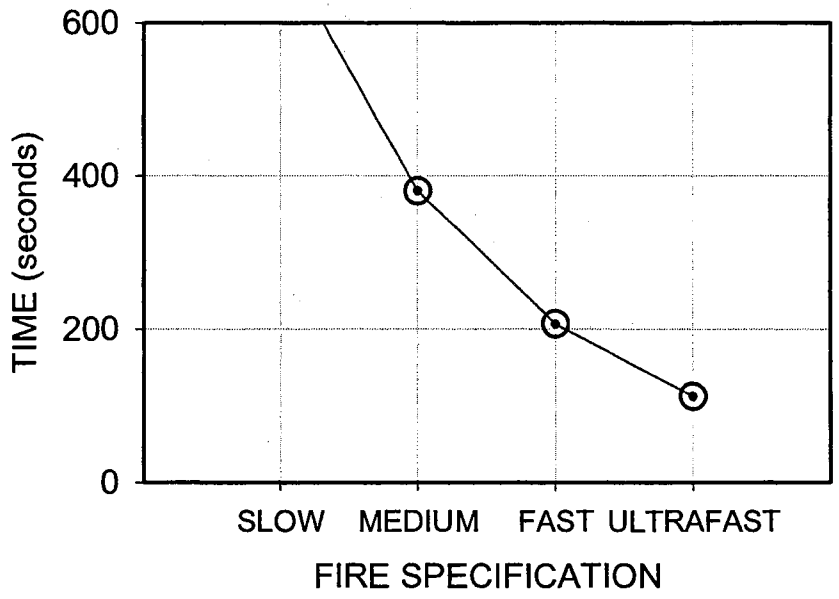

Figure 5. 7 Flashover Time vs. Fire Specification

5.1.6 Fire location

In Figure 5. 8, the result of different fire location is shown, for a fire located in the center of the room, at a side-wall of the room, and in a corner of the room (Parameter Number 7). It is seen that the progressive confinement of the walls (over the three fire locations considered) reduces cooling air entrainment into the fire plume and leads to more rapid temperature rise in the upper smoke layer. This qualitative reasoning explains the results seen in the calculations – that reduced time is required for flashover conditions with corner fires vs. side-wall fires vs. center-room fires.

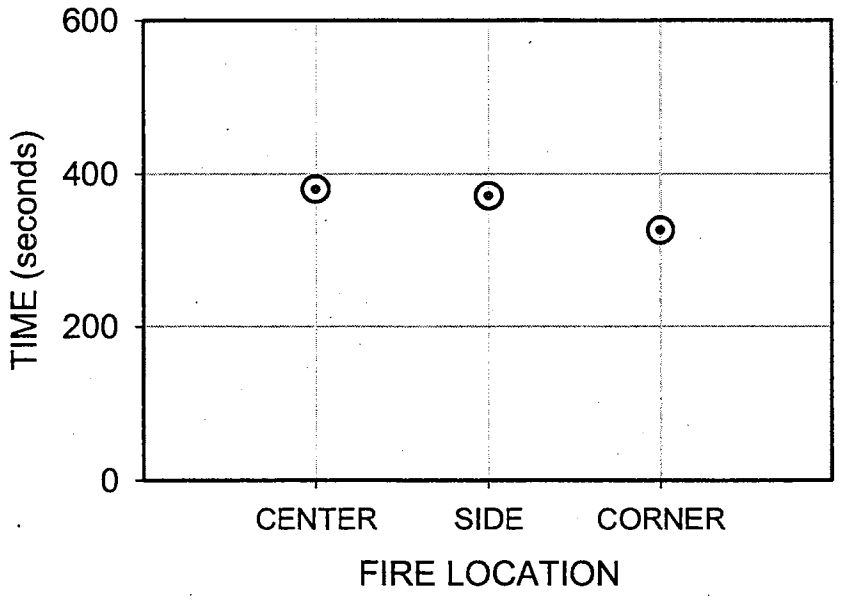

Figure 5. 8 Flashover Time vs. Fire Locaion

5.1.7 Wall and Ceiling Material

Seven wall and ceiling materials were considered, so as to illuminate on the effect of their properties on the time to reach flashover conditions. The array of materials considered here are: gypsum of thickness 1/2", 5/8", and 3/4", common brick 3", light concrete 6", normal concrete 6", and glass fiber 3.5" with properties given in Table 5. 1. Conductivity and the associated property thermal diffusivity (equal to conductivity divided by the product of density times specific heat) is the major parameter affecting heat transfer rates through the material for short time exposures. For longer time exposures, the thickness of the material may also come into play (in fact, when the time exposure is such that the thermal penetration distance exceeds thickness of the material). The effect of the type of material specified on the relatively short time to reach flashover (Parameter Number 8) is shown in Figure 5. 9.

Table 5. 1 The Properties of the Wall and Ceiling Material

Material	Thickness (m)	Conductivity (W/mK)	Specific Heat (J/kgK)	Density (kg/m^3)	Emissivity
Gypsum 1/2"	0.013	0.160	900	790	0.90
Gypsum 5/8"	0.016	0.160	900	790	0.90
Gypsum 3/4"	0.019	0.160	900	790	0.90
Common Brick	0.076	0.720	835	1920	0.90
Light Concrete	0.150	0.125	1050	525	0.94
Normal Concrete	0.150	1.750	1000	2200	0.94
Glass Fiber	0.088	0.040	720	105	0.90

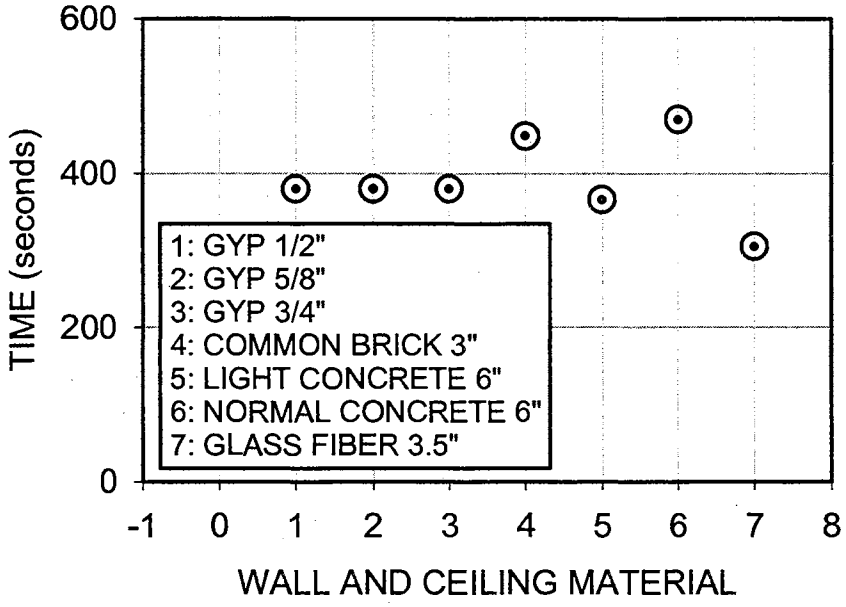

Figure 5. 9 Flashover Time vs. Wall and Ceiling Material

5.1.8 Fire Radiation Fraction

Five different fire radiation fraction values (Parameter Number 9) are considered, which cover a large and exhaustive range (10 to 60 percent of fire heat loss by radiation). Most common fires have radiation heat losses within this range. The effect on the calculated time to reach flashover is given in Figure 5. 10. We observe that the radiation factor has virtually no effect on the time to reach flashover. This may be because the total heat from the fire exhibits itself as heat convected in the plume above the fire and as heat radiated from the fire, and that whatever the particular split is between the two, the

totality of the heat generated is still within the room and affects the temperature in the smoke layer in a very similar fashion.

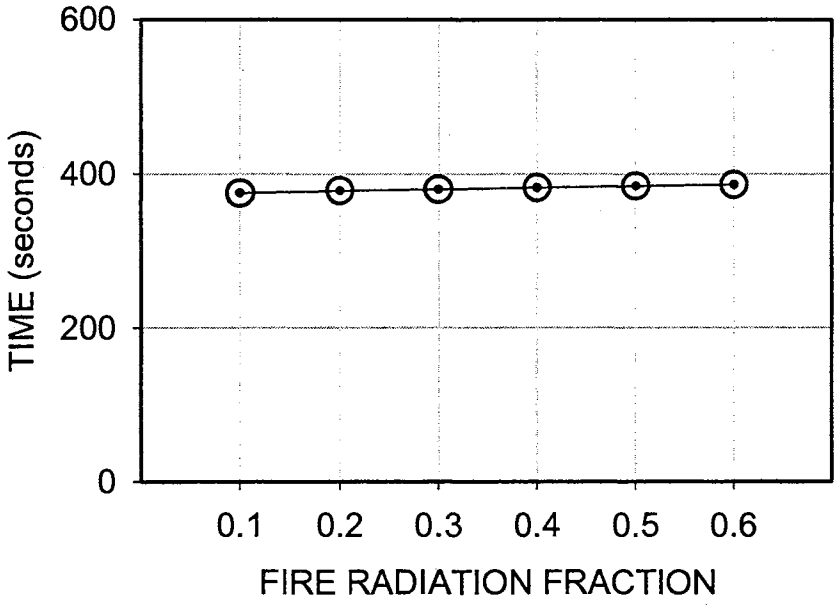

Figure 5. 10 Flashover Time vs. Fire Radiation Fraction

5.1.9 Fire Maximum Heat Release Rate

The effect of specified fire maximum heat release rate (Parameter Number 10) on the time to flashover is covered in Figure 5. 11. When the maximum heat release rate is 1 MW, flashover occurs in about 900 seconds, and this is off the scale. Flashover occurred at about 380 seconds for all the other cases considered, that is, when the maximum heat release rate was 2 MW or greater. The reason for all these times being equal is that, for the values of the other parameters specified, the upper layer temperature reached 600°C (1112°F) during the growth phase of the medium growth rate fire, that is,

before the heat release rate actually reached 2 MW. For other problem parameters (for example, fire growth rate, room size, etc), this may not necessarily be the case.

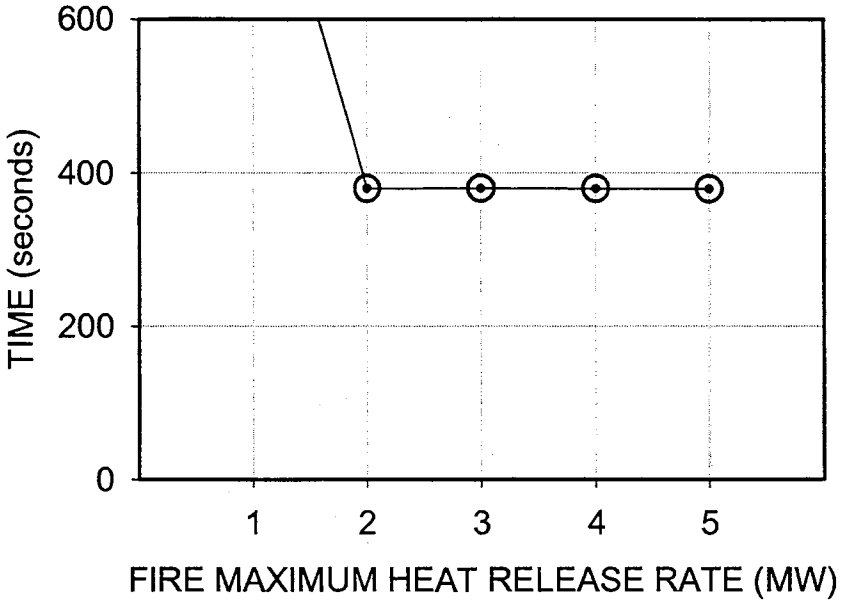

Figure 5. 11 Flashover Time vs. Maximum Heat Release Rate

5.1.10 Multiple Parameter Variations

Above results of sections 5.1.1 through 5.1.10 are indicating the effect of a single parameter change when the other parameters are held their standard (default) values. The standard values and the variation of each parameter are generally within the normal range of residential house fires. Note that, if any of their default values are changed, the effect of variation of a parameter may be different than illustrated above. For example, the effect of vent height above the floor with different widths of the vent might be different than given earlier in section 5.1.3. Also the effect of vent height above the floor

on the time to reach flashover may be more significant with a slower fire growth than the medium (default) growth fire just considered. All these effects are shown in Figure 5. 12.

Time to reach flashover conditions are calculated for a larger vent (3 m wide × 1 m high) and a smaller vent (1 m wide × 1 m high) with two different fire growth rates (i.e. Slow and Medium). The calculated time to reach flashover conditions with different vent heights above floor are then plotted in Figure 5. 12. The vent height above floor has no effect on the time to reach flashover within the confines of the standard values of the other parameters. The vent height also has very little effect on the time to reach flashover in almost all cases, except small effect is found with a larger vent and for a slower growth fire.

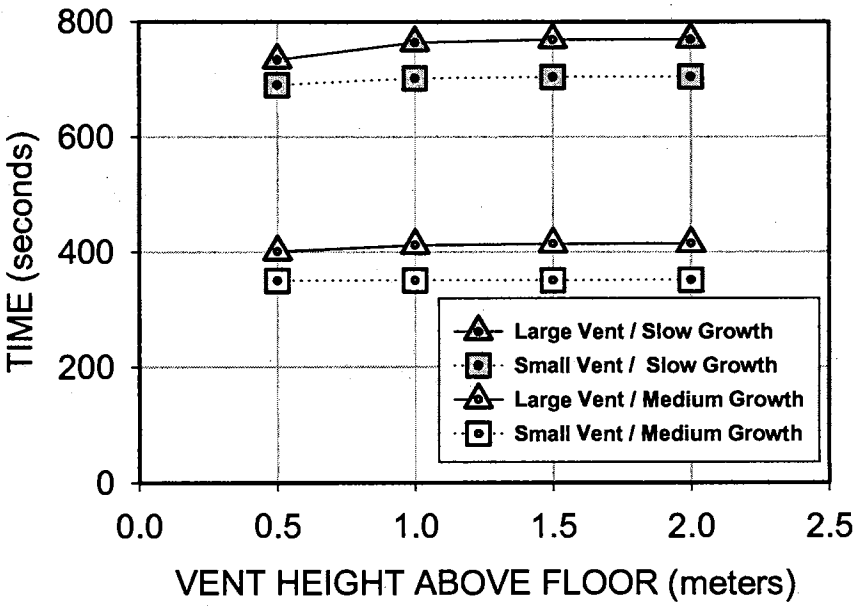

Figure 5. 12 Flashover Time vs. Vent Height above Floor of Different Vent Sizes and Fire Growth Rates

5.1.11 Closure

Flashover is characterized by the rapid transition in fire behavior from localized burning of fuel to the involvement of all combustibles in the enclosure. The objective of the present contribution was to calculate the development of flashover in a typical single room fire, and show the effect of ten key parameters on the time required to reach flashover conditions. It was found that the major parameters affecting flashover were fire growth rate, ventilation opening area, wall and ceiling martial and room area in the normal range of residential fires. The parameters with little effect to the time to reach flashover have been found vent height above the floor, ceiling height, fire location, and fire radiation heat loss fraction in the normal range of residential fires.

5.2 Comparison of Flashover Theories

In this section, a comparison of flashover theories is undertaken using the Thomas, Babrauskas and the FASTLite (CFAST) theories, concentrating on the similarities and differences between the theories in their assessment of the major parameters affecting flashover.

5.2.1 Four Alternative Theories

The time to reach flashover is characterized in the FASTLite computer program by the criterion of the upper layer temperature reaching 600°C (1112°F). The FASTLite (CFAST) computer program single room simulation is used for calculations, and results are compared with the alternative simpler theories of Thomas and Babrauskas.

Calculations to be exhibited are made with these parameters held at their standard (default) values, except those that vary in order to show the parameters effect in the figures and tables. That is, calculations to be exhibited all have vent height = 2 m, ceiling height = 2.4 m, fire location in center of flow, wall and ceiling material to be 0.016 meter (5/8") thick gypsum, fire radiation fraction = 0.3, and fire maximum heat release rate = 3 MW.

During fire growth, conduction heat loss is most pronounced through the ceiling and walls, with little heat loss through the floor. In the Thomas flashover criterion, the total enclosure surface area is used, but the contribution of floor area to the total surface area is sometimes omitted. The calculations will clarify this effect. In the case of the Thomas theory, including the floor area in the total enclosure surface area is indicated by "Thomas 1", while excluding it is indicated by "Thomas 2."

5.2.2 Calculations of Flashover Time

Previous studies (see section 5.2.2 and Kim and Lilley, 1997) have shown that the major parameters affecting flashover are fire growth rate, ventilation opening area, and room area. Hence, the focus of the calculations, and how the various theories differ, will be on precisely these important parameters.

Figure 5. 13 shows the calculation of the time to reach flashover conditions versus fire growth specification and ventilation factor, for a room of floor area 3 x 4 m^2. Figure 5. 14 through Figure 5. 17 show similar calculations with room areas 4 x 6 m^2, 6 x 8 m^2, 8 x 12 m^2 and 12 x 16 m^2 respectively. Notice that the effect of greater room size is to increase the time required to reach flashover, in the case of Thomas and CFAST

theories. It has no effect with the Babrauskas theory, since enclosure surface area does not play a part in the Babrauskas theory. It may also be noted that, as room size increases, the CFAST theory gives very large flashover times, which are at odds with the other theories considered.

These data are conveniently given in Table 5. 2, where fire growth specification, room size, ventilation factor and flashover theory being used are all considered. These four parameters affect strongly the calculated time from inception of the fire to reach flashover conditions. Notice the very large flashover times calculated via the CFAST theory in the case of the largest room area considered. Also notice that Xs in some locations in this table indicates that flashover conditions were never reached in the CFAST computer calculations, for the particular values of largest room size and the two largest ventilation factors considered.

Table 5. 3 gives an indication of the variance between the four flashover theories for each of the situations considered in Table 5. 2. One can thus judge the extent to which the theories differ in their calculation of time to reach flashover conditions. Each line of maximum, minimum, average, and normalized range (= (max− min) / *average*) is obtained via observation of the four "times to flashover" given by the four theories (Thomas 1, Thomas 2, Babrauskas and CFAST) for the one situation of interest. When flashover was not predicted by one of the four theories, the calculation was made on the basis of the other three alone. Slow fire growth with large rooms appear in general to have large discrepancies between the alternate theories, as observable via the "normalized range" values, and cases where flashover was not predicted by one of the theories.

5.2.3 Closure

A comparison of flashover theories was undertaken using the Thomas, Babrauskas and the FASTLite theories, concentrating on the similarities and differences between the theories in their assessment of the major parameters affecting flashover. The time to flashover is reduced with smaller vent size in the wall and faster growing fire. All theories considered correlate with this. With small rooms, all theories give similar calculations of the time to reach flashover. With medium sized rooms, Babrauskas gives shorter times to flashover, as compared with the other theories, especially for small vent sizes. With large sized rooms, Babrauskas gives even shorter times to flashover, as compared with the other theories, and FASTLite gives excessively long times to flashover for the small vent and did not predict the occurrence of flashover with medium and large vents.

Table 5. 2 Calculated time (seconds) to Reach Flashover According to Ventilation Factor, Rapidity of Fire Growth, Room Area (all rooms' heights are 2.4 m) and Four Different Theories [T1 = Thomas 1 theory including floor area in total surface area; T2 = Thomas 2 theory excluding floor area in total surface area; B = Babrauskas theory; CF = CFAST computer calculations to reach 600°C]

Vent factor		6 $m^{5/2}$ (2 m high × 2.12 m wide)				4 $m^{5/2}$ (2 m high × 1.41 m wide)				2 $m^{5/2}$ (2 m high × 0.71 m wide)			
		T1	T2	B	CF	T1	T2	B	CF	T1	T2	B	CF
Slow	3×4	957	940	1239	934	814	794	1012	786	638	613	716	602
	4×6	1009	977	1239	950	874	837	1012	858	714	668	716	747
	6×8	1094	1034	1239	1088	971	903	1012	969	830	749	716	874
	8×12	1237	1129	1239	2041	1129	1010	1012	1283	1010	875	716	1077
	12×16	1464	1277	1239	X*	1374	1174	1012	X*	1278	1060	716	2040
Medium	3×4	479	470	620	467	407	397	506	393	319	307	358	301
	4×6	505	488	620	506	437	418	506	462	357	334	358	411
	6×8	547	517	620	705	486	451	506	545	415	375	358	486
	8×12	618	564	620	1677	565	505	506	916	505	437	358	716
	12×16	732	639	620	X*	687	587	506	X*	639	530	358	1689
Fast	3×4	239	235	239	233	203	198	253	196	160	153	179	151
	4×6	252	244	239	300	218	209	253	250	178	167	179	226
	6×8	274	259	239	524	243	226	253	354	207	187	179	284
	8×12	309	282	239	1500	282	252	253	739	253	219	179	542
	12×16	366	319	239	X*	344	293	253	X*	320	265	179	1518
Ultra-Fast	3×4	120	118	120	117	102	99	127	98	80	77	89	75
	4×6	126	122	120	208	109	105	127	145	89	83	89	123
	6×8	137	129	120	437	121	113	127	264	104	94	89	193
	8×12	155	141	120	1418	141	126	127	653	126	109	89	457
	12×16	184	160	120	X*	172	147	127	X*	160	132	89	1432

* X indicates that flashover conditions is never reached.

Table 5. 3 Indication of the Variance between the Four Flashover Theories for each of the Situations Considered in Table 5. 2

Vent factor		$6\ m^{5/2}$ (2 m high × 2.12 m wide)				$4\ m^{5/2}$ (2 m high × 1.41 m wide)				$2\ m^{5/2}$ (2 m high × 0.71 m wide)			
		Max.	Min.	NR*	Ave.	Max.	Min.	NR*	Ave.	Max.	Min.	NR*	Ave.
Slow	3×4	1239	934	0.30	1018	1012	786	0.27	851	716	602	0.18	642
	4×6	1239	950	0.28	1044	1012	837	0.20	895	747	668	0.11	711
	6×8	1239	1034	0.18	1114	1012	903	0.11	964	874	716	0.20	792
	8×12	2041	1129	0.65	1411	1283	1010	0.25	1108	1077	716	0.39	919
	12×16	1464	1239	0.17	1327	1374	1012	0.31	1187	2040	716	1.04	1273
Medium	3×4	620	467	0.30	509	506	393	0.27	426	358	301	0.18	321
	4×6	620	488	0.25	530	506	418	0.19	456	411	334	0.21	365
	6×8	705	517	0.31	597	545	451	0.19	497	486	358	0.31	408
	8×12	1677	564	1.28	870	916	505	0.66	623	716	358	0.71	504
	12×16	732	620	0.17	663	687	506	0.31	593	1689	358	1.66	804
Fast	3×4	239	233	0.03	237	253	196	0.27	213	179	151	0.18	161
	4×6	300	239	0.24	259	253	209	0.19	233	226	167	0.31	187
	6×8	524	239	0.88	324	354	226	0.48	269	284	179	0.49	214
	8×12	1500	239	2.16	583	739	252	1.27	382	542	179	1.22	298
	12×16	366	239	0.41	308	344	253	0.31	297	1518	179	2.35	570
Ultra-Fast	3×4	120	117	0.02	118	127	98	0.27	106	89	75	0.18	80
	4×6	208	120	0.61	144	145	105	0.34	121	123	83	0.41	96
	6×8	437	120	1.54	206	264	113	0.97	156	193	89	0.86	120
	8×12	1418	120	2.83	458	653	126	2.01	262	457	89	1.88	196
	12×16	184	120	0.42	154	172	127	0.30	148	1432	89	2.96	454

* NR = normalized range = (Max - Min)/Average

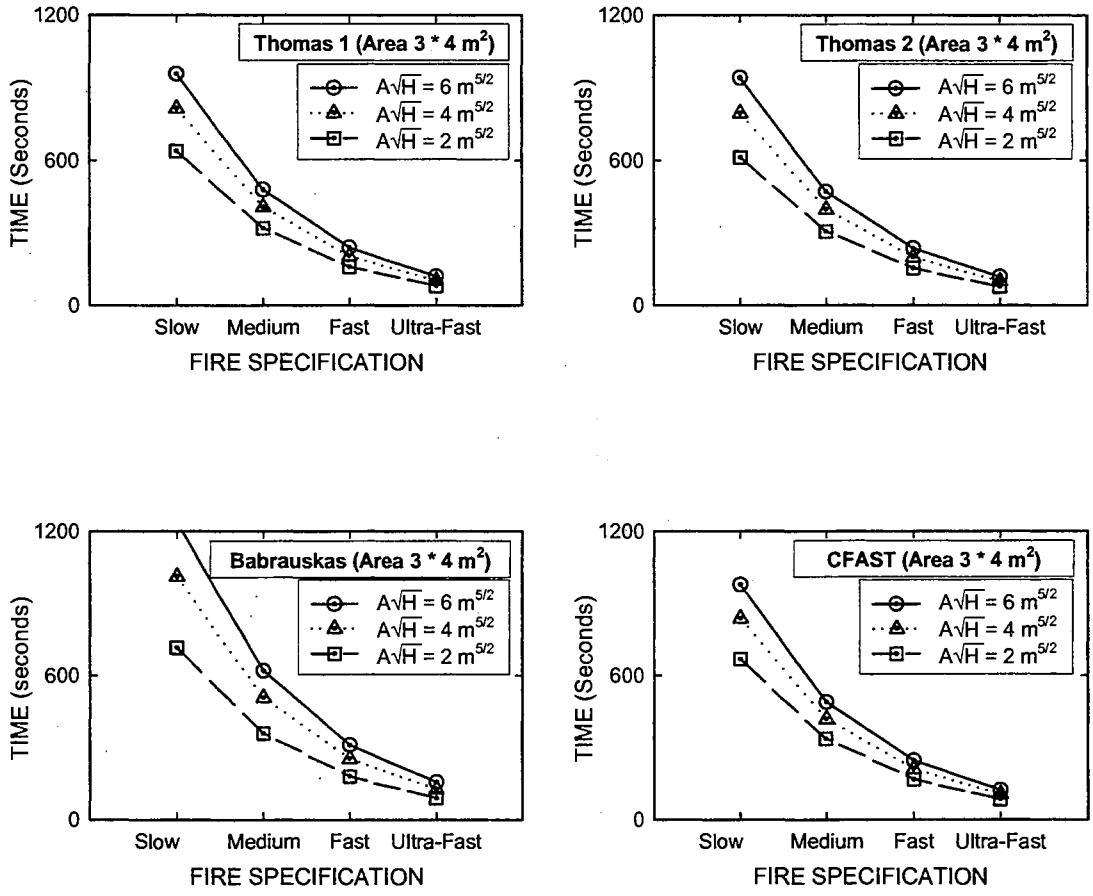

Figure 5. 13 Time to Reach Flashover Conditions Versus Fire Growth Specification and Ventilation Factor, for a Room of Area 3 x 4 m^2

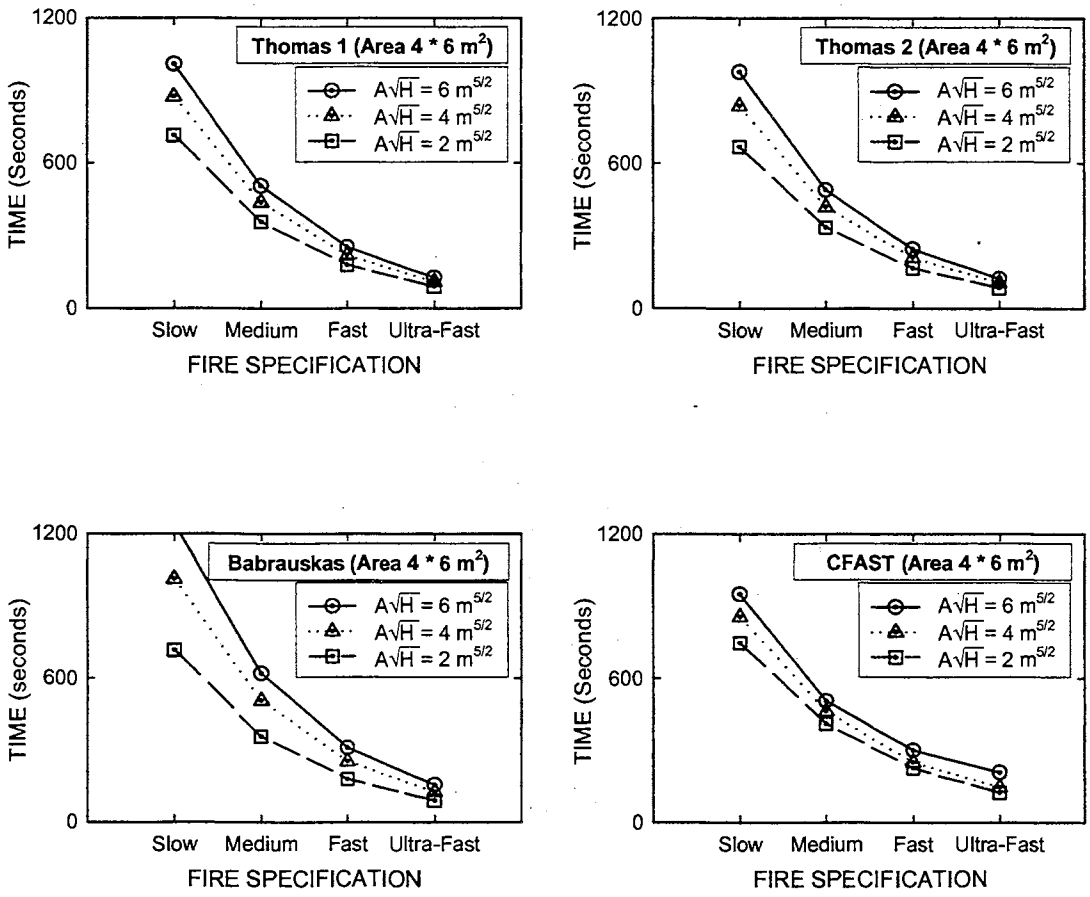

Figure 5. 14 Time to Reach Flashover Conditions Versus Fire Growth Specification and Ventilation Factor, for a Room of Area 4 x 6 m^2

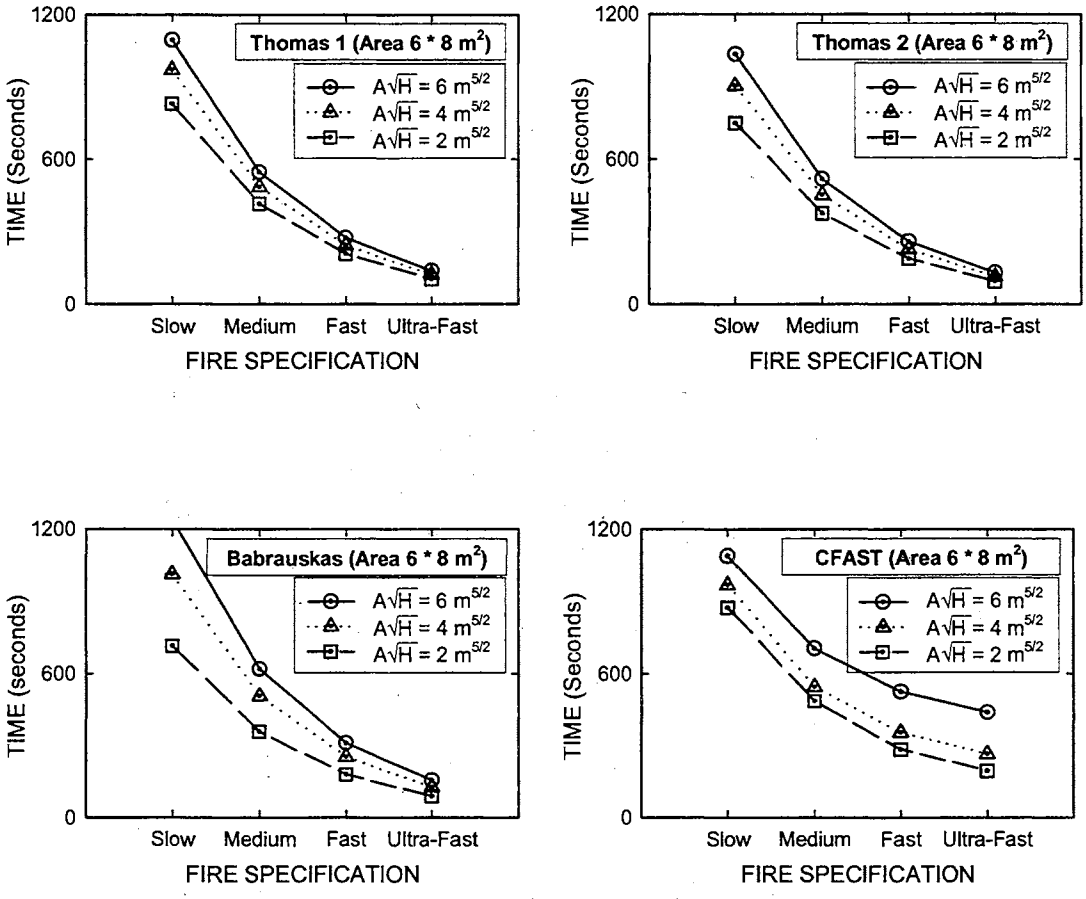

Figure 5. 15 Time to Reach Flashover Conditions Versus Fire Growth Specification and Ventilation Factor, for a Room of Area 6 x 8 m^2

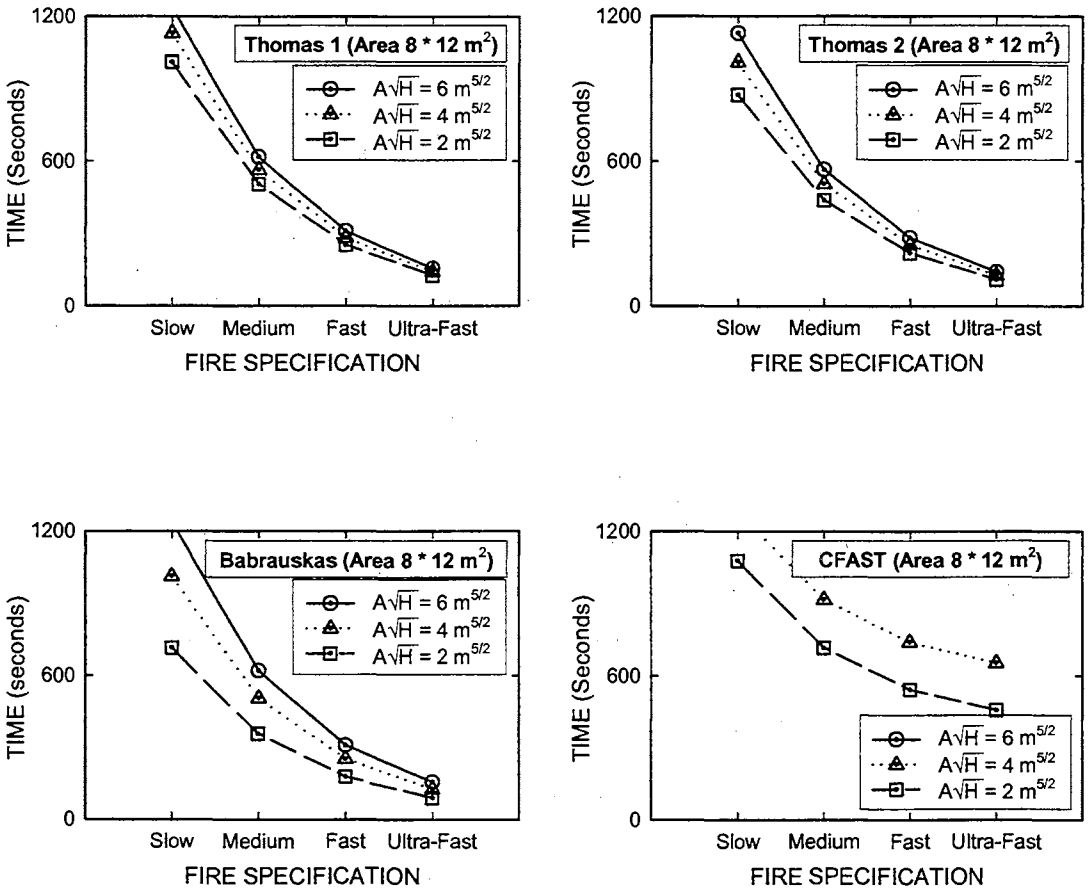

Figure 5. 16 Time to Reach Flashover Conditions Versus Fire Growth Specification and Ventilation Factor, for a Room of Area 8 x 12 m^2

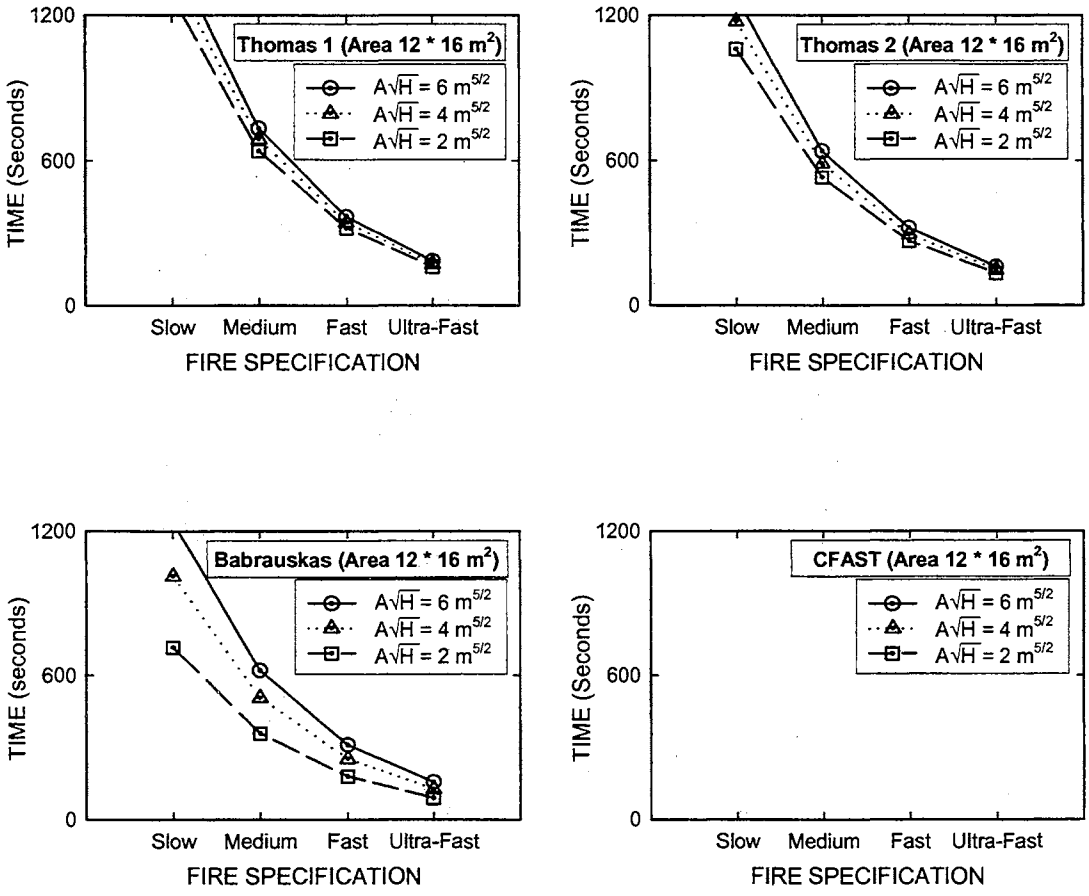

Figure 5. 17 Time to reach flashover conditions versus fire growth specification and ventilation factor, for a room of area 12 x 16 m^2

5.3 Burning Rates of Typical Items

Computer codes are available that permit calculations to be made of the effect of a given specified fire on the subsequent environment in a structural fire. Things like temperature of the smoke layer, its depth from the ceiling downwards, its optical density, ceiling, wall and floor temperatures, floor surface heat flux rate, etc are calculated a function of time in all the rooms of a typical multi-room structural fire. However, the accuracy of these calculations is strongly dependent upon the correctness of the initial fire specifications. This section deals with how we can model a fire specification from experimental heat release data.

5.3.1 The t^2-fire Growth Simulation

Emphasis is often placed on the growth phase of the fire. Slow, medium, fast and ultra-fast fire growths may be specified by the t^2-fire growth model, where, after an initial incubation period,

$$\dot{Q} = \alpha_f (t - t_0)^2 \qquad (5.1)$$

where α_f is a fire-growth coefficient (kW/s^2) and t_0 is the length of the incubation period (s). The coefficient α_f appears to lie in the range 10^{-3} kW/s^2 for very slowly developing fires to 1 kW/s^2 for very fast fire growth. The incubation period (t_0) will depend on the nature of the ignition source and its location, but data are now becoming available (see Babrauskas, 1995) on fire growth rates on single items of furniture

(upholstered chairs, beds, etc.) which may be quantified in these terms. Suggested values for the coefficient α_f are also given in the formula section of Makefire - a subset of the FPETool Computer Program. The specification there for the fire-growth coefficient α_f (kW/s^2) is:

Slow	0.002778 kW/s^2
Medium	0.011111 kW/s^2
Fast	0.044444 kW/s^2
Ultra-fast	0.177778 kW/s^2

and these correspond to growth times of the fire from zero size to 1 MW total heat output in

Slow	600 seconds
Medium	300 seconds
Fast	150 seconds
Ultra-fast	75 seconds

5.3.2 Characterization of Experimental Data Using Five Parameters

Experimental furniture calorimeter data are available for a variety of items, giving heat release rate $\dot{Q}$ (kW) vs. time (seconds). Each of these tables is in conformity with several parameters that completely characterize the situation, as given in Figure 5. 18:

t_0 = time to the onset of ignition

t_{1MW} = time to reach 1 MW

t_{lo} = level-off time

t_d = time at which $\dot{Q}$ decay begins

t_{end} = time at which $\dot{Q}$ equals zero

Notice that both the ascent and decent are characterized by t^2-fire activity:

$$\dot{Q} = \alpha_g (t - t_0)^2 \tag{5.2}$$

$$\dot{Q} = \alpha_d (t_{end} - t)^2 \tag{5.3}$$

where α_g and α_d are the fire-growth and fire-decay coefficients (kW/s^2), respectively.

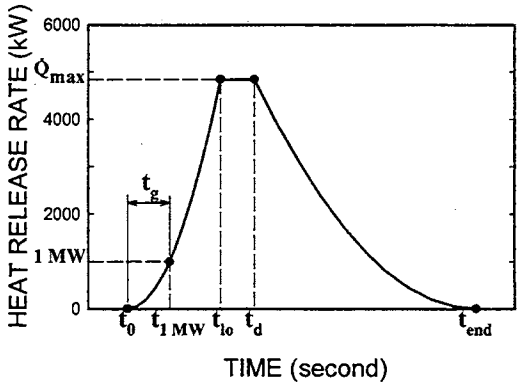

Figure 5. 18 Heat Release Rate vs. Time in t^2-fire Characterization

These heat release rates $\dot{Q}$ (in kW) vs. time t (in seconds) are active only in the growth $(t_0 \le t \le t_{lo})$ and decay $(t_d \le t \le t_{end})$, respectively. The maximum heat release rate $\dot{Q}_{\max}$ (kW) occurs when $t_{lo} \le t \le t_d$. The growth time to reach 1 MW = 1,000 kW of heat release rate $\dot{Q}$ is $t_{1MW} - t_0$ seconds, and this is related to the fire-growth parameter α_g (kW/s^2) via

$$\alpha_g = \frac{1000}{(t_{1MW} - t_0)^2} \tag{5. 4}$$

Similarly the fire-decay parameter α_d (kW/s^2) is found via

$$\alpha_d = \frac{\dot{Q}_{max}}{(t_{end} - t_d)^2} \tag{5. 5}$$

Also note that the maximum heat release rate $\dot{Q}_{\max}$ (kW) is related to other parameters via:

$$\dot{Q}_{\max} = 1000\left[\frac{t_{lo} - t_0}{t_{1MW} - t_0}\right]^2 \tag{5. 6}$$

In order to characterize in the above fashion the actual experimental data of heat release rate versus time, one proceeds as follows:

1. First, one decides the values to be taken for the three key parameters $\dot{Q}_{\max}$ (maximum heat release rate), t_{lo} (time to reach $\dot{Q}_{\max}$) and t_d (time to start decay). Adjustments are made in order to ensure that the modeled total heat release during the time interval of from t_0 to t_d seconds matches the experiment to within 1 % for most items (within 5 % for all items).

2. Then, the time to onset of ignition t_0 with associated value of fire-growth parameter α_g is chosen so as to match the total heat release during the growth phase of from t_0 to t_{lo} seconds. The correspondence of t_0, t_{lo} and α_g is automatic since a t^2-fire growth is being assumed.

3. Finally, the end time t_{end} with associated value of fire-decay parameter α_d is chosen so as to match the total heat release during the decay phase of from t_d to t_{end} seconds. Again, the correspondence of t_d, t_{end} and α_d is automatic since a t^2-fire decay is being assumed.

Figure 5. 19 shows an example of t^2-fire characterization of an item (Chair 5 in Table 5. 5). Modeled data are given for heat release rate $\dot{Q}$ (kW) vs. time (seconds) in figures of Kim and Lilley (2000a). Careful perusal and interpretation of the figures will enable the discerning reader to deduce what the values of the defining parameters are. However, for completeness, the data are given directly in Table 5. 4 through Table 5. 7 respectively as follows:

1. Furniture calorimeter data from FASTLite (see Portier et al, 1996).
2. Furniture calorimeter data from HAZARD (see Peacock et al, 1994).
3. Furniture calorimeter data from Building and Fire Research Laboratory (see BFRL Website, 1999).
4. Cone calorimeter data from HAZARD (see Peacock et al, 1994).

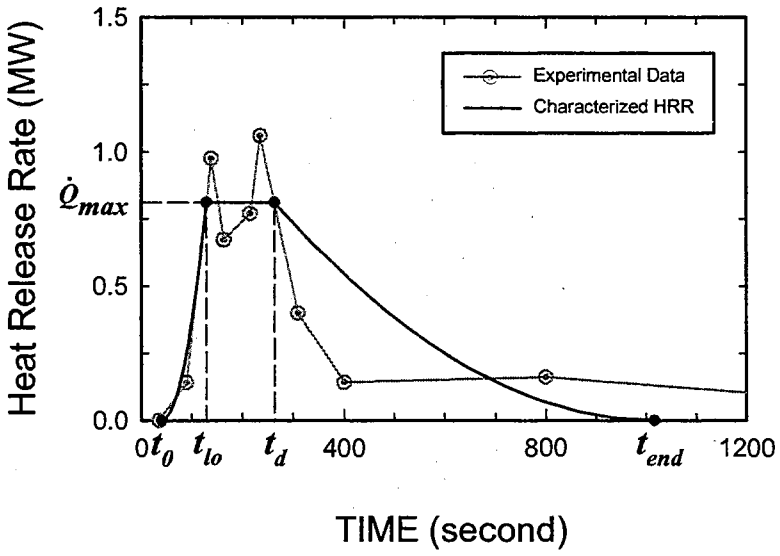

Figure 5. 19 An Example of t^2-fire Characterization (Chair 5 in Table 5. 5)

Finally $\dot{Q}$ vs. t is given by

$$\dot{Q} = 0 \qquad 0 \le t \le t_0 \tag{5. 7}$$

$$\dot{Q} = \alpha_g (t - t_0)^2 \qquad t_0 \le t \le t_{lo} \tag{5. 8}$$

$$\dot{Q} = \alpha_g \left(t_{lo} - t_0\right)^2 \qquad t_{lo} \le t \le t_d \tag{5.9}$$

$$\dot{Q} = \alpha_d \left(t_{end} - t\right)^2 \qquad t_d \le t \le t_{end} \tag{5.10}$$

$$\dot{Q} = 0 \qquad t_{end} \le t \le \infty \tag{5.11}$$

with the parameters taken directly from the tables for the particular item under consideration.

5.2.3 Closure

The ability to determine fire growth in terms of when the second and subsequent objects may ignite (and their burning rates) and whether or not "flashover" occurs depends strongly on the initial fire specification. The focus of this entire document was to characterize the initial item on fire (in terms of burning rate versus time) so as to more accurately be able to calculate fire growth and the possible occurrence of flashover.

Heat release rates of typical items in fires were needed as a prerequisite for estimating fire growth and temperatures in structural fires. That is, these burning rates were required to be specified by the user as input to single-room and multi-room structural fire computer codes like CFAST, FASTLite, FPETool and HAZARD. Data was given here that permit burning items to be specified in a permit burning items to be specified in a useful modeled way, taking a t^2-fire for the growth and decay periods, with a constant maximum heat release rate between these two periods.

Table 5. 4 Heat Release Rate vs. Time in t^2-fire Characterization of FASTLite Data

CODE	DESCRIPTION	t_0	t_{1MW}	t_{lo}	t_d	t_{end}
Wardrobe 1	1/2" Plywood wardrobe, clothing on 16 hangers	0	35	60	90	500
Wardrobe 2	1/8" Plywood wardrobe, clothing on 16 hangers	0	40	100	110	140
Wardrobe 3	1/8" Plywood wardrobe, FR paint, clothing on 16 hangers	0	30	70	80	400
Wardrobe 4	1/8" Plywood wardrobe, FR paint, clothing on 16 hangers	0	90	150	160	450
Wardrobe 5	3/4" Particle-board wardrobe, thin plastic coating	0	150	170	670	2000
Chair 1	Chair, one-piece wood-reinforced urethane foam	0	1000	650	660	1900
Chair 2	Chair, polypropylene foam frame, urethane foam, polyolefin fabric	0	100	140	160	500
Chair 3	Chair, thin wood frame, California foam, polyolefin fabric	0	200	175	176	900
Chair 4	Chair, urethane foam frame, urethane foam, polyolefin fabric	0	60	60	210	430
Chair 5	Chair, wood frame, California foam, Haitian cotton fabric	0	350	275	475	1000
Chair 6	Chair, wood frame, California foam, polyolefin fabric	0	50	70	90	315
Chair 7	Chair, wood frame, FR cotton stuffing, Haitian cotton fabric	0	2000	210	310	1000
Chair 8	Chair, wood frame, FR cotton stuffing, polyolefin fabric	0	400	275	475	1000
Chair 9	Chair, wood frame, urethane foam, cotton fabric	0	200	90	310	550
Chair 10	Chair, wood frame, urethane foam, cotton fabric	0	75	50	250	1250
Chair 11	Chair, wood frame, urethane foam, cotton fabric, polyester batting	0	425	347	367	1000
Chair 12	Chair, wood frame, urethane foam, polyolefin fabric	0	80	160	170	420
Chair 13	Chair, wood frame, urethane foam, quilted cotton/polyolefin, polyester batting	0	200	187	200	500
Bed	Innerspring mattress and boxspring, cotton felt/urethane/sisal spring cover	0	1100	680	1080	1300
Lounge chair 1	Lounge chair, metal frame, urethane foam, plastic-coated fabric	0	350	170	220	350
Lounge chair 2	Lounge chair, one-piece molded glass fiber, metal legs	0	120	20	21	150
Lounge chair 3	Lounge chair, one-piece molded thermoplastic	0	275	230	430	900
Lounge chair 4	Lounge chair, wood frame, latex foam/cotton stuffing, plastic-coated fabric	0	500	130	140	300
Loveseat 1	Loveseat, mixed foam and cotton batting stuffing, cotton fabric	0	400	350	400	2000
Loveseat 2	Loveseat, wood frame, California foam, polyolefin fabric	0	80	130	160	400
Loveseat 3	Loveseat, Wood frame, urethane foam, plastic-coated fabric	0	350	330	430	1500
Metal wardrobe 1	Metal wardrobe, clothing on 16 hangers	0	250	125	150	500
Metal wardrobe 2	Metal wardrobe, clothing on 8 hangers	0	50	40	47	200
Patient lounge chair	Patient lounge chair, metal frame, urethane foam cushion	0	170	80	90	150
Sofa 1	Sofa, metal frame, urethane foam, plastic-coated fabric	0	500	260	460	800
Sofa 2	Sofa, wood frame, California foam, polyolefin fabric	0	100	170	250	430

Table 5. 5 Heat Release Rate vs. Time in t^2-fire Characterization of HAZARD Data (Furniture Calorimeter)

CODE	DESCRIPTION	t_0	t_{1MW}	t_{lo}	t_d	t_{end}
Bed 1	Double bed,bedding,night table;gyp bd walls;test R1 (85-2998)	169	211	230	230	936
Bed 2	Double bed,bedding,night table;plywood walls;test R5 (85-2998)	164	239	360	430	998
Chair 1 (F21)	Upholstered chair,F21,wood frame,pu foam-fr,olefin	126	218	260	260	607
Chair 2 (F23)	Chair,F23,wood frame,fr cotton batting,olefin test 24 (82-2604)	0	538	450	450	1932
Chair 3 (F25)	Upholstered chair,F25,wood frame,pu foam,olefin,test 29	106	215	260	260	679
Chair 4 (F28)	Uphols.chair,F28,wood frame,pu/pe/ctn bedding,cotton test 28	82	478	420	420	1184
Chair 5 (F30)	Uphols.chair,F30,pu frame,pu foam,olefin,test 30 (82-2604)	40	140	130	263	1017
Chair 6	Bean bag chair,vinyl/ps foam beads,c05 nbs tn 1103	88	748	545	718	1228
Chair 7	Chair,molded flexible pu frame,pu cover test 64 (83-2787)	644	1662	1330	1330	2685
Chair 8	Easy chair,molded ps foam frame,pu pad&cover,c07,test 48	38	245	240	240	883
Christmas Tree	Christmas tree,spruce,dry, vtt 285,no.17	290	327	320	350	478
Cooking Oil	Cooking Oil,Corn;Cottonseed;Etc In 12in.Pan	0	15	5	1000	1000
Curtain	Curtain,Cotton,0.31kg/M2,Item 9	123	229	175	175	411
Loveseat (F31)	Loveseat,F31,wood frame,pu foam(fr),olefin test 37 (82-2604)	71	165	229	249	701
Mattress 1	Mattress,m05,pu foam,rayon ticking,bedding	269	437	480	480	933
Mattress 2	Mattress+boxspring(westchase hilton) test 67 (83-2787)	144	858	606	980	2233
Sofa (F32)	Upholstered\sofa,F32,wood\frame,pu foam-fr,olefin test 38	74	154	211	283	651
Trash Bags	Trash bags (3),paper	0	100	58	111	517
TV Set	Television set,b/w,wood cabinet,exp.3	304	984	670	670	1872
Wardrobe	Wardrobe closet,plywood,fr paint nbsir83-2787 test 42	70	113	170	170	358
Waste Basket	Wastepaper basket,polyethylene,milk cartons,exp.7	115	2034	350	350	1264

Table 5. 6 Heat Release Rate vs. Time in t^2-fire Characterization of Building and Fire Research Laboratory Data

CODE	DESCRIPTION	t_0	t_{1MW}	t_{lo}	t_d	t_{end}
Bunk Bed	BFRL* in February 1996.	186	211	240	240	445
Koisk	Western Fire Center in the summer of 1995.	817	1129	1230	1230	3300
Loveseat		48	222	350	371	866
Mattress (Center)	BFRL in February 1996.	9	173	145	219	959
Mattress (Corner)	BFRL in February 1996.	85	294	295	321	484
Small Dresser	BFRL in February 1996.	112	346	423	423	870
Sofa		26	222	390	399	931
Wooden Pallet	BFRL in February 1996.	0	467	634	664	1616
Workstation (2 panels)	Sponsored by GSA** and performed at BFRL in 1991.	132	244	280	280	3276
Workstation (3 panels)	Sponsored by GSA and performed at BFRL in 1991.	283	386	550	550	1142

* BFRL – Building and Fire Research Laboratory

** GSA – General Services Administration

Table 5. 7 Heat Release Rate vs. Time in t^2-fire Characterization of HAZARD Data (Cone Calorimeter)

CODE	DESCRIPTION	t_0	t_{1MW}^*	t_{lo}	t_d	t_{end}
Cotton Fabric	Cotton fabric,fr (test 803a), Fabric	29	89	45	45	206
Fir Board	Douglas fir (828), Board	2	32	15	15	1502
Fir Plywood Board 1	Douglas fir plywood,1/2in.thick (435), Board	74	124	92	604	1193
Fir Plywood Board 2	Douglas fir plywood,1/2in.thick (446), Board	0	28	13	309	1829
Gypsum Board 1	Gypsum board,1/2in.thick (434)	228	280	243	246	274
Gypsum Board 2	Gypsum board,1/2in.thick (448)	6	66	30	30	102
Mattress Composite	Mattress ass'y m05,pu foam,rayon ticking (test 296), Composite	8	44	28	111	164
Oak Board 1	Red oak,7/8in.thick (1454)	156	191	166	1684	2310
Oak Board 2	Red oak,7/8in.thick (1456), Board	0	26	11	707	1802
Oak Board 3	Red oak,7/8 in.thick (1468) , Board	0	28	13	806	1354
Pine Board 1	Pine (838) , Board	14	19	16	637	940
Pine Board 2	Pine (842) , Board	111	198	137	834	1511
Pine Board 3	White pine (wood),0.75 in (test 487) , Board	0	8	3	587	4048
Pine Board 4	White pine (wood),0.75 in (test 493) , Board	40	67	47	1097	4176
PMMA Sheet 1	PMMA 1" black (cb) w/frame (test 1461), Sheet	0	123	115	804	1032
PMMA Sheet 2	PMMA 1" black (cb) w/frame (test 1470), Sheet	148	218	197	1689	2240
Polyisocyanurate Foam 1	Rigid polyisocyanurate foam,2 in (test 438), Foam	0	40	9	9	61
Polyisocyanurate Foam 2	Rigid polyisocyanurate foam,2 in (test 449) , Foam	0	15	6	6	1127
Polystyrene Foam	Polystyrene foam,2 in (test 437) , Foam	84	268	201	201	417
Polyurethane Foam 1	Flexible polyurethane foam,fr,2 in (test 725) , Foam	15	112	80	80	158
Polyurethane Foam 2	Rigid polyurethane foam,gm-29/gm-30 (test 257) , Foam	0	33	15	15	260
Polyurethane Foam 3	Rigid polyurethane foam,fr,gm-31 (test 258) , Foam	0	36	12	12	115
Polyvinyl Sheet	Polyvinyl chloride,0.5 in thick (test 333), Sheet	12	102	37	703	768
Rayon Fabric	Rayon fabric (test 804a), Fabric	26	73	40	40	71
Wool Fabric	Wool fabric/neoprene padding (test 722), Composite	23	62	45	45	167
Cotton Fabric	Cotton fabric,fr (test 803a), Fabric	29	89	45	45	206
Fir Board	Douglas fir (828), Board	2	32	15	15	1502
Fir Plywood Board 1	Douglas fir plywood,1/2in.thick (435), Board	74	124	92	604	1193
Fir Plywood Board 2	Douglas fir plywood,1/2in.thick (446), Board	0	28	13	309	1829
Gypsum Board 1	Gypsum board,1/2in.thick (434)	228	280	243	246	274
Gypsum Board 2	Gypsum board,1/2in.thick (448)	6	66	30	30	102

* In this table, t_{1MW} refers to the time to reach 1 MW/m^2.

5.4 Temperature and Smoke Prediction in a Small House Fire

Temperature and smoke level predictions in several rooms of a structural fire are possible with a variety of available computer codes. The accuracy and applicability of the results are greatly enhanced though the comparison of the calculations with experimental data. Experimental work assists in understanding fire behavior in structural fires. Temperature measurements at different locations during a house fire provide necessary data for the development of mathematical models, which attempt to simulate the fire on a computer. In this section, a small 46 square meters single-level house (Tulsa, Oklahoma) was the subject of a complete experimental burn, with temperature measurements and fire observations during the entire burn. The CFAST computer code is used to calculate temperatures and smoke levels in the various rooms of the house during the burn. Seven fire scenarios are considered in the simulation. The first five scenarios progressively increase realism regarding the actual fire specification, and they establish a methodology for fire simulation in which flashover occurrence, window breakout and fire initiation in the next room occurs in a sequential fashion. Thus, the fire spreads and grows through the structure. The last two scenarios are added to illustrate the effect of the specified maximum heat release rate on the calculations.

The experimental facility is described, followed by discussion about instrumentation, temperature measurement technique, and experimental results. The prediction method and computational results follow, including important events in the fire, flashover in the sequence of rooms, and smoke temperature and smoke layer heights. Computational results give the expected trends (deduced from local point

temperature measurements) of initial temperature surge, rate of general temperature rise in the upper layer, peak and leveling off temperatures, and time to reach flashover in each room. Noteworthy conclusions are then presented.

5.4.1 The Experiment

A small 46 square meters single-level house (Tulsa, Oklahoma) was selected as the experimental facility. The house was of relatively cheap, simple construction, with 0.1 meters thick wood frame walls, and composition shingle pitch roof. The floor plan is seen in Figure 5. 20 with north direction to the top. Rooms 1, 2, 3, and 4 correspond to the bedroom, living room, kitchen/dining room, and utility, respectively. The two rooms (Room 5 and 6) to the west of the bedroom are a clothes closet and bathroom.

The house was only partially furnished. The fuel load was very light. Room 1 contained only a double-bed mattress and box-spring set located along the east wall. Room 2 contained a 2-seater couch along the south wall, a single chair on the west wall, and a TV set in the NE corner. The kitchen/dining area (Room 3) contained standard items below the counter top, wood cabinets above, a spare range/oven appliance, a 3-seater couch, and a bean bag. Finally, the utility (Room 4) contained a wood crib and a washing machine. Rooms 1 and 2 were thinly carpeted; Rooms 3 and 4 had linoleum-covered floors. All external windows and doors were closed, except for the utility exit door to the outside, which permitted smoke to exit near the top and fresh air to enter near the bottom. All internal doors were open.

In the complete burn, the temperatures of each room was measured with nine well-insulated K-type thermocouples, which were located as given in Table 5. 8. All

thermocouples (TCs from here on) were positioned at least 0.15 meters away from nearby surfaces. Their positions are illustrated in Figure 5. 20. They were attached as follows:

TC 1 - to curtain rail of the window
TC 2 - to handle of the open door
TC 3 - to outlet socket
TC 4 - to curtain rail of the window
TC 5 - to outlet socket
TC 6 - to SE corner of upper cabinets
TC 7 - to NW corner of spare oven range
TC 8 - to light fixture in ceiling
TC 9 - to outlet socket

Table 5. 8 Thermocouple Locations (Small House at Tulsa, OK)

Room	TC #	Location
Room 1 (Bedroom)	1	0.3 meters from ceiling
	2	1.2 meters from floor
	3	0.3 meters from floor
Room 2 (Living)	4	0.3 meters from ceiling
	5	0.3 meters from floor
Room 3 (Kitchen)	6	0.3 meters from ceiling
	7	0.3 meters from floor
Room 4 (Utility)	8	0.3 meters from ceiling
	9	0.3 meters from floor

The well-insulated K-type thermocouples (chromel-alumel) permitted temperatures up to 1375 °C (2507 °F) to the measured with high accuracy and without thermal damage to the wires and insulation. The thermocouple measurement stations were wired to the external temperature measuring instruments positioned about 20 meters to the NW of the structure. Unfortunately, thermocouple TC 8 fell down and was then covered with ceiling material in the early stages of the fire, so the upper layer temperature of room 4 is not available.

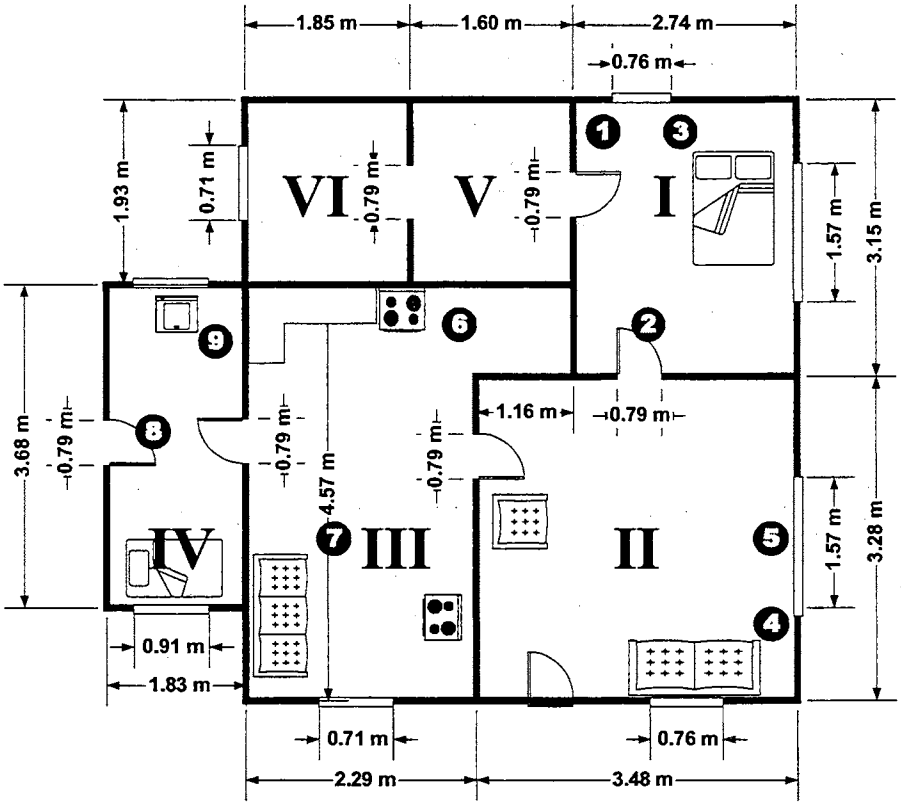

Figure 5. 20 Floor Plan of the Structure Indicating Room Numbers and Thermocouple Locations (Small House at Tulsa, OK)

5.4.2 The Simulation

CFAST, which is the most popular, is used to simulate a small house fire. Most previous researchers simulate one- and/or three-room building fires with a fire only in a room. In this study, seven fire scenarios are calculated for the small 46 square meters single-level house with six rooms. Scenarios take in more fire spreading and window breaking out as scenario number increases. Note that rooms 5 and 6 just provide additional volume to room 1, with no opening to the outside.

Scenario 1. For this study, a typical mattress with polyurethane foam and bedding (Mattress 1 in Table 5. 5) is used to estimate the heat release rate in the first room for scenario 1. This fire has a Medium-Fast growth and a Slow-Medium decay with 1.6 MW maximum heat release rate as shown in the first panel of Figure 5. 21. The fire-growth coefficient is 0.035431 kW/s^2 and the fire-decay coefficient is 0.007687 kW/s^2. This fire shows just growth and decay, burning out without full room involvement, and is included for comparison purposes with the more realistic fires of the other scenarios.

Scenario 2. The same growth rate of the above typical mattress is used as the main fire in room 1 for scenario 2 (see mattresses and beds in Table 5. 4 through Table 5. 6). As this fire in room 1 grows, flashover occurs in room 1 (as 600 °C is reached in the upper smoke layer near the ceiling) and its two windows break out. This fire now is permitted to grow to a maximum of 2 MW maximum heat release rate (estimated from

the availability of air through the openings and fuel load available) and levels off as shown in Figure 5. 22.

Scenario 3. This is the same as scenario 2, plus a Medium growth fire (with fire-growth coefficient of 0.011111 kW/s^2) in room 2 begins at the instant of room 1 flashover. This room 2 fire grows to a maximum of 2 MW then has a constant heat release rate. Both windows in room 2 break out at the instant of room 2 flashover, which occurs before the maximum heat release rate has been reached. This is illustrated in Figure 5. 23.

Scenarios 4 and 5. These scenarios parallel scenario 3, but take in a subsequent fire in room 3 (scenario 4) and subsequent fires in rooms 3 and 4 (scenario 5), respectively. In these cases, medium growth fires are specified (reaching a maximum of 2 MW and leveling off) as shown in Figure 5. 24 and Figure 5. 25. Again, windows break out at the instant of flashover in each room.

Scenarios 6 and 7. These scenarios are the same as scenario 5, but the maximum heat release rates are set to be 1 MW and 3 MW for scenarios 6 and 7 respectively (see Figure 5. 28 and Figure 5. 29). These scenarios are calculated to illustrate the effect of the specified maximum heat release rate, comparing with scenario 5 (2 MW maximum heat release rate). The time to reach flashover in each room may now differ from other scenarios, because the time required to reach the specified 600 °C upper layer temperature may differ.

The first five scenarios are considered in the simulation, with progressively increasing realism regarding the actual fire specification of fire spreading from one room to the next as the previous room reaches flashover. The specified fires and the breaking out of windows for each scenario are summarized in Table 5. 9. The CPU time of scenario 5 is 1 minute and 17 seconds using Intel Pentium III 800 Mhz CPU (3 minutes and 52 seconds on Intel Celeron 366 machine).

Table 5. 9 Fire Scenarios (Small House at Tulsa, OK)

Scenario #	Style of the Specified Fires
1	Fire of typical mattress with polyurethane foam and bedding in room 1 (Medium-Fast fire growth and Slow-Medium decay) No window breakout.
2	Medium-Fast growth fire in room 1 to a maximum of 2 MW then constant HRR Both windows in room 1 break out at room 1 flashover
3	As Scenario 2, plus Medium growth fire in room 2 begins at room 1 flashover to a maximum of 2 MW then constant HRR Both windows in room 2 break out at room 2 flashover
4	As Scenario 3, plus Medium growth fire in room 3 begins at room 2 flashover to a maximum of 2 MW then constant HRR The window in room 3 breaks out at room 3 flashover
5	As Scenario 4, plus Medium growth fire in room 4 begins at room 3 flashover to a maximum of 2 MW then constant HRR Both windows in room 4 break out at room 4 flashover
6	As Scenario 5, except a maximum heat release rate of 1 MW for all fires in each room
7	As Scenario 5, except a maximum heat release rate of 3 MW for all fires in each room

5.4.3 Experimental Results

The fire began on the mattress in the bedroom which was furthest away from the utility room. Only natural combustibles were used, with crumpled paper and a plastic garbage bag being ignited on the bed in Room 1. Fire spread rapidly throughout the structure. Temperatures were recorded every minute, with Figure 5. 21 giving the measured smoke layer temperatures graphically in °C over the first 20 minutes of the burn. Soon after the 20 minute mark temperature measurements were terminated, since burn through of the roof and collapse of some ceilings and walls had occurred. Thus, the thermocouples were no longer in their original locations. Important events were as indicated in Table 5. 10.

Table 5. 10 Important Events (Small House at Tulsa, OK)

Min.	Event
0	Ignition
3	Temperatures surge in bedroom (flashover)
6	Temperatures surge in living room
14	Temperatures surge in kitchen and utility
20	Flames penetrating well through roof
30	Many walls down, external blazing fire, black smoke
40	Flames die down, most walls down

At the 2 minute mark flames were about 0.6 meters high covering an area of about 1.5 meters x 0.6 meters on top of the mattress. Half a minute later flames extended up to the ceiling and ceiling collapse began. The videotape technicians departed from the first observation point in the living room (Room 2) and exited the building through

the west door. At 3 minutes, temperatures above 800 °C were recorded on TC2 (located 1.2 meters above the floor near the handle of the open door between the bedroom and living room). Smoke exited the upper part of the only external opening (the west doorway) while air was being sucked in at the bottom of the doorway. At the 5 minute mark flames had spread to the living room, and even the ceiling in the kitchen began caving in from the effects of the hot smoke layer emerging from the east side of the house to exit via the west doorway. Temperatures in the bedroom row ranged from about 540 °C near the floor to 700 °C near the ceiling, with close to 870 °C at 1.2 meters above the floor in the doorway connecting through to the living room. At 6 minutes, both thermocouples in the living room recorded over 870 °C, while those in the bedroom had subsided slightly to register between 650 to 760 °C.

At the 10 to 12 minute mark the fire in the living room appeared to have subsided, with only modest flames seen near the floor with thick smoke above. Soon after this, the fire grew rapidly. Fire first penetrated through to the kitchen area at the 13 minute mark, with upper regions showing rolling flames. Flames were observed from floor to ceiling in the kitchen just before the 14 minute mark, with flames emerging through the upper part of the west doorway. Temperatures at both locations in the kitchen were now in the range of 870 to 930 °C. At 14 minutes, flames extended from floor to ceiling in the utility room also, with flames extending from open window exits on all sides of the house. Approximate experimental times to reach flashover in each room are represented in Table 5. 11, obtained from point measurements and physical observations.

At 16 minutes, high radiation heat levels were felt at the instrument location to the NW of the structure. Flames began emerging through the roof. At 20 minutes, flames were well penetrating almost the entire roof, in addition to other open exits, and heavy black smoke was observed. The entire interior was an inferno from here onwards, with external walls on the north side of the building having now collapsed. Most other walls had also partially collapsed by 30 minutes, and the fire burned profusely with lots of black smoke. At the 40 minute mark, flames had died down and most walls had collapsed.

Table 5. 11 Experimental Time (approximate) to Reach Flashover in Each Room, These Data Being Deduced from Point Measurements and Physical Observations

Room #	Flashover Time from Start of the First Fire	Flashover Time from Start of Fire in Each Room
1	3 min 30 sec	3 min 30 sec
2	7 min 30 sec	4 min 00 sec
3	13 min 30 sec	6 min 00 sec
4	14 min 00 sec	0 min 30 sec

5.4.4 Computational Results

The small 46 square meter single-level house with six rooms is modeled and calculated via the computer code CFAST with five fire scenarios, with progressively increasing realism regarding the actual fire specification of fire spreading from one room to the next as the previous room reaches flashover. Two more scenarios are added then to illustrate the effect of the specified maximum heat release rate on the calculations.

CFAST requires knowledge or estimation of the heat release rate history versus time, and this must be specified by the user prior to making calculations of the effect of that given fire scenario on the fire spread, temperatures and smoke levels throughout the rooms of the structure. A typical mattress with polyurethane foam and bedding is used to estimate the heat release rate (abbreviated to HRR on figures) in the first room for scenario 1. This fire has Medium-Fast growth and Slow-Medium decay with 1.6 MW maximum heat release rate as shown in Figure 5. 22. The calculated results of upper layer smoke temperatures and layer heights are presented graphically in Figure 5. 22. Notice that room 1 reaches the onset of flashover in 3 minutes and 24 seconds, and temperatures are further increased until the heat release rate reaches the maximum specified value of 1.7 MW at 3 min 31 sec. Thereafter temperatures in all the rooms decrease and the previously descending smoke layer now has the interface ascending towards the ceiling. As expected, all these temperatures of scenario 1 are much lower than the experimental house burn values, since there is deliberately no attempt in this simulation to permit the fire in room 1 to reach full room involvement, nor to let the fire spread into other rooms. This scenario 1 is included so as to let the reader perceive the effects of a simple fire specification prior to venturing to more realistic scenarios.

The same fire growth rate (of the typical mattress being used in the main fire in room 1) is retained for the fire in room 1 for scenarios 2 through 5. This first fire in room 1 now is specified to grow to a maximum of 2 MW heat release rate and then levels off as shown for scenarios 2 through 5 in Figure 5. 23. Scenarios 2 through 5 thereby simulate the occurrence of flashover in room 1 when the upper layer temperature in room 1 reaches 600 °C. Scenarios 3 through 5 permit fire spread into the next room,

flashover in this next room, and then the initiation of a subsequent fire in the next room, etc. These five scenarios are described in detail earlier in discussion about the prediction method, and portrayed in Table 5. 9. First five scenarios give progressively increasing realism regarding the actual house burn, in which the fire actually spread into subsequent rooms of the house as the burn evolved, with each room becoming fully involved in a sequential fashion.

Figure 5. 23 shows the results of the scenario 2 simulation. This fire has Medium-Fast growth to a maximum heat release rate of 2 MW as shown in the first panel of the figure. The calculated results of upper layer smoke temperatures and layer heights are presented graphically in the lower parts of this figure for rooms 1 through 4. Room 1 flashover occurs at 3 minutes and 24 seconds, the same time to reach flashover as scenario 1 because their fires have same growth rate. After opening windows of room 1 at the time of flashover, and leveling off the heat release rate soon afterwards, the temperatures and smoke levels in all the rooms also tend to level off.

In scenarios 3 through 5, a medium growth fire (reaching a maximum of 2 MW and leveling off) is used for sequential fires in other rooms as shown in Figure 5. 24 through Figure 5. 26. Such medium t^2-fires are characteristic of common residential natural burns. As each room reaches flashover (600 °C being reached in the upper smoke layer), window breakout occurs and a subsequent fire begins in the next adjacent room. To clarify, scenario 3 is the same as scenario 2, plus a Medium growth fire in room 2 begins at the instant of room 1 flashover. This room 2 fire grows to a maximum of 2 MW then has a constant heat release rate. Both windows in room 2 break out at the instant of room 2 flashover, which occurs before the maximum heat release rate is

reached. Calculations of upper layer smoke temperatures and layer heights in rooms 1 through 4 are illustrated in Figure 5. 24 for scenario 3.

Scenarios 4 and 5 parallel scenario 3, but include a subsequent fire in room 3 (scenario 4) and subsequent fires in rooms 3 and 4 (scenario 5), respectively. In these cases, medium growth fires are specified (reaching a maximum of 2 MW and leveling off) with flashover occurring when the upper smoke layer temperature reaches 600 °C. Again, windows break out at the instant of flashover in each room. The fire specification and computed results for scenarios 4 and 5 are given in Figure 5. 25 and Figure 5. 26.

The first five fire scenarios progressively increases realism regarding the actual fire specification of fire spreading from one room to the next as the previous room reaches flashover. The calculated time to reach flashover in each room (using the flashover criterion that the upper smoke layer temperature reaches 600 °C) with the most realistic simulation of scenario 5 is represented in Table 5. 12. Notice that, in the case of the small room 4, the calculated temperatures are very close to reaching the flashover criterion for about two minutes before actually satisfying the flashover criterion embodied in the computer code. That is, the time quoted in this table (for flashover in room 4) is probably longer than it would actually be. In general, the calculated flashover times in Table 5. 12 are in very good agreement with the corresponding experimental values given in Table 5. 11.

Figure 5. 26 shows the results of the most realistic simulation of scenario 5, consisting of four sequential fires in the four main rooms of the house, four flashovers and four sets of window breakouts. Temperatures and smoke layer heights are affected as these events occur. This scenario is a new and novel method in the simulations of

real-world fires. General upper layer temperature calculations exhibit the expected trends (deduced from local point measurements) of initial temperature surge, rate of general temperature rise, peak and leveling off temperatures, and time to reach flashover in each room.

Table 5. 12 Calculated time (approximate) to Reach Flashover in Each Room, Simulation with Scenario 5, Assuming 600 °C for Occurrence of Flashover in Each Room

Room #	Flashover Time from Start of the First Fire	Flashover Time from Start of Fire in Each Room
1	3 min 24 sec	3 min 24 sec
2	8 min 35 sec	5 min 11 sec
3	13 min 48 sec	5 min 13 sec
4	18 min 38 sec	4 min 50 sec

To illustrate more closely the comparison of the experiments and the calculations, Figure 5. 27 amalgamates point-temperature measurements and general upper layer temperature calculations. Exact agreement is not expected because of the use of point measurements and averaged upper layer calculations. For simplicity, not all the fire scenarios are included, but scenarios 1, 3, and 5 are sufficient to illustrate the greater realism of the "most-realistic" scenario 5. The figure shows upper layer averaged temperature calculations versus time in the three rooms, and includes point-temperature measurements. It may be seen that, as the scenarios number increases, the calculations show the trends more correctly. That is, in terms of temperature rise, magnitude of peak and level-off temperature, and time to reach flashover in each of the rooms. Note again

that the calculations illustrate general upper layer average temperatures, whereas thermocouple point measurements are very localized. In particular, thermocouples in room 2 were located on one side of the room and would be affected by local burning and local fuel load.

In the calculations of scenarios 2 through 5, a maximum heat release rate of 2 MW has been used for each fire. This was estimated from the availability of air through the sequence of door opening and fuel load available. To justify this choice of 2 MW, two further scenarios have been calculated with 1 MW and 3 MW maximum heat release rates.

Scenarios 6 and 7 illustrate the effect of the specified maximum heat release rate on the calculations. These two scenarios are the same as scenario 5, except that the maximum heat release rate of all fires in each room is now different. The same fire growth rate of the typical mattress being used in the main fire in room 1 is retained for the fire in room 1. This first fire in room 1 now is specified to grow to the maximum heat release rate of 1 MW and 3 MW for each scenario 6 and 7, and then levels off as shown in the top panels of Figure 5. 28 and Figure 5. 29. As in scenario 5, medium growth fires are added in subsequent rooms as the fire progresses, but now their maximum heat release rates are 1 MW and 3 MW, respectively, in scenarios 6 and 7. Heat release rates, upper layer temperatures and smoke layer heights of each scenario are depicted in Figure 5. 28 and Figure 5. 29. As we expect, higher temperatures and lower layer heights are observed as the bigger maximum heat release rate are specified.

To illustrate more closely the comparison of the experiments and the calculations of scenarios 5 through 7, Figure 5. 30 amalgamates point-temperature measurements and

general upper layer temperature calculations. Again exact agreement is not expected because of the use of point measurements and averaged upper layer calculations. The upper layer temperatures of scenarios 5 through 7 are compared with measurements in Figure 5. 30. Too cold temperatures and slow rise of temperature are seen for scenario 6 (1 MW maximum heat release rate), and too hot and fast for scenario 7 (3 MW maximum heat release rate). The 2 MW maximum heat release rate shows greater realism in the calculations with respect to the trend of temperature rise rate and temperature magnitude.

The time to reach flashover is represented graphically in Figure 5. 31 for experiment and scenarios 5 through 7. The results of scenario 6 (1 MW) show very longer times to reach flashover in each room than the observations from experiment. The same amount of time is required to reach flashover in room 1 for scenarios 5 and 7, because room 1 reaches flashover before the heat release rate reaches 2 MW. Slightly shorter (but similar) times are required to reach flashover in other rooms with scenario 7 comparing to scenario 5. However we observed clearly in Figure 5. 30 that the upper layer temperatures of scenario 7 were too high and rise too fast.

Now it can be concluded that scenario 5 is the most realistic simulation in terms of fire growth methodology and maximum fire size in each room for the small house burn. Scenario 5 has the closest trend to the experiment in the rise and the magnitude of temperatures, and in the time to reach flashover in each room.

5.4.6 Closure

In the experiment, it is to be noted that the fire load was very low and only natural combustibles were used to initiate the fire. Despite this, two noteworthy conclusions may be drawn from the experiment. All rooms reached temperatures in excess of 870 °C (≅ 1600 °F) at some time during the burn. Fire spread rapidly throughout the structure, with almost total roof collapse in 30 minutes.

In the calculations, seven scenarios have been calculated using CFAST and represented graphically, showing the results of smoke temperatures and smoke layer heights of each room. A new and novel methodology for multi-room fire simulation has been introduced. It consists of sequential fire spreading to the next room when flashover conditions occur in the previous room. Also windows break out at the instant of flashover. It has been found that scenario 5, which fully implements the new methodology, is the most realistic simulation. The results of scenario 5 follow the trend of the experiments in the rate of temperature rise and the magnitude of temperatures, and in the time to reach flashover. Studies of this type assist in the understanding of structural fires, and the development of computer modeling studies, and assessment of their predictive capability.

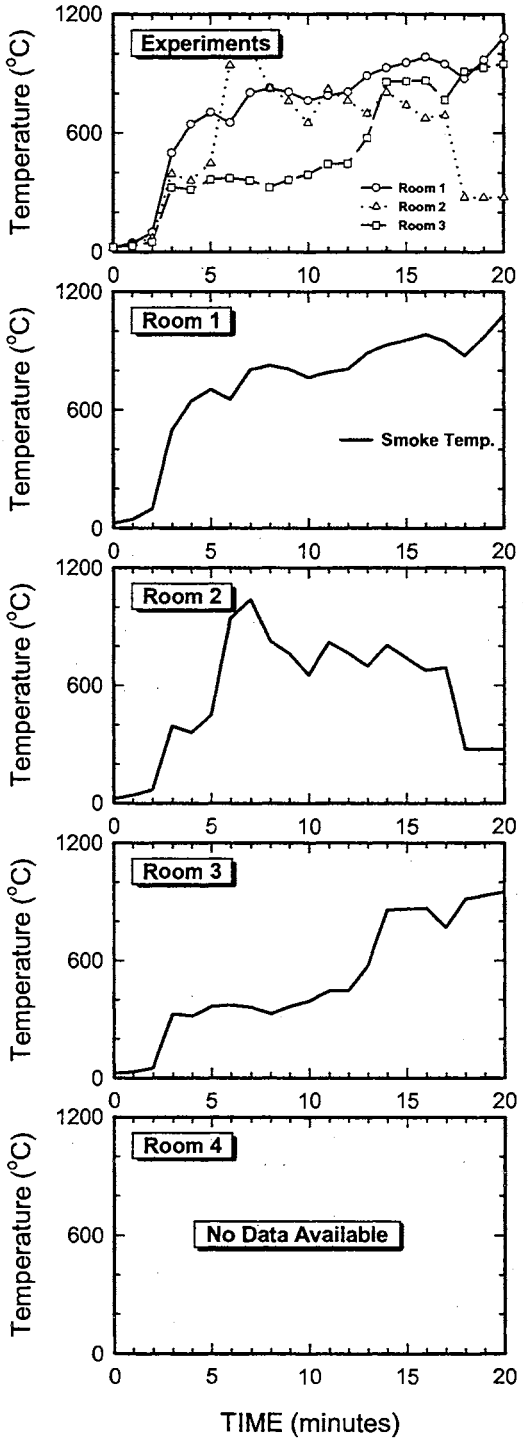

Figure 5. 21 Experimental Upper Layer Smoke Temperatures Measured 0.3 Meter from Ceiling (Small House at Tulsa, OK)

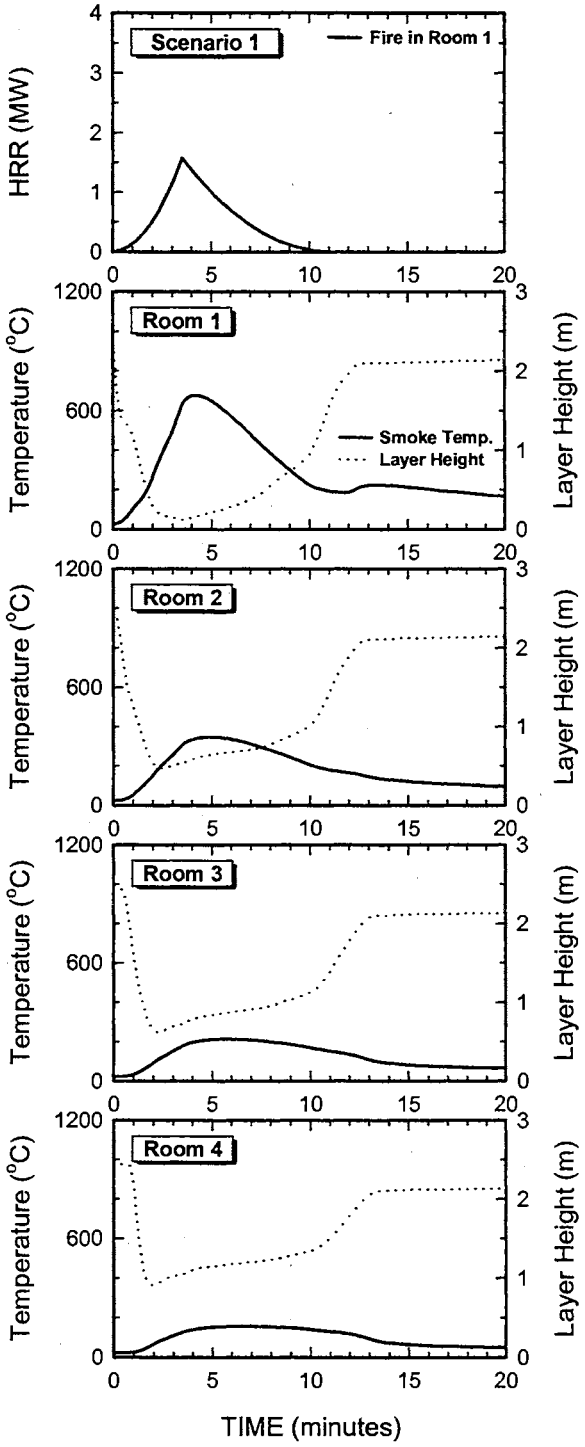

Figure 5. 22 **Scenario 1**: Fire of Typical Mattress with Polyurethane Foam and Bedding in Room 1 (Medium-Fast Growth and Slow-Medium Decay Fire), with No Window Breakout

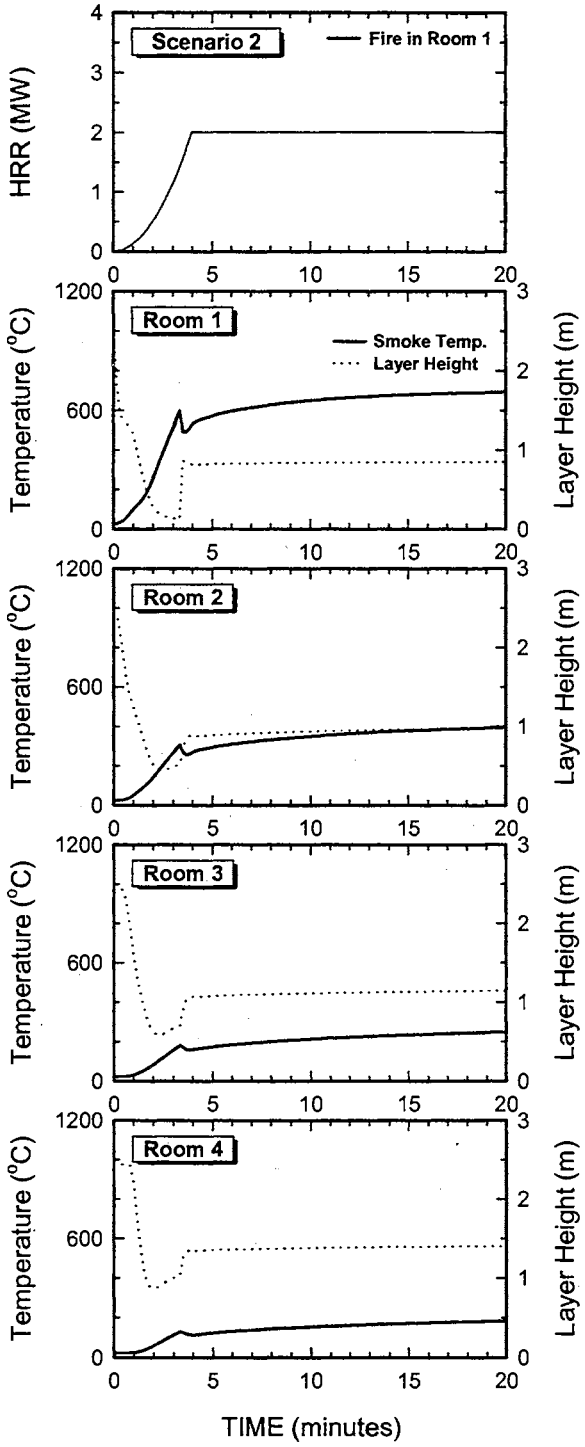

Figure 5. 23 **Scenario 2**: Medium-Fast Growth Fire in Room 1 to a Maximum of 2 MW then Constant HRR, with Both Windows in Room 1 Breaking Out at Room 1 Flashover

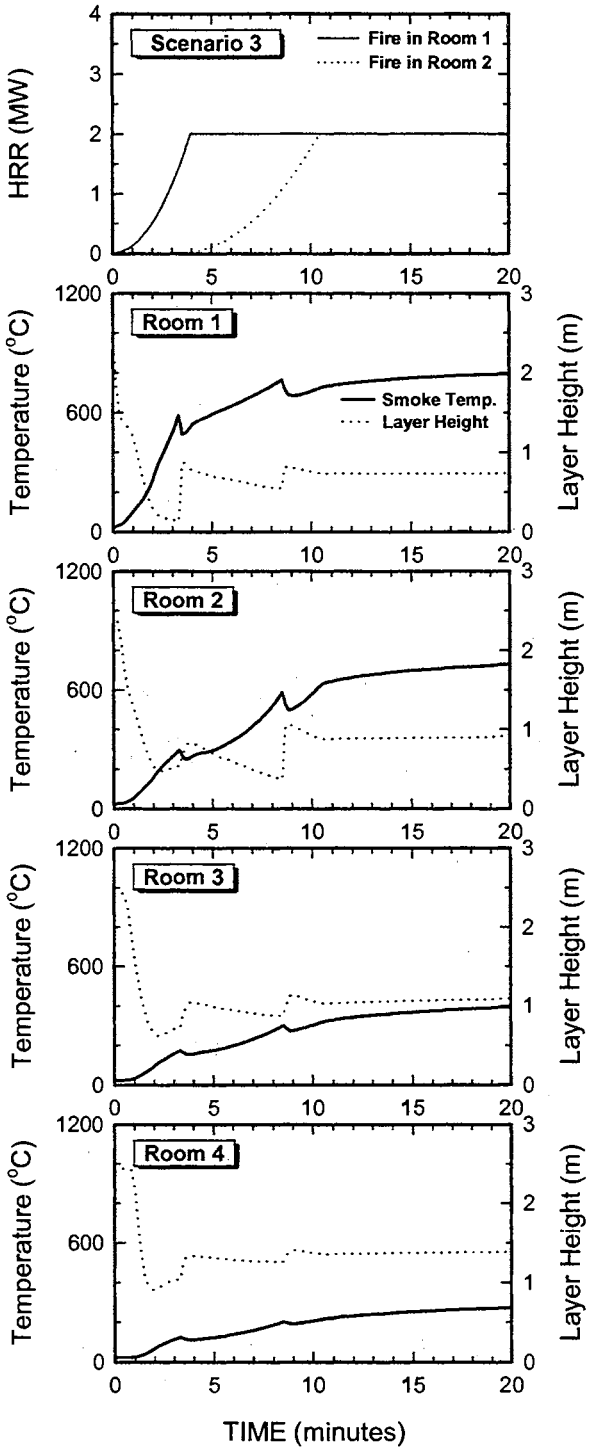

Figure 5. 24 **Scenario 3**: As Scenario 2 Plus Medium Growth Fire in Room 2 Begins at Room 1 Flashover to a Maximum of 2 MW then Constant HRR, with Both Windows in Room 2 Breaking Out at Room 2 Flashover

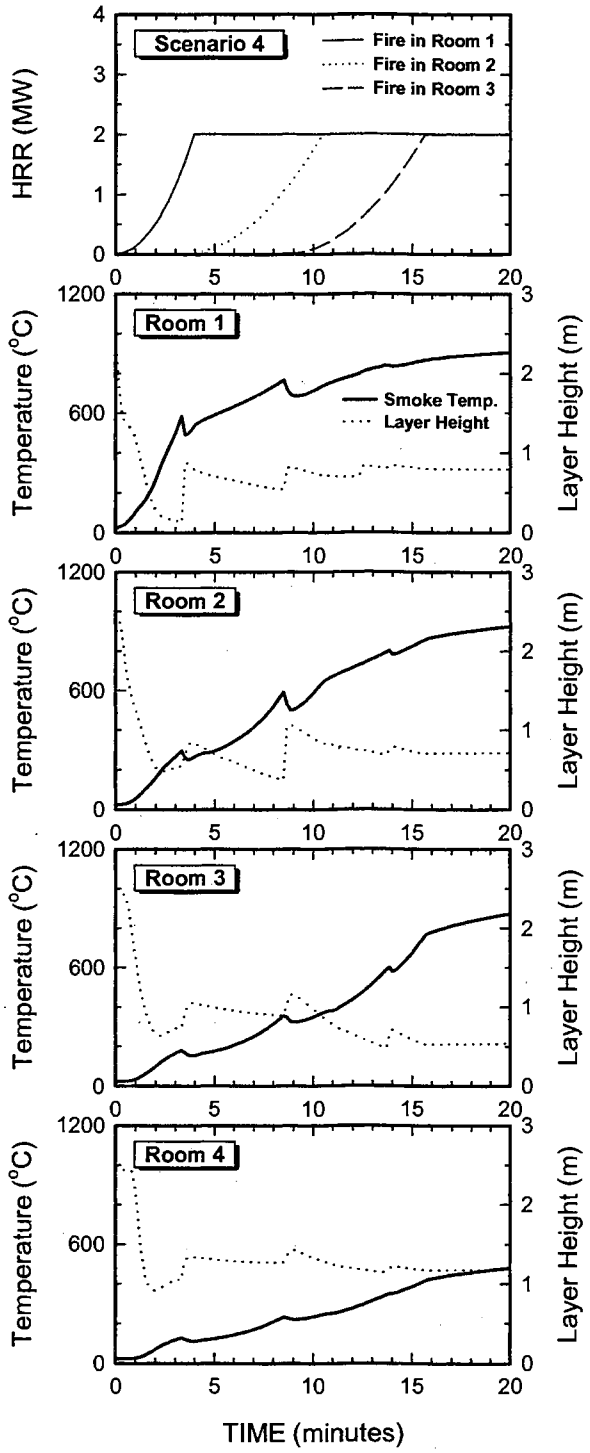

Figure 5. 25 **Scenario 4**: As Scenario 3 Plus Medium Growth Fire in Room 3 Begins at Room 2 Flashover to a Maximum of 2 MW then Constant HRR, with the Window in Room 3 Breaking Out at Room 3 Flashover

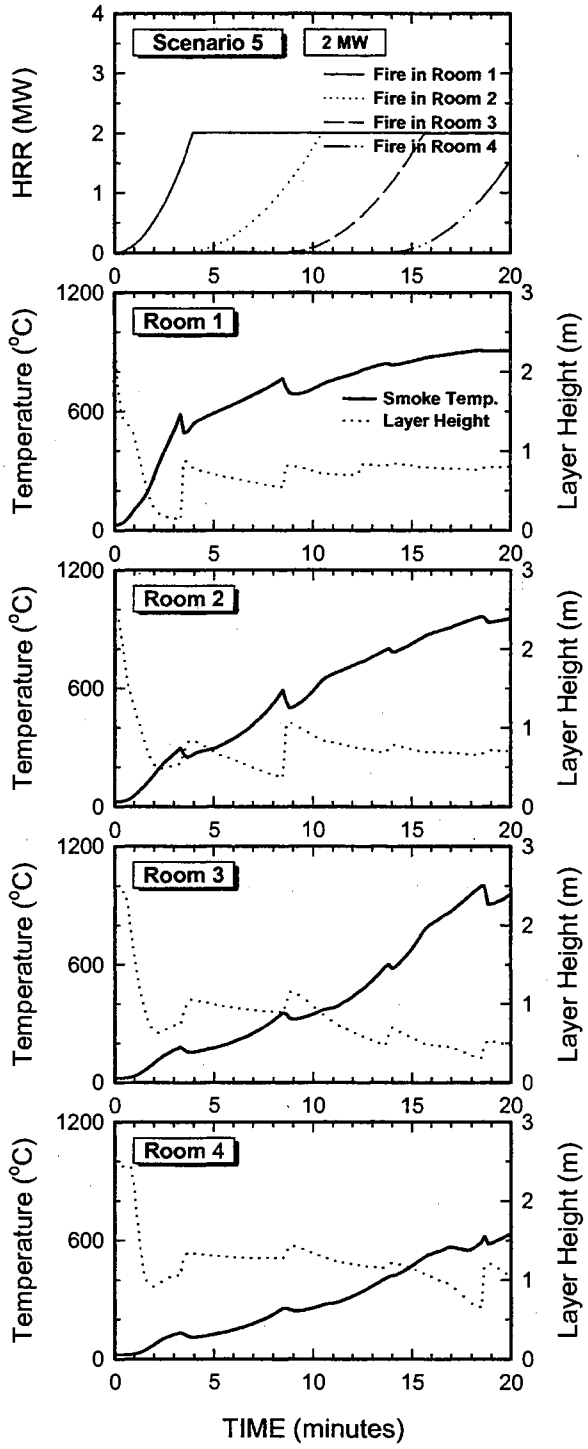

Figure 5. 26 **Scenario 5**: As Scenario 4 Plus Medium Growth Fire in Room 4 Begins at Room 3 Flashover to a Maximum of 2 MW then Constant HRR, with Both Windows in Room 4 Breaking Out at Room 4 Flashover

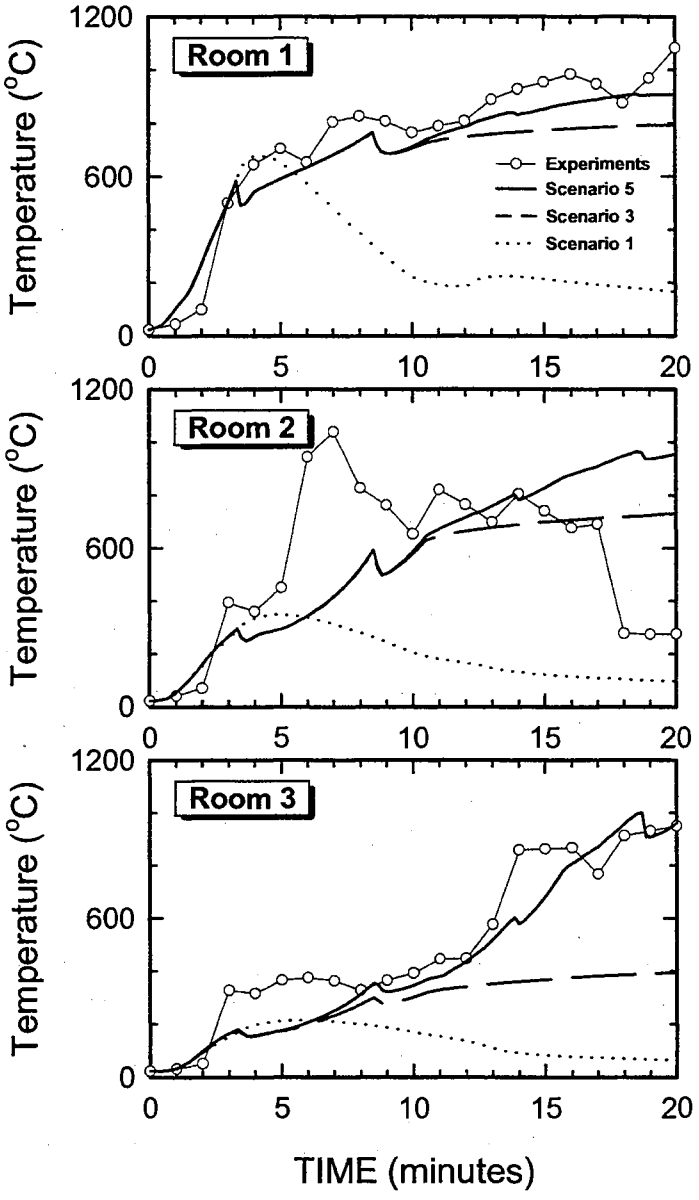

Figure 5. 27 Comparison of Upper Layer Temperatures Among Experiments and Scenarios 1, 3, and 5

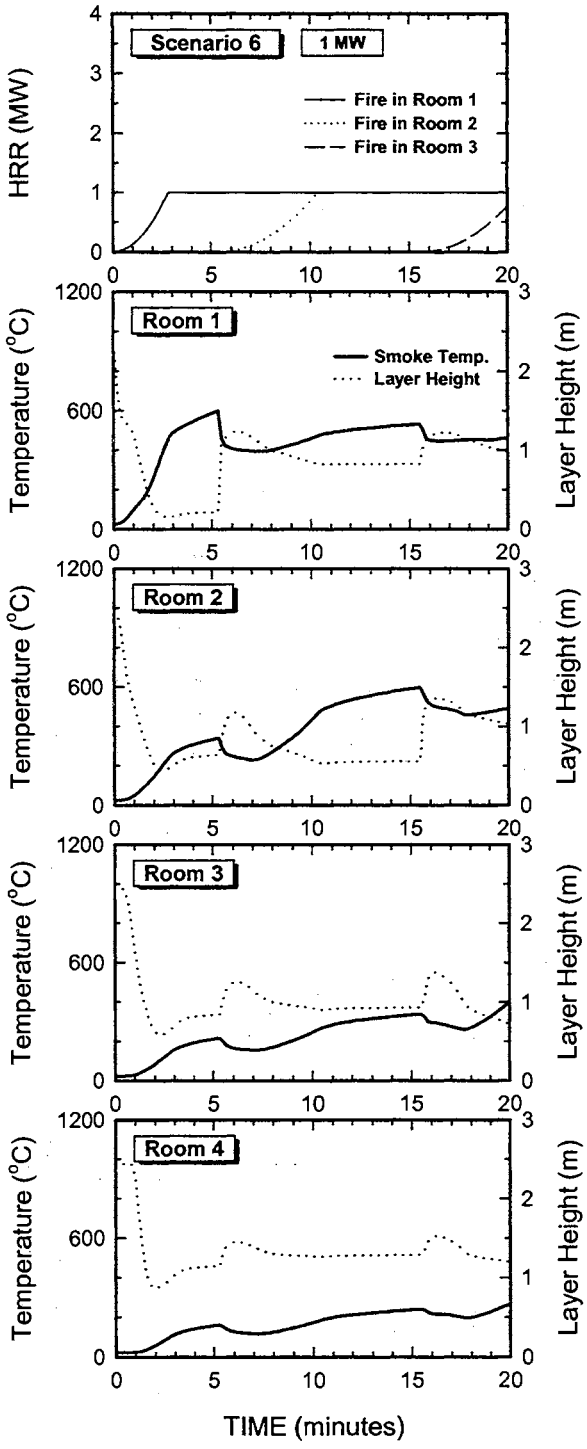

Figure 5. 28 **Scenario 6**: As Scenario 5 with 1 MW Maximum HRR for All Fires

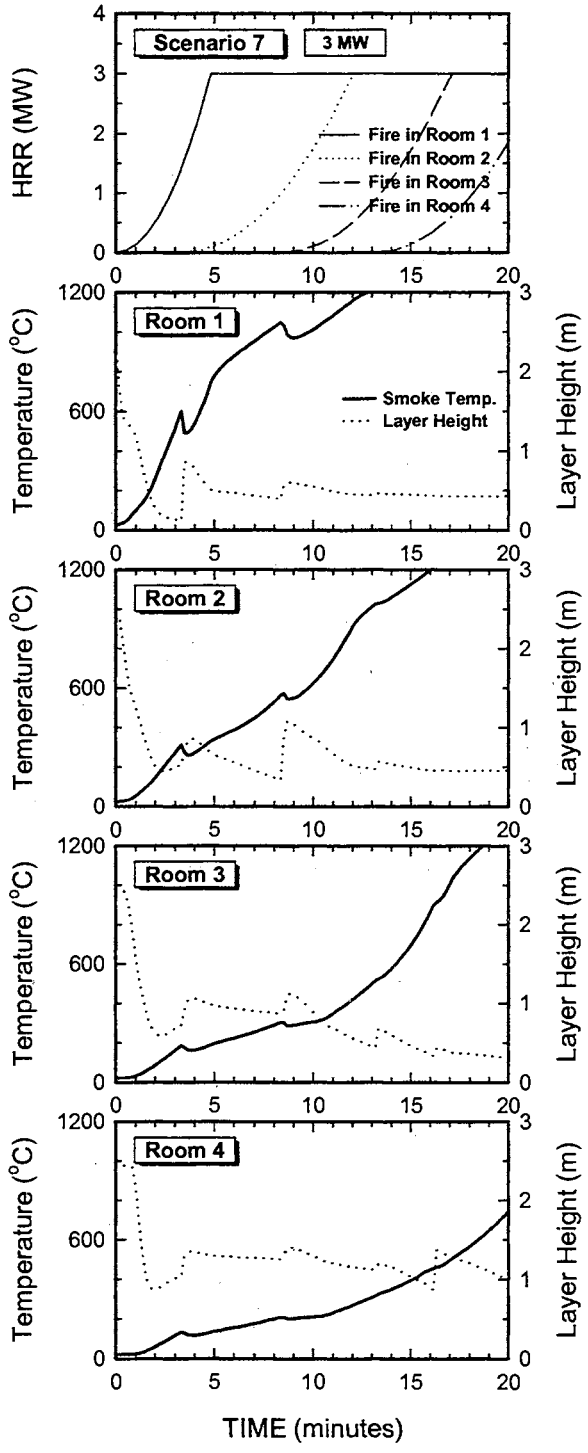

Figure 5. 29 **Scenario 7**: As Scenario 5 with 3 MW Maximum HRR for All Fires

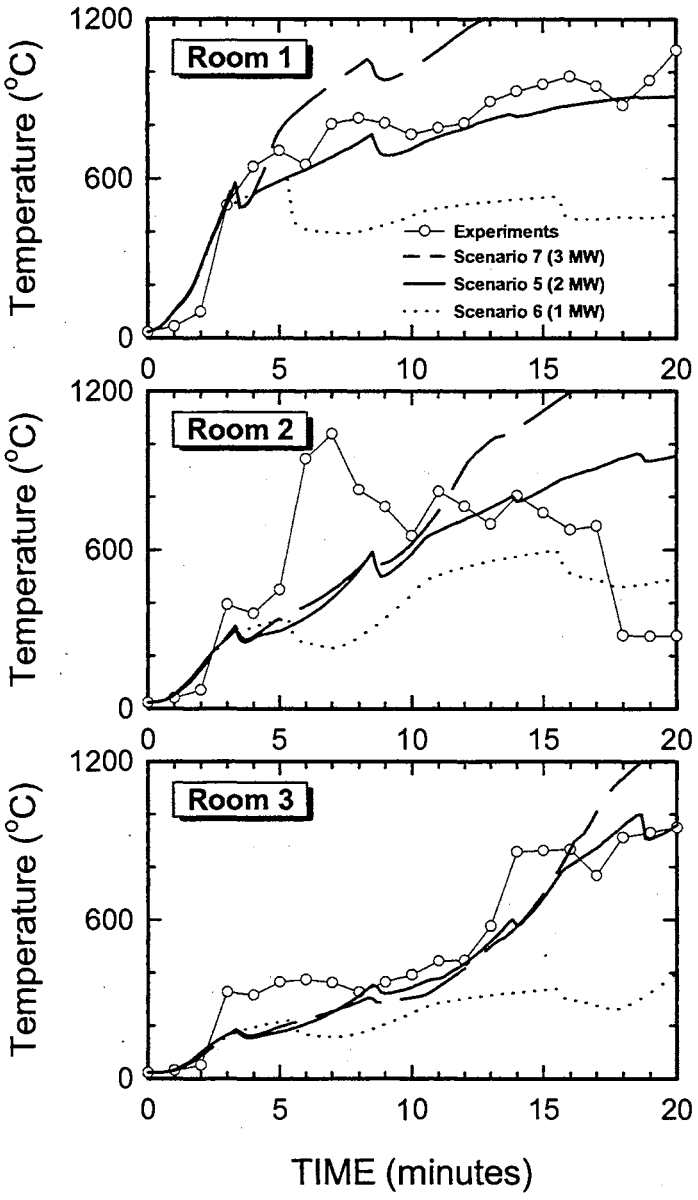

Figure 5. 30 Comparison of Upper Layer Temperatures Among Experiments and Scenarios 5, 6, and 7 (2, 1, and 3 MW of Maximum HRR Respectively)

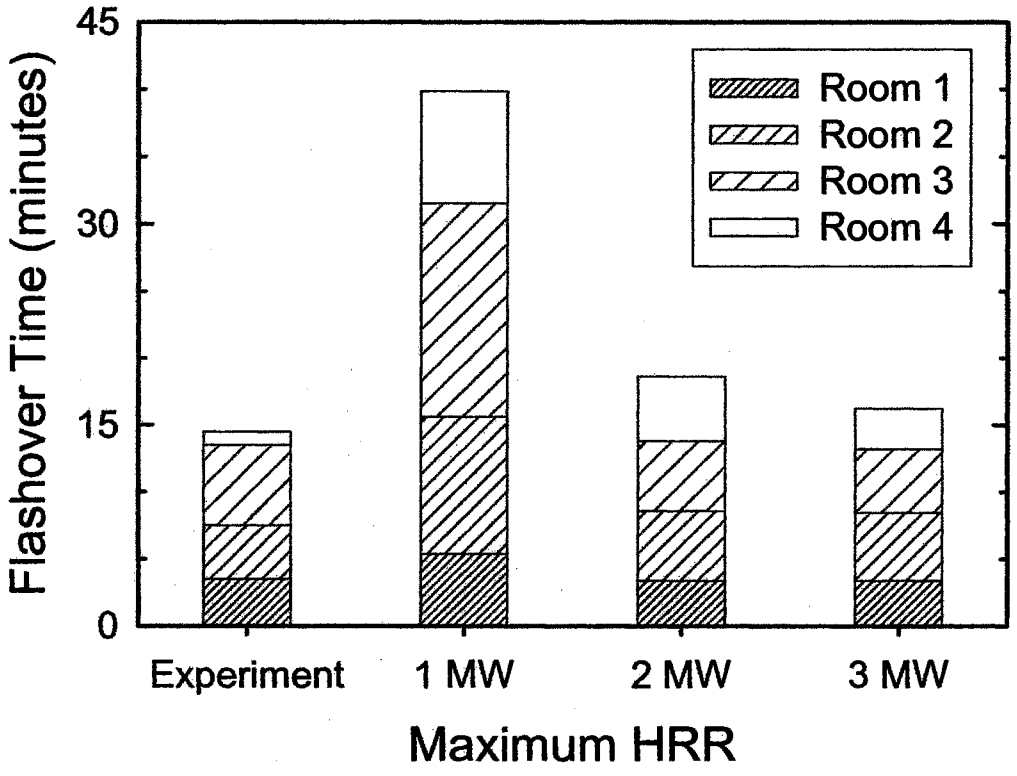

Figure 5. 31 Comparison of Time to Reach Flashover for Each Room Among Experiments and Scenarios 5, 6, and 7 (2, 1, and 3 MW of Maximum HRR Respectively)

Figure 5.23 Comparison of Time to Reach Flashover for Back Room Among Experiments and Scenarios 5, 6, and 7 (2, 1, and 3 MW of Maximum HRR Respectively)

5.5 Temperature and Smoke Prediction in a Large House Fire

In this section, a large house (area about 170 square meters, with 10 rooms) at Woodward, Oklahoma was subjected to a complete experimental burn, with temperature measurements and fire observations during the entire burn. The CFAST computer code is used to calculate temperatures and smoke levels in the various rooms of the house during the burn (with 10 different rooms). Four fire scenarios are considered in the simulation, with increasing realism regarding the actual fire specification.

A simpler calculation (with 3 different rooms) has also done to see if the similar results would be shown with the 10 room simulation. It was found that results for smoke temperature and smoke layer heights were very similar, leading to the conclusion that a 3-room simulation of a 10-room building gives adequate modeling capability of the real structural fire.

The experimental facility is described, followed by discussion about instrumentation, temperature measurement technique, and experimental results. The prediction method and computational results follow, including important events in the fire, flashover in the first room, and smoke temperature and smoke layer heights. Computation results give the expected trends (deduced from local point temperature measurements) of initial temperature surge and decay, peak and leveling off temperatures, especially with respect to the northwest bedroom with a closed door. The effect of weather a door of a room would have been open was investigated computationally, with results illustrating far more dangerous smoke temperature and smoke level in the room.

5.5.1 The Experiment

A large house with an attic was selected as the experimental facility. Figure 5. 32 shows the floor plane of a multi-room house that was the subject of a complete burn, with north direction to the top. Then small rooms were on the first floor (area about 170 square meters), with a large attic above. The house was fully furnished with furniture and a large amount of old clothes in the closets and the attic area. All external windows and doors were boarded up, except for the west-side living room door which remained open. This door was opened at about 45 degrees.

All internal doors were open, except that leading to the northwest bedroom (room 3) which was closed. The heights of all doors are 2.1 meters. This closed door of the northwest bedroom had a larger than normal gap of about one inch (2.54 centimeters) below and a gap of about a half inch (1.27 centimeters) above. Fire began near to the projecting corner of the L-shaped kitchen area (room 1). Only natural combustibles were used. A wastebasket with crumpled paper was first ignited. Fire spread rapidly to an adjacent dry Christmas tree (about 2 meters tall), and then ignition of a wooden shelf unit occurred.

Fire rapidly spread to the living room and west porch area (aided by the open door). Eight K-type thermocouples with ceramic fiber insulated wires were strategically located in the burn room near the fire (one near the ceiling, one near the vertical center, and one near the floor), in the living room (one near the ceiling, one near the floor), in the closed-off northwest bedroom (one near the ceiling), and in the attic (one near the ceiling, one near the floor). Temperature up to 1375 °C could be measured with high

accuracy and without damage to the wires or insulation. The temperature measuring locations are illustrated in Figure 5. 32 and Table 5. 13.

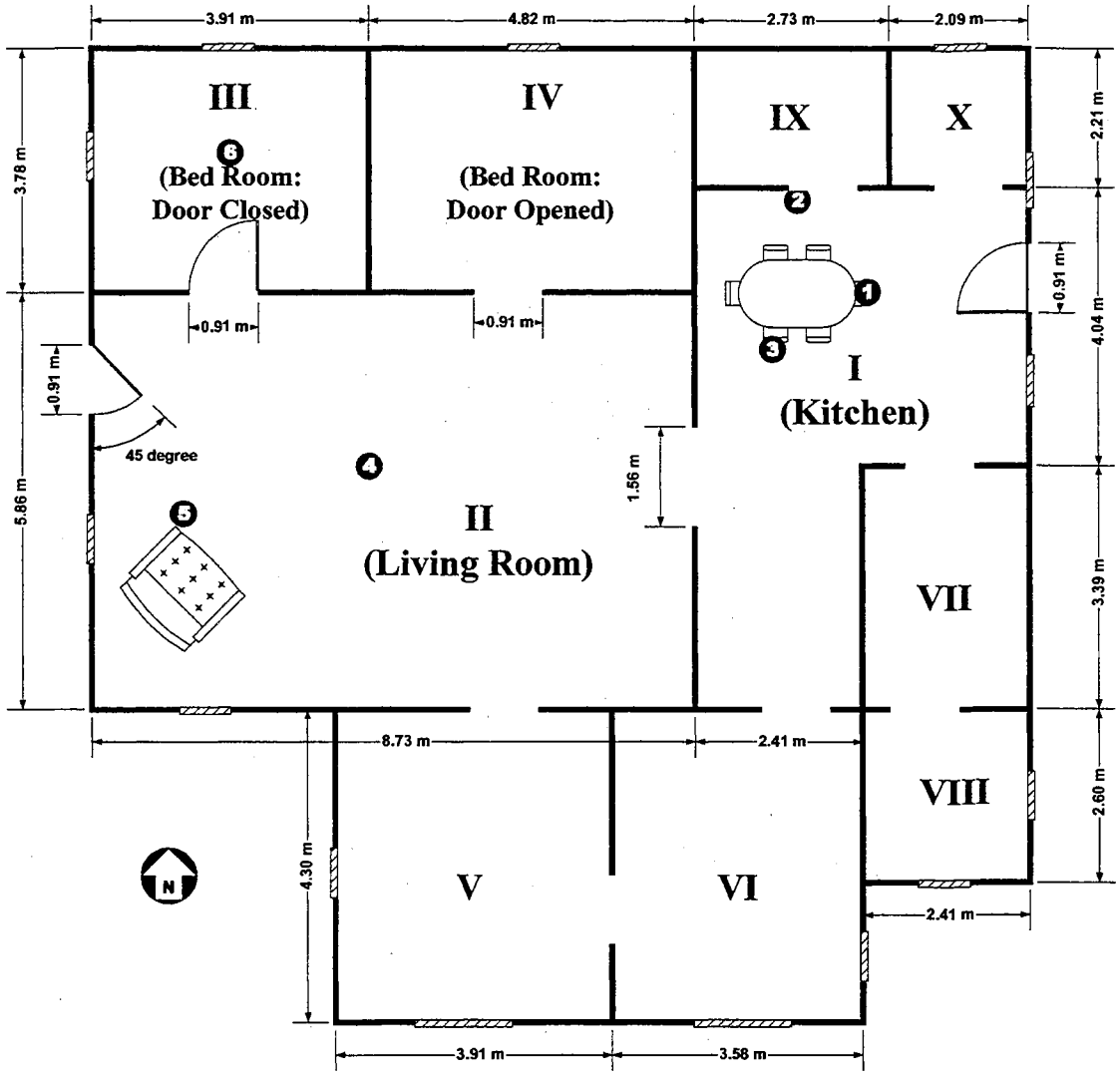

Figure 5. 32 Floor Plan of the Structure Indicating Room Numbers and Thermocouple Locations of 10-room simulation for Scenario 1 and 2 (Large House at Woodward, OK)

Table 5. 13 Thermocouple Locations (Large House at Woodward, OK)

Room	TC #	Location
Room 1 (Kitchen)	1	0.15 meters from ceiling
	2	1.2 meters from floor
	3	0.3 meters from floor
Room 2 (Living)	4	0.3 meters from ceiling
	5	0.3 meters from floor
Room 3 (Bedroom)	6	0.3 meters from ceiling
Attic	7	0.3 meters from ceiling
	8	0.15 meters from floor

5.5.2 The Simulation

The large 170 square meters house with ten rooms and a large attic is modeled via CFAST with six fire scenarios. Note that external openings are boarded up, except for the door to the west from living room (room 2). The opening size was deduced from the 45-degree opened.

Scenario 1. A wastebasket, a Christmas tree, and a plywood wardrobe (Waste Basket and Christmas Tree in Table 5. 5, and Wardrobe 3 in Table 5. 4) are used together to estimate the heat release rate in the first room for this scenario 1. In the experiment these three items were ignited within a few seconds and for simplicity in the calculations, they are ignited instantly at the beginning of this simulation. This combined fire has a much faster growth than Ultra-fast growth, and a Fast decay with 6.0 MW maximum heat release rate. This fire shows just growth and decay, burning out without full room

involvement, and is included for comparison purposes with the more realistic fires of the other scenarios.

Scenario 2. The same fire of the above three items is used as the main fire in room 1 for this scenario 2. This main fire decays as same as scenario 1, with the following reason. As the fire in room 1 grows, flashover occurs in room 1 (as 600 °C is reached in the upper smoke layer near the ceiling). A Medium growth fire (with fire-growth coefficient of 0.011111 kW/s^2) in room 2 begins at the instant of room 1 flashover. This room 2 fire grows to a maximum of 3 MW then has a constant heat release rate. The maximum 3 MW fire size was determined by consideration of available air through the open door to the outside. This room 2 fire may block the fresh air from outside to get to the room 1. Hence, the main fire in the room 1 (no opening to the outside) will decay.

Scenario 3. A simpler simulation is suggested. The fire specification is the same as scenario 2, but the building is simulated as a 3-room house. The nearby small rooms except room 3 are added to get larger new "rooms", designed as room 1 and room 2 (see Figure 5. 33). The door of room 3 (to room 2) is still closed.

Scenario 4. This is same as scenario 3, but the door of room 3 (to room 2) is open. This scenario is calculated to see the effect of open door.

Scenarios 5 and 6. These scenarios are the same as scenario 2, but the maximum heat release rates of the fire in room 2 are set to be 2 MW and 4 MW for scenarios 5 and 6 respectively (Figure 5. 44 and Figure 5. 45). In addition, the door to the outside has to be fully opened in scenario 6 to permit 4 MW maximum. The maximum heat release rate is about 3.1 MW in room 2 without the fully open door. These scenarios are calculated to illustrate the effect of the specified maximum heat release rate, and to justify the choice of the maximum heat release rate.

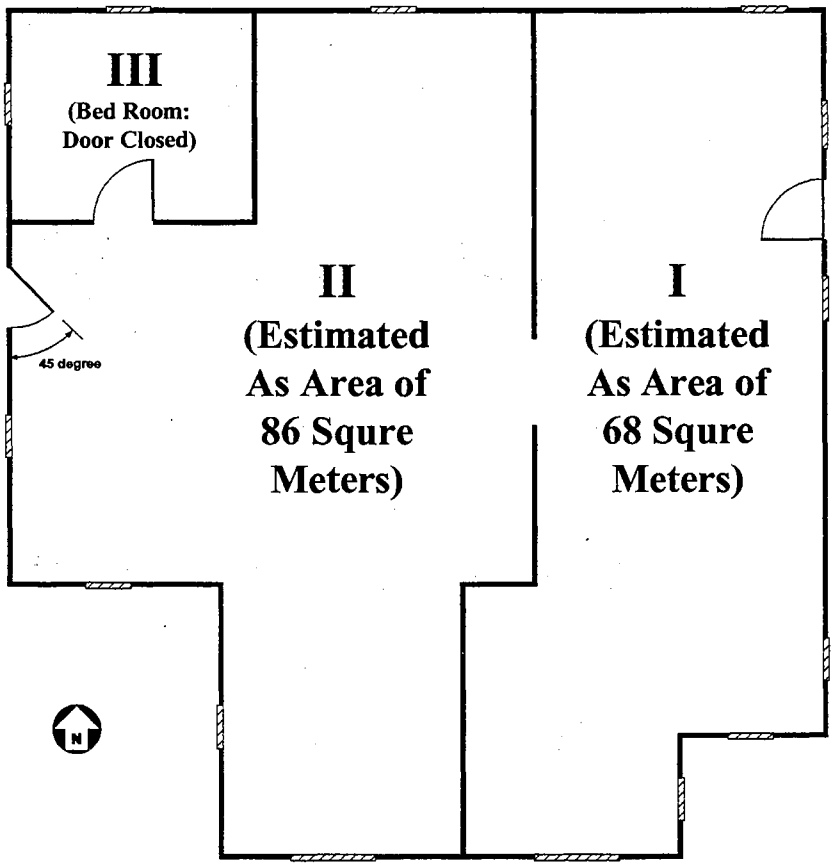

Figure 5. 33 Floor Plan of 3-room simulation for Scenarios 3 and 4
(Large House at Woodward, OK)

Six fire scenarios are considered in the simulation, with scenario 2 having greatest realism regarding the actual fire specification of fire spreading from the first room to the next as the previous room reaches flashover. The specified fires for each scenario are summarized in Table 5. 14. The designed main fire sizes in room 1 are different than the actually being used ones in the calculations. It will be explained in the later section.

Table 5. 14 Fire Scenarios (Large House at Woodward, OK)

Scenario #	Style of the Specified Fires
1	Fire of three items of a waste basket, a Christmas tree, and a plywood wardrobe in room 1 (Ultra-fast fire growth and Fast decay) 10-room building 45 degree open door to the outside
2	As Scenario 1, plus Medium growth fire in room 2 begins at room 1 flashover to a maximum of 3 MW then constant HRR 10-room building 45 degree open door to the outside
3	As Scenario 2, but simpler simulation with the closed door of room 3 3-room building 45 degree open door to the outside
4	As Scenario 3, but with the open door of room 3 3-room building 45 degree open door to the outside
5	As Scenario 2, except a maximum heat release rate of 2 MW of the fire in room 2 10-room building 45 degree open door to the outside
6	As Scenario 2, except a maximum heat release rate of 4 MW of the fire in room 2 10-room building Full open door to the outside

5.5.3 Experimental Results

Only natural combustibles were used, the fire began on the wastebasket with crumpled paper in the kitchen, which has a open door large way to the living room. Fire spread rapidly to the adjacent dry Christmas tree, and then to the wooden shelf unit in a few seconds. Fire rapidly spread to the living room and the front porch area (west-side of living room). Temperatures were recorded during entire the 180 minutes of the burn. Figure 5. 34 gives the measured smoke layer temperatures graphically in °C over the first 30 minutes of the burn. After that, burn through of the roof and collapse of a large part of ceilings and walls occurred.

Table 5. 15 Important Events (Large House at Woodward, OK)

Min.	Event
0	Ignition
5	Flames on front porch
16	Porch roof falls
30	Lots of flame at west end West roof area collapses Attic venting
37	All roof now collapsed Black smoke
56	Most walls down

The temperatures of kitchen and living room surged right after ignition and initial fire spread. At the 2 minute mark, smoke temperatures of the kitchen and the living room reached about 800 °C and 650 °C respectively at the thermocouple measurement locations. The fire appeared to have subsided from 2 minutes to 4 minutes, and then they

surged again. Flames started on the front porch at about 5 minute mark. At the 7 minute mark, the temperature in the kitchen and the living room were recorded over 400 °C and 800 °C respectively, and then subsided again. These two rooms' temperatures started to increase again at about the 15 minute mark. The porch roof started to fall at about 16 minute mark. At 20 minutes, the smoke temperature of the attic started to increase, and it reached over 500 °C at 30 minutes. At that time, lots of flame was seen at the west end of building, and collapse of the west roof had occurred. Heavy black smoke was observed. The entire interior was an inferno from here onwards. Flames can be found on the roof and through all windows at about 37 minutes. All roof was collapsed at about the 45 minute mark, and most walls were down at 56 minutes. These events were as summarized in Table 5. 15.

5.5.4 Computational Results

The large 170 square meter single-level house with 10 rooms is modeled and calculated via the computer code CFAST. The heat release rate of a wastebasket, a Christmas tree, and a plywood wardrobe are amalgamated to estimate the heat release rate (called the designed fire) in the first room. However, the size of the fire in room 1 is constrained automatically in the CFAST program by the ventilation limit. The required amount of oxygen for the designed heat release rate (maximum of 6.0 MW) is higher than the available amount. Figure 5. 35 shows the heat release rate of the combination of three items, and the reduced heat release rate actually used in the calculations of each scenario.

The calculated results of upper layer smoke temperatures and layer heights are presented graphically in Figure 5. 36. Notice that room 1 reaches the onset of flashover in just 60 seconds, and temperatures are further increased until the heat release rate reaches the maximum constrained value of 5.1 MW at about 70 seconds. Thereafter temperatures in all the rooms decrease and the previously descending smoke layer now has the interface ascending towards the ceiling. For the room 1, the calculated temperature has a very good agreement (less than 5 % difference of the maximum temperature at 2 min) with the measured one in the being of the fire. After about 6 minutes, all room temperatures are much lower than the experimental point measurements would suggest. This result was expected, since there is deliberately no attempt in this simulation to let the fire spread into other rooms. This scenario 1 is included so as to let the reader perceive the effects of a simple fire specification prior to venturing to more realistic scenarios.

Figure 5. 37 shows the comparison of upper layer temperatures and layer heights of room 3 and room 4 in scenario 1. The difference between two rooms (reasonable same sizes to compare) is the opening of doors. The upper layer temperature of the door-closed room 3 is much lower than the corresponding temperature of the door-opened room 4. The smoke layer height of room 4 (open door) is a lot lower than room 3 (closed door) during the time of the fire. When this fire subsides, the smoke of room 4 ventilates more quickly than room 3, because of its fully open door.

The same fire is retained for the fire in room 1 for scenario 2, which also permits the fire to spread into the adjacent living room (room 2). A subsequent fire in this next room is initiated when the temperature of room 1 reaches 600 °C (flashover of room 1 at

60 sec). The fire in room 1 (no direct opening to the outside) did not progress to reach full room involvement. This scenario gives greater realism regarding the actual house burn, in which the fire actually spreads into the adjacent living room as the burn evolved.

A medium growth fire (reaching a maximum of 3 MW and leveling off) is added in room 2 on the constrained main fire in room 1 as shown in the first panel of Figure 5. 38. The calculated results of upper layer smoke temperatures and layer heights are presented graphically in the lower parts of this figure for rooms 1 through 4. Room 1 flashover occurs at 60 seconds, which is the same as with scenario 1. This is because the fire specification in the house is exactly the same until the next sequential fire in room 2 is initiated.

Figure 5. 38 shows the results of the realistic simulation of scenario 2, consisting of the original room 1 fire plus one sequential fire in room 2 (living room) of the house. Temperatures and smoke layer heights are affected because of this second fire. Generally, calculated upper layer temperatures exhibit similar trends as found in the experimental data. The room 3 temperature remains about 20 °C, somewhat expected because of its closed door connection to the fire in the rest of the house.

Figure 5. 39 shows a comparison of upper layer temperatures and layer heights between room 3 (closed door) and room 4 (open door) from the calculated results of scenario 2. This figure may be compared with the Figure 5. 37 which was for scenario 1. Notice that in the case of scenario 2 (with the continuing fire in room 2) the temperatures continue to rise in room 3. This was not the case with scenario 1, which had fire growth and decay in room 1 only and with no fire in room 2. Also smoke levels descend quickly and remain at low levels in room 3, and decrease slowly in room 4. Comparing the

results of room 3 and room 4, one can see that there is a 10 minutes difference in the time available before the smoke has fallen to floor (22 vs. 2 minutes).

A simpler version of scenario 2 has been performed. The Figure 5. 40 shows the results of the simpler simulation of scenario 3, consisting of the 3-room simulation. The results of this scenario (3-room simulation) are in very good agreement with the results of scenario 2 for smoke temperatures and levels in room 1 (kitchen), room 2 (living room), and room 3 (bedroom with closed door). The temperature difference between them is in the maximum of 15 percent, and average error is 2.5 %. The bigger differences at the first two minutes due to the door heights of 2.1 meters, where the building height is 2.4 meters. After smoke layer goes down enough, error was very small. The smoke levels are also very similar. The setup time and calculation time can save a lot with this simpler simulation. The CPU of the 3-room simulation is about 25 % of the CPU time of the 10-room simulation (4 vs. 16 minutes on Intel Celeron 366 machine). This assumption that nearby small rooms can be merged into single larger rooms can be very usefully for faster simulations.

Figure 5. 41 shows the results of scenario 4, and the values may be compared with the results of scenario 3 in Figure 5. 42. The upper layer temperature and smoke height of room 3 of scenario 4 shows very similar trend as room 4 of scenario 2, so Figure 5. 42 gives very similar discussion as in Figure 5. 39. All these results of the 3-room simulation give confidence in the possibility of using the use simpler and quicker FASTLite program to simulate multi-room building fires with more than 3 rooms.

To illustrate more closely the experiments and the calculations, Figure 5. 42 amalgamates point-temperature measurements and general upper layer temperature

calculations. Exact agreement is not expected because of the use of point measurements and averaged upper layer calculations. The figure shows upper layer averaged temperature calculations versus time in the three rooms, and includes point-temperature measurements. It may be seen that the calculation of scenario 2 shows the trends more correctly. Also the calculation of simpler scenario 3 (3-room simulation) shows very similar results as compare with scenario 2 (10-room simulation), as previously mentioned.

In the calculations of scenario 2 through 4, a maximum heat release rate of 3 MW has been used for the fire in room 2. This was estimated from the availability of air through the door to the outside and fuel load available. To justify this choice of 3 MW, two further scenarios have been calculated with 2 MW and 4 MW maximum heat release rates.

Scenario 5 and 6 illustrate the effect of the specified maximum heat release rate on the calculations. These two scenarios are the same as scenario 2, except that the maximum heat release rate of the fire in room 2 is now different. Same fire specification is used in room 1, but the fire in room 2 now is specified to grow to the maximum heat release rate of 2 MW and 4 MW (same medium growth as scenario 2) for each scenario 5 and 6. Heat release rates, upper layer temperatures and smoke layer heights of each scenario are depicted in Figure 5. 44 and Figure 5. 45. As we expect, higher temperatures in room 2 are observed as the bigger maximum heat release rate are specified, whereas the door to the outside is fully opened in scenario 6.

To illustrate more closely the comparison of the experiments and the calculations of scenarios 2, 5, and 6, Figure 5. 46 amalgamates point-temperature measurements and

general upper layer temperature calculations. Note that exact agreement is not expected as described above. The upper layer temperatures of scenarios 2, 5, and 6 are compared with measurements in Figure 5. 46. Too cold temperatures are seen for scenario 5 (2 MW maximum heat release rate), and too hot for scenario 6 (4 MW maximum heat release rate). Note also that the door to the outside had to be fully opened in scenario 6 to provide enough air, which means that the results are not representation of the actual fire. So, scenario 6 is a simulation just for comparison purposes.

When a maximum of 4 MW heat release rate was specified in room 2 without changing the opening to the outside (45 degree open), the CFAST computer program automatically reduced the maximum heat release rate to approximately 3.1 MW (by the limit of the size of the opening). The results from this calculation are not much different from scenario 2 (3 MW maximum), so it is not presented in this thesis.

Scenario 2 has the closest trend to the experiment in the rise, decay, and magnitude of temperatures (see Figure 5. 43 and Figure 5. 46).

5.5.6 Closure

In the experiment, it is to be noted that the fire load was about 3 MW (heat release rate) and only natural combustibles were used to initiate the fire. Despite this, two noteworthy conclusions may be drawn from the experiment. Two first rooms' smoke temperatures reaches over 600 °C (≅ 1100 °F) in just two minutes after the ignition of the fire. Fire spread rapidly throughout the structure, with almost total roof collapse in 37 minutes.

In the calculations, four 10-room scenarios have been calculated using CFAST and represented graphically, showing the results of smoke temperatures and smoke layer heights of each room with similar trends of surge, maximum, and decay of the temperature measurements.

The effect of weather a door of a room would have been open was investigated computationally, with results illustrating far more dangerous smoke temperature and smoke level in the room.

Two simpler 3-room scenarios have used to make calculations. These calculations were very comparable to the previous ones for smoke temperatures and smoke level heights, indicting the accuracy and usefulness of a quicker simulation. This simpler 3-room simulation allows faster calculation in two ways which are saving CPU time and possibility of using the simpler program like FASTLite.

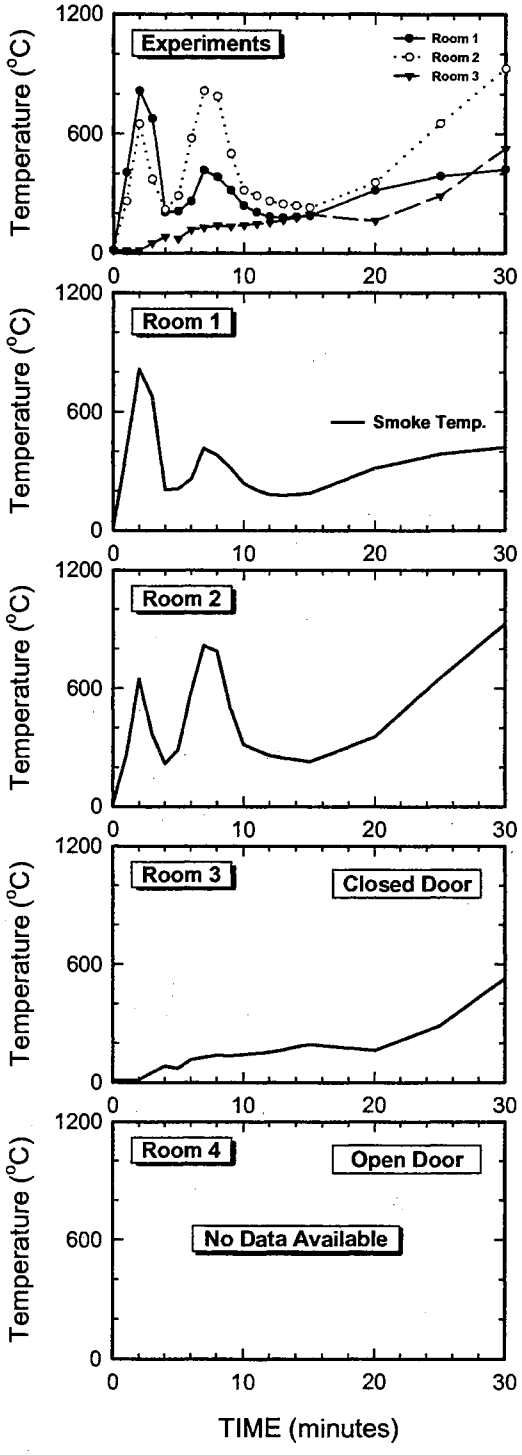

Figure 5. 34 Experimental Upper Layer Smoke Temperatures Measured 0.3 Meter from Ceiling (Large House at Wardwood, OK)

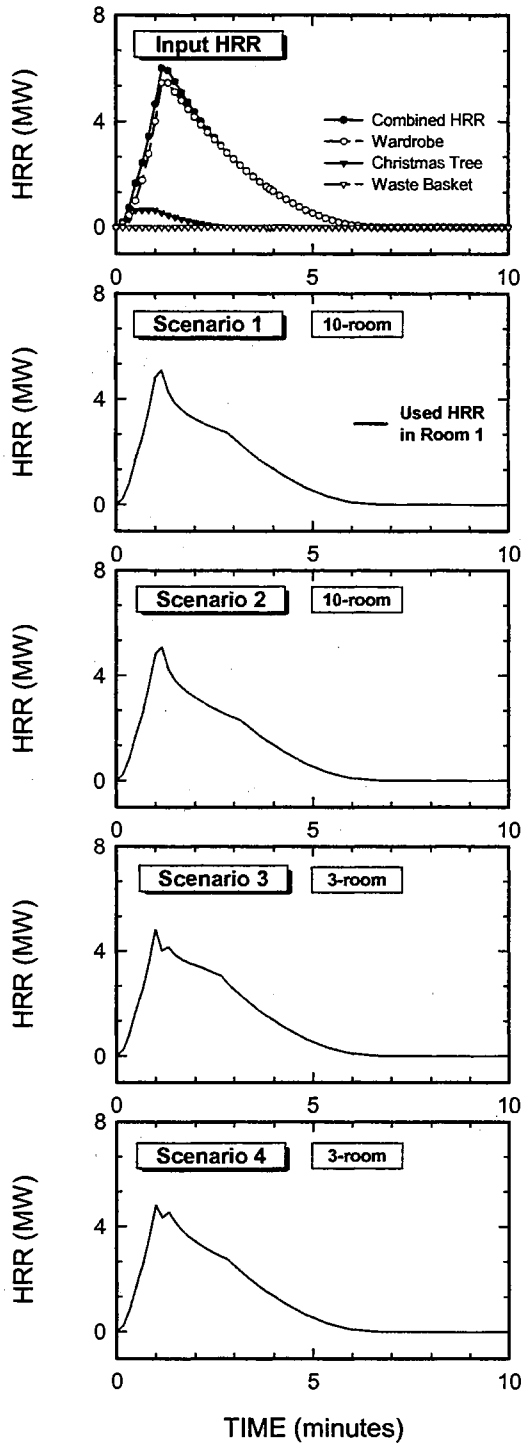

Figure 5. 35 Designed (Input) and Constrained Heat Release Rates in Room 1 by Ventilation limit of Each Scenario (Large House at Wardwood, OK)

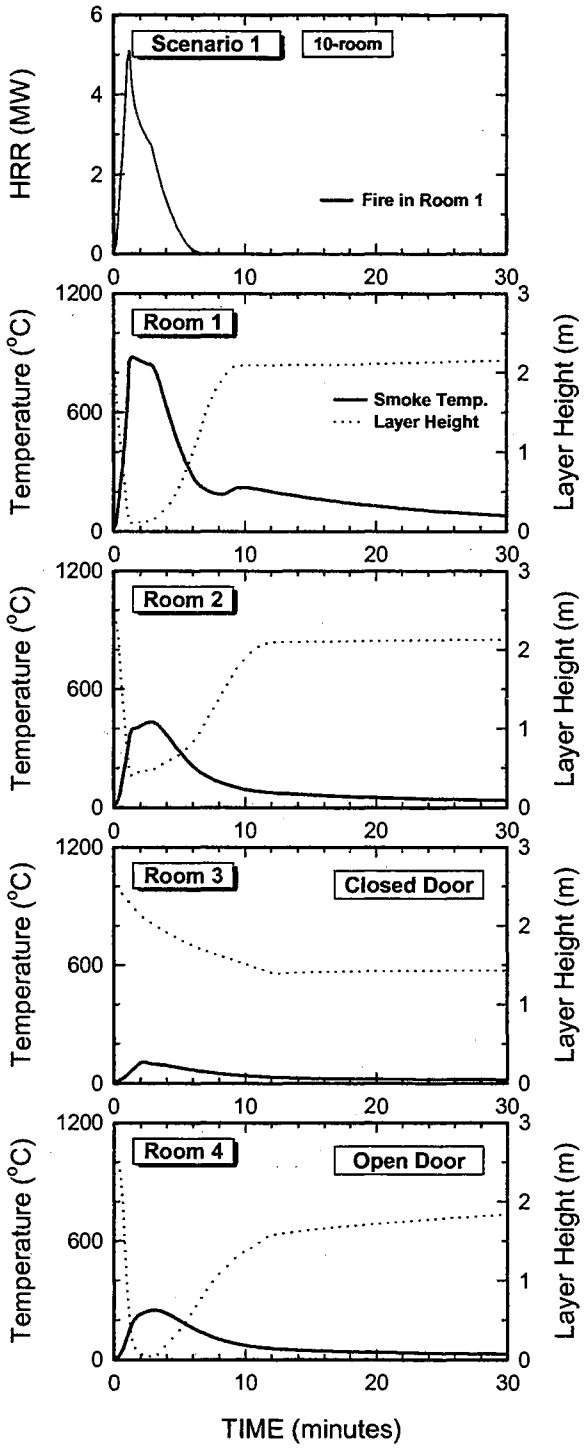

Figure 5. 36 **Scenario 1**: Fire of Typical Wastepaper Basket, Christmas Tree, and Wardrobe in Room 1 (Ultra-Fast Growth and Ultra-Fast Decay Fire)

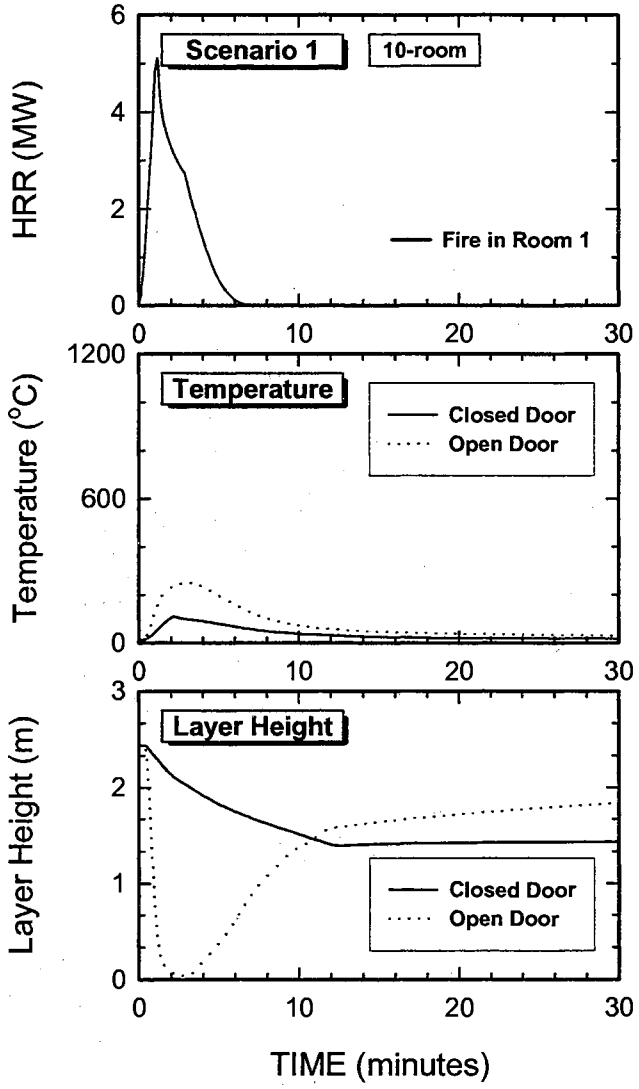

Figure 5. 37 Comparison of Upper Layer Temperatures and Layer Heights Between Room 3 (Room with Closed Door) and Room 4 (Room with Open Door) from Calculated Results of Scenario 1

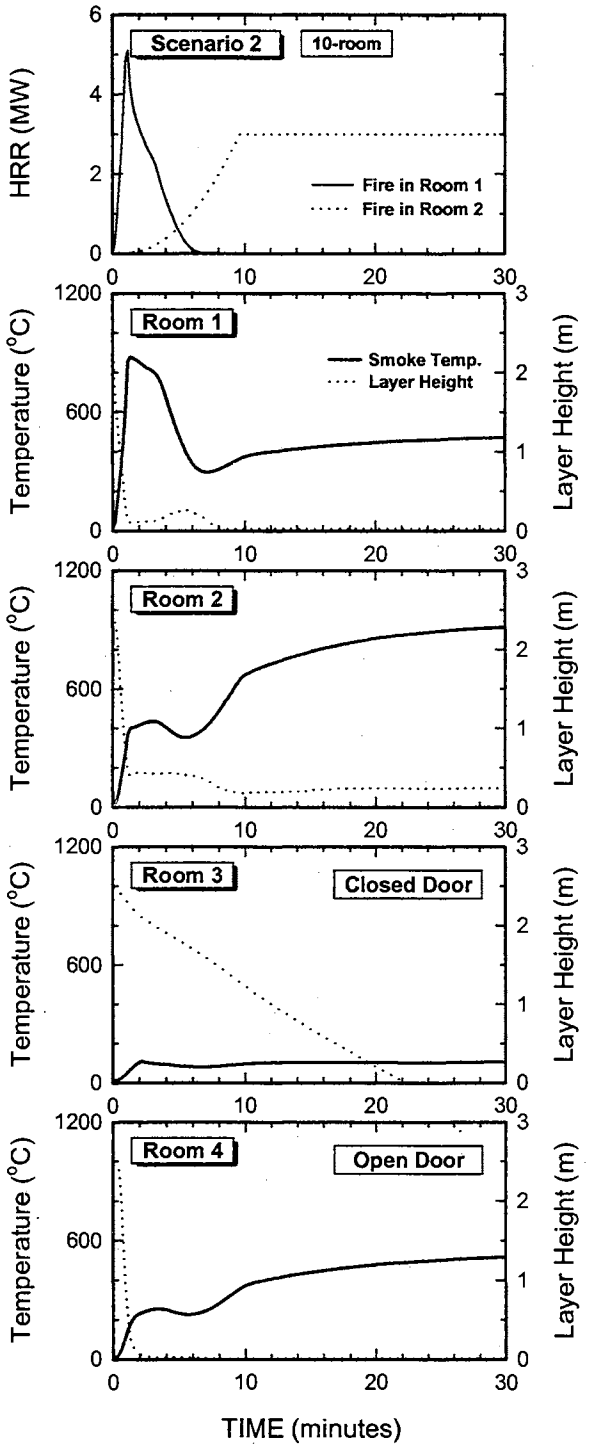

Figure 5. 38 **Scenario 2**: As Scenario 1 Plus Medium Growth Fire in Room 2 Begins at Room 1 Flashover to a Maximum of 3 MW then Constant HRR

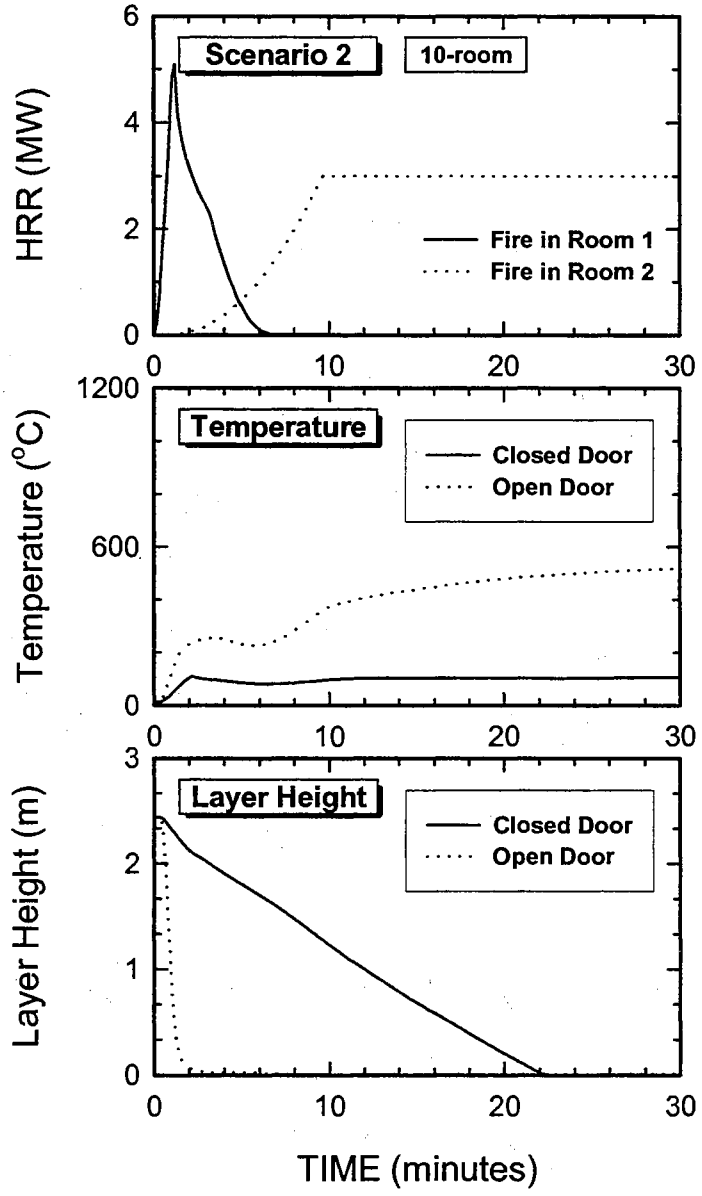

Figure 5. 39 Comparison of Upper Layer Temperatures and Layer Heights Between Room 3 (Room with Closed Door) and Room 4 (Room with Open Door) from Calculated Results of Scenario 2

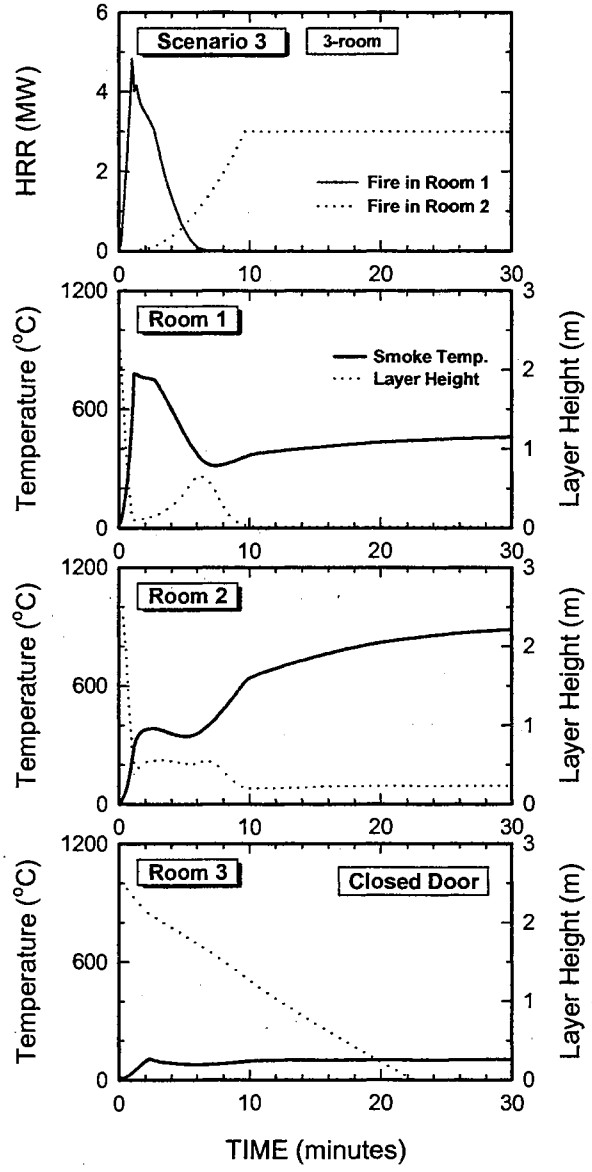

Figure 5. 40 **Scenario 3**: Simpler Version of Scenario 2 (Same As Scenario 2, Except 3-room House Simulation Instead of 10-room House Simulation)

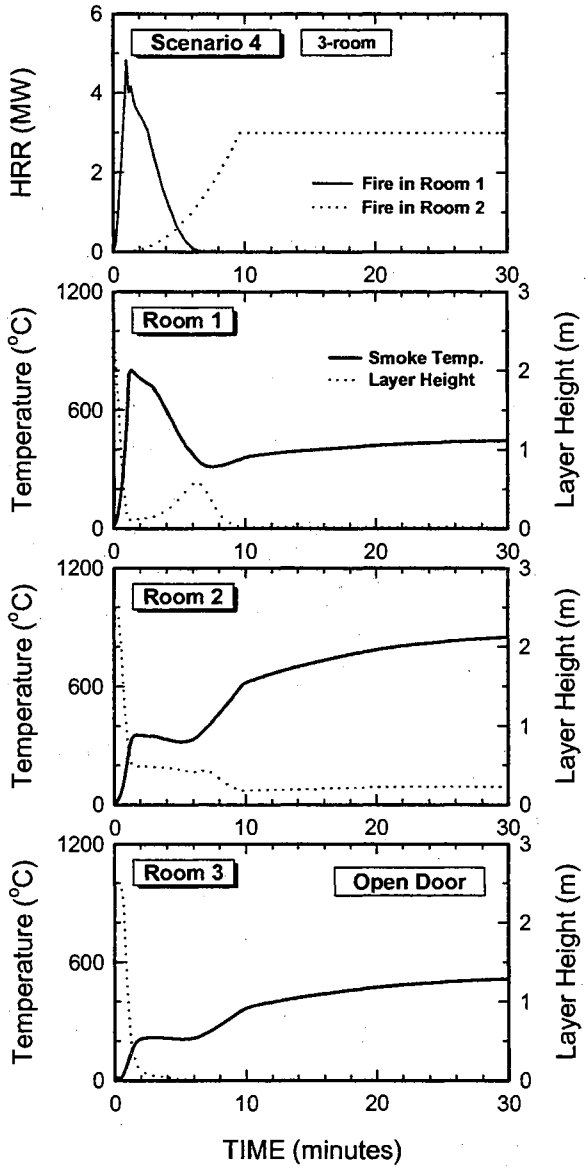

Figure 5. 41 **Scenario 4**: Simpler Version of Scenario 2 (Same As Scenario 3, Except the Door of Room 3 Open)

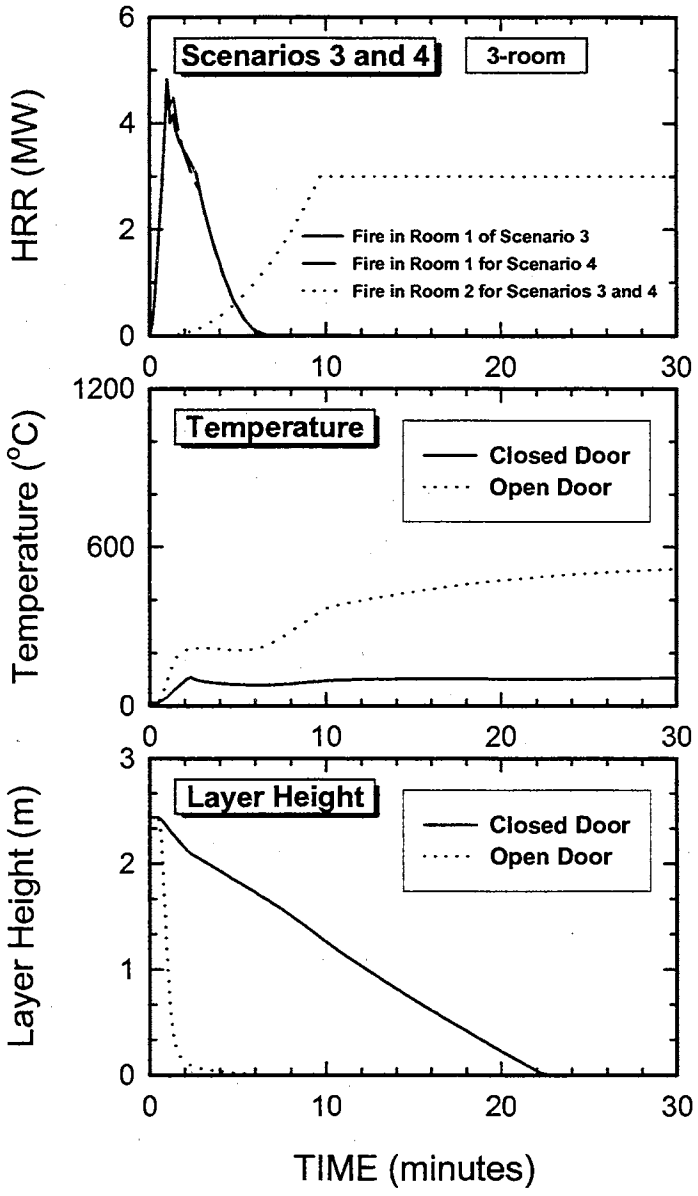

Figure 5. 42 Comparison of Upper Layer Temperatures and Layer Heights Between Room 3 (Room with Closed Door) and Room 3 (Room with Open Door) from Calculated Results of Scenarios 3 and 4

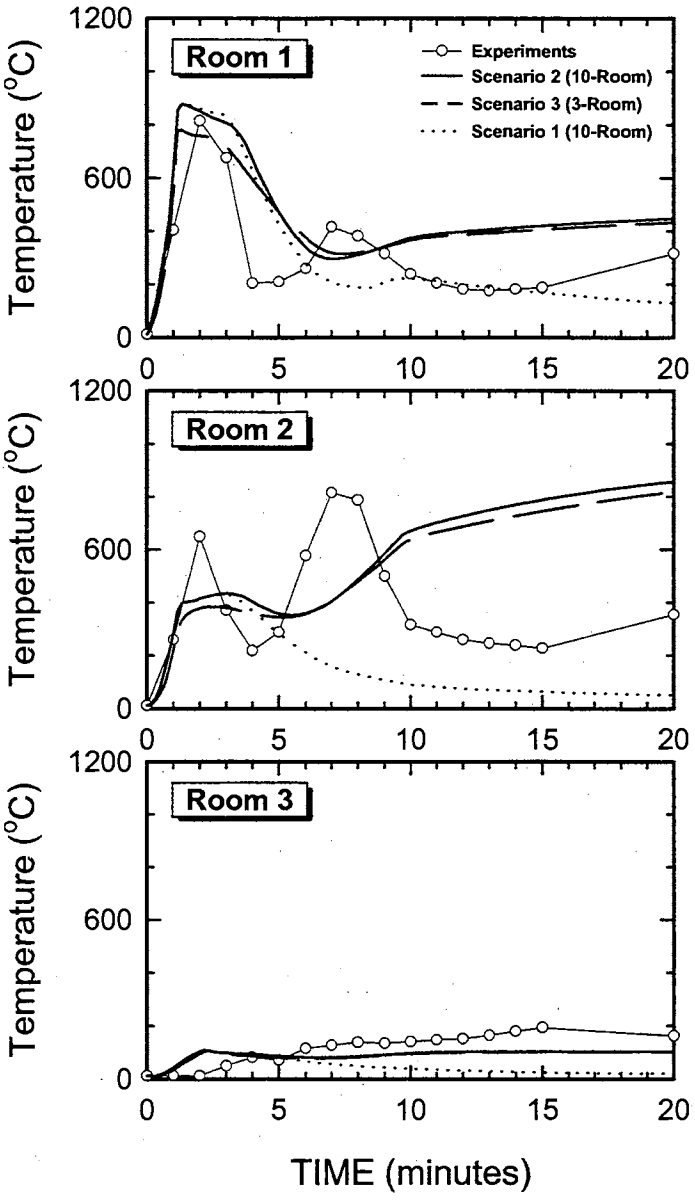

Figure 5. 43 Comparison of Upper Layer Temperatures Among Experiments and Scenarios 1, 2, and 3

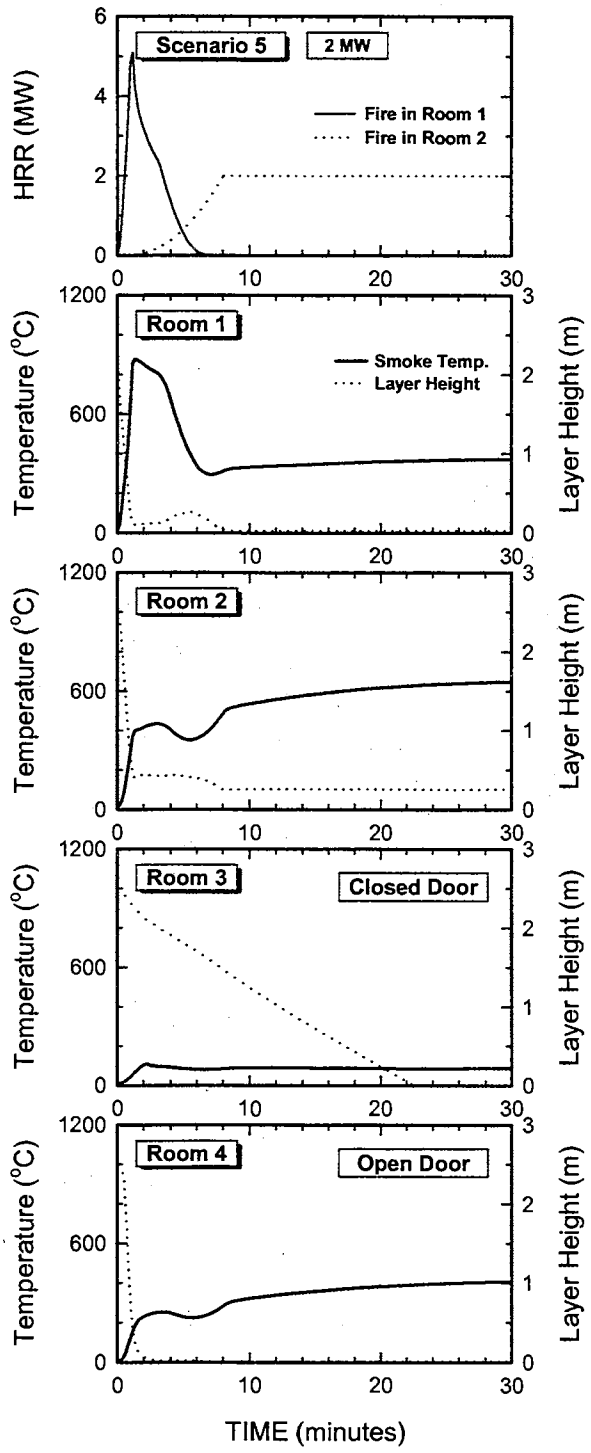

Figure 5. 44 **Scenario 5**: As Scenario 2 with 2 MW Maximum HRR for the Fire in Room 2

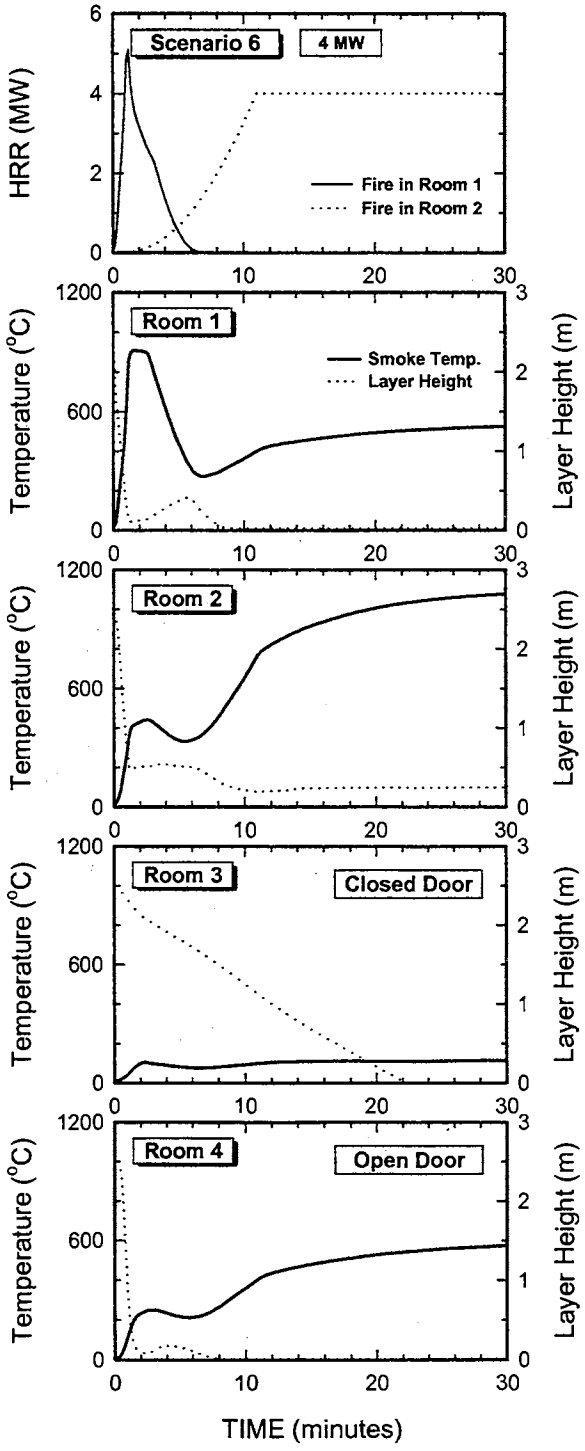

Figure 5. 45 **Scenario 6**: As Scenario 2 with 4 MW Maximum HRR for the Fire in Room 2

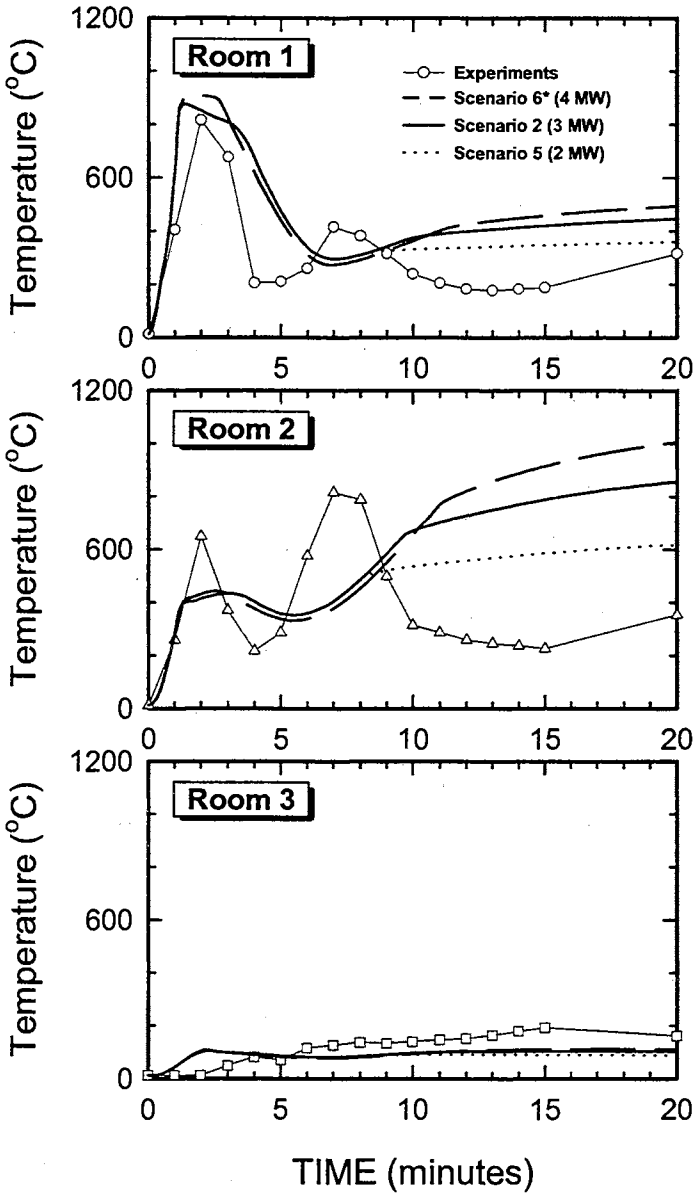

Figure 5. 46 Comparison of Upper Layer Temperatures Among Experiments and Scenarios 2, 5, and 6* (3, 2, and 4 MW of Maximum HRR Respectively)

* Note that the door to the outside is fully open in Scenario 6 to allow 4 MW maximum HRR in Room 2.

CHAPTER VI

CONCLUSIONS

The ultimate goal of this study was to improve scientific understanding of fire behavior leading to flashover in structural fires. Subtopics related to this goal include: burning rates, radiant ignition, fire spread rates, ventilation limit imposed by size of openings, flashover criteria, and fire modeling. These are the main components related to the scientific understanding of fire growth, smoke generation and flashover problem involved in real-world structural fires. Useful computer codes are available that permit calculations to be made, once the user supplies input data about the building and specification of the fires, in terms of heat release rate versus time for each fire in the building.

Major conclusions are:

1. The major parameters affecting time to reach flashover have been found as fire growth rate, ventilation open area, wall and ceiling martial, and room area.

2. Parameters with little effect to the time to reach flashover have been found vent height above the floor, ceiling height, fire location, and fire radiation heat loss fraction.

3. Conditions for flashover to occur in one-room building may be determined on the basis any of four simple algebraic models.

4. The time to reach flashover with a specified fire growth rate may be determined by any of four models with similar results for a room with normal size floor area, but different results for a room with large floor area.

5. Burning rates of typical items have been characterized in a consistent fashion, thereby simplifying their direct input into any modeling simulation of a fire in a structure, including the CFAST and FASTLite computer codes.

6. Calculations of temperature and smoke development in house fires can be made with the CFAST computer code on the basis of sequential room fires starting and reaching flashover.

7. A new appropriate methodology (ignition, fire spread, flashover and window breakout) that permits fire development calculations has been found, developed, used, and applied successfully to multi-room structural fires. It consists of fire spreading to the next room when flashover conditions occur in the previous room. Also windows break out in the flashover room at the instant of flashover.

8. Calculations of upper layer temperature (using the new methodology) have shown the expected trends (deduced from local point temperature measurements) of initial temperature surge, rate of general temperature rise in the upper layer, peak and leveling off temperatures, and time to reach flashover in each room.

9. The new methodology has been found to be applicable to small and large house structures.

10. A simpler 3-room simulation can be used to simulate large house structural fires. Results are similar to the more complete 10-room simulation. It permits faster calculations and gives the possibility to use a simpler program like FASTLite.

REFERENCES

Alpert, R. L. and Ward, E. J., (1983). "Evaluating Unsprinklered Fire Hazards," SFPE TR 83-2, Society of Fire Protection Engineers, Boston, MA, 1983.

Alvord, D. M., (1995). "CFAST Output Comparison Method and Its Use in Comparing Difference CFAST Versions," NISTIR 5705, p. 51, August 1995.

ASME, (1973). "Prediction of the Dispersion of Airborne Effluents," ASME, NY, 1973.

ASTM, (1967). "Standard Method of Test for Surface Flammability of Materials Using a Radiant Heat Energy Source," ASTM E 162-67, American Society for Testing and Materials, Philadelphia, PA, 1967.

ASTM, (1969). "Standard Method of Test for Surface Flammability Using and 8-ft (2.44 m) Tunnel Furnace," ASTM E 286-69, American Society for Testing and Materials, Philadelphia, PA, 1969.

ASTM, (1995a). "Standard Guide for Evaluating the Predictive Capability of Fire Models," ASTM E 1355, Annual Book of ASTM Standards, Vol. 04.07, American Society for Testing and Materials, Philadelphia, 1995.

ASTM, (1995b). "Standard Guide for Guide for Documenting Computer Software for Fire Models," ASTM E 1472, Annual Book of ASTM Standards, Vol. 04.07, American Society for Testing and Materials, Philadelphia, 1995.

Babrauskas, V., (1979). "COMPF2-A Program for Calculating Post-Flashover Fire Temperatures," National Bureau of Standards, U.S., Technical Note 991, 1979.

Babrauskas, V., (1980). "Estimating Room Flashover Potential," Fire Technology, 16, 2, pp. 94-104, May, 1980.

Babrauskas, V., (1981a). "A Closed-form Approximation for Post-flash-over Compartment Fire Temperatures," Fire Safety Journal, 4, 63, pp. 63-73, 1981.

Babrauskas, V., (1981b). "Will the Second Item Ignite," Report NBSIR 81-2271, National Bureau of Standards, Gaithersburg, MD, 1981.

Babrauskas, V., (1984). "Upholstered Furniture Room Fires - Measurements, Comparison with Furniture Calorimeter Data, and Flashover Predictions," Journal of Fire Sciences, Vol. 2, pp. 5-19, Jan.-Feb., 1984.

Babrauskas, V., (1985). "Free-Burning Fires," Proceedings SFPE Symposium: Quantitative Methods for Fire Hazard Analysis, University of Maryland, College Park, MD, 1985.

Babrauskas, V., (1995). "Burning Rate," Chapter 3-1, The SFPE Handbook of Fire Protection Engineering, 2nd Ed., NFPA and SFPE, Quincy, MA, 1995.

Babrauskas, V. and Grayson, S. J., eds., (1992). "Heat Release in Fires," Elsevier Applied Science, 1992.

Babrauskas, V. and Krasny, J. F., (1985). "Fire Behavior of Upholstered Furniture," NBS Monograph, National Bureau of Standards, Gaithersburg, MD, 1985.

Babrauskas, V. and Williamson, R. B., (1979). "Post-flashover Compartment Fires-Application of a Theoretical Model," Fire and Matls., 3, 1, 1979.

Babrauskas, V., Lawson, R. L., Walton W. D., and Twilley, W. H., (1982). "Upholstered Furniture Heat Release Rates Measured with a Furniture Calorimeter," NBSIR 82-2604, National Bureau of Standards, Gaithersburg, MD, 1982.

Beard, A., (1990). "Evaluation of Fire Models: Overview," Unit of Fire Safety Engineering, University of Edinburgh, Edinburgh, UK, 1990.

Beard, A., (1992). "Evaluation of Fire Models: Part I – Introduction," Fire Safety Journal, 19, pp. 295-306, 1992.

Belles, D. W., (1991). "Health Care Facilities," Fire Protection Handbook, 17th Ed., National Fire Protection Association (NFPA), Chapter 8-3, Quincy, MA, 1991.

Belyer, C., (1991). "Introduction to Fire Modeling," Fire Protection Handbook, 17th Ed., National Fire Protection Association (NFPA), Chapter 8-9, Quincy, MA, 1991.

Bennett, W. W., and Hess, K. M., (1984). "Investigating Arson," Thomas Publishers, Springfield, IL, 1984.

Berlin, G. N., (1988). "Probability Models in Fire Protection Engineering," The SFPE Handbook of Fire Protection Association, Quincy, MA, 1988.

Berry, D. J., (1989). "Fire Litigation Handbook," 2nd Printing, NFPA, Quincy, MA, 1989.

Blinov, V. I. and Khudiakov, G. N., (1957). "Certain Laws Governing Diffusive Burning of Liquids," Academiia Nank, SSSR Doklady, pp. 1094-1098, 1957.

Brenan, K. E., Campbell, S. L., and Petzold, L. R., (1989) "Numerical Solution of Initial-Value Problems in Differential-Algebraic Equations," Elsevier Science Publishing, New York, 1989.

Bryan, J. L., (1990). "Automatic Sprinkler and Standpipe Systems," NFPA, Quincy, MA, 1990.

Budnick, E. K. and Evans, D. D., (1986). "Hand Calculations for Enclosure Fires," Fire Protection Handbook, 16th Ed., National Fire Protection Association (NFPA), Section 21-3, 1986.

Budnick, E. K., Evans, D. D., and Nelson H. E., (1991). "Simplified Calculations for Enclosure Fires," Chapter 11, Section 10 in Fire Protection Handbook, 17th Ed., NFPA, Quincy, MA, 1991.

Bukowski, R. W., (1990). "Reconstruction of a Fatal Residential Fire at Ft. Hood, Texas," First HAZARD I Users' Conference, National Institute of Standards and Technology, Gaithers-burg, MD, June 5-6, 1990.

Bukowski R. W., (1996). "Modeling a Backdraft Incident: The 62 Watts St., (New York) Fire," Fire Engineers Journal, Vol. 56, No. 185, pp. 14-17, November 1996.

Bukowski R. W., Peacock, R. D., Jones, W. W., and Forney, C. L., (1989). "Technical Reference Guide for the HAZARD I Fire Hazard Assessment Method," Handbook 146, Vol. II, National Institute of Standards and Technology, June 1989.

Bukowski, R. W. and Spetzler R. C., (1992). "Analysis of the Happyland Social Club Fire With HAZARD I," Fire and Arson Investigator, Vol. 42, No. 3, pp.36-47, 1992.

Campbell, J. A., (1991b). "Confinement of Fire in Buildings," Chapter 6, Section 6 in Fire Protection Handbook, 17th Ed., NFPA, Quincy, MA, 1991.

Carlson, G. P., ed., (1982). "Fire Cause Determination," IFSTA, Stillwater, OK, 1982.

Carroll, J. R., (1979). "Physical and Technical Aspects of Fire and Arson Investigation," Thomas, Springifeld, IL, 1979.

Chow, C-Y, (1979). "Computational Fluid Mechanics," Wiley, NY, 1979.

Clarke, F. B., (1991). "Fire Hazards of Materials: an Overview," Fire Protection Handbook, 17th Ed., NFPA, Quincy, MA, 1991.

Cole, L. S., (1992). "The Investigation of Motor Vehicle Fires," 3rd Edition, Lee Books, Novato, CA, 1992.

Collier, P. C. R., (1996). "Fire in a Residential Building: Comparisons Between Experimental Data and a Fire Zone Model," Fire Technology, Third Quarter, pp. 195-215, 1996.

Combustion Institute, (1979). "Colloquium on Fire and Explosion," 17th Symposium on Combustion, The Combustion Institute, Pittsburgh, PA, 1979.

Cooper, L. Y., (1982). "A Mathematical Model for Estimating Available Safe Egress Time in Fires," Fire and Materials, Vol. 6, Nos. 3 and 4, 1982, (See also NBSIR 80-2172, Feb., 1981).

Cooper, L. Y., (1983). "A Concept for Estimating Available Safe Egress Time in Fires," Fire Safety Journal, Vol. 5, 1983.

Cooper, L. Y., (1984). "Smoke Movement in Rooms of Fire Involvement and Adjacent Spaces," Fire Safety Journal, Vol. 7, pp. 33-46, 1984.

Cooper, L. Y., (1988). "Compartment Fire-Generated Environment and Smoke Filling," Section 2, Chapter 7 of SFPE, 1988.

Cooper, L. Y., (1990). "An Algorithm and Associated Computer Subroutine for Calculating Flows through a Horizontal Ceiling Flow Vent in a Zone-Type Compartment Fire Model," NISTIR 4402, National Institute of Technology, Oct., 1990.

Cooper, L. Y., Harklerod, M., Quintiere, J., and Rinkmen, W., (1982). "An Experimental Study of Upper Hot Layer Stratification in Full Scale Multiroom Fire Scenarios," Journal of Heat Transfer, Vol. 104, pp. 741-749, 1982.

Cote, A. E. and Bugbee, P., (1988). "Principles of Fire Protection," NFPA, Quincy, MA, 1988.

Cote, A. E. and Linville, J. L., eds., (1990). "Industrial Fire Hazards Handbook," NFPA, Quincy, MA, 1990.

Cox, G., and Kumar, S., (1987). "Field modeling of fire in forced ventilated enclosures," Combust. Sci. Technol., 52 7-23, 1987.

Crowl, D. A. and Louvar, J. F., (1990). "Chemical Process Safety: Fundamentals with Applications," Prentice Hall, Englewood Cliffs, NJ, 1990.

Davis, W. D., and Cooper, L. Y., (1991). "Computer Model for Estimating the Response of Sprinkler Links to Compartment Fires With Draft Curtains and Fusible Link-Actuated Ceiling Vents," Fire Technology, 27 (2), pp. 113-127, 1991.

Davis, W. D., Forney, G. P., and Klote, J. H., (1991). "Field Modeling of Room Fires," NISTIR 4673, NIST, Gaithersburg, MD, 1991.

Dayan, A. and Tien, C. L., (1974). "Radiant Heating from a Cylindrical Fire Column," Combustion Science and Technology, Vol. 9, p. 41, 1974.

Deal, S., (1990). "A Review of Four Compartment Fires with Four Compartment Fire Models," Fire Safety Developments and Testing, Proceedings of the Annual Meeting of the Fire Retardant Chemicals Association., Ponte Verde Beach, Florida, 33-51., October 21-24, 1990.

DeHaan N., (1991). "Interior Finish," Fire Protection Handbook, 17th Ed., NFPA, Quincy, MA, 1991.

DeHaan, J. D., (1997). "Kirk's Fire Investigation," 4rd Edition, Prentice-Hall, Englewood Cliffs, NJ, 1997.

Dembsey, N. A., Pagni, P. J., and Williamson, R. B., (1995). "Compartment Fire Experiments: Comparison with Models," Fire Safety Journal, Vol. 25, pp. 187-227, 1995.

Dong, M. C., (1989). "A Multicompartment Model for the Spread of Fire, Smoke and Toxic Gases," M.S. Report, Oklahoma State University, Stillwater, OK, 1989.

Drysdale, D. D., (1986). "An Introduction to Fire Dynamics," John Wiley and Sons, 1986.

Drysdale, D. D., (1991). "Chemistry and Physics of Fire," Chapter 4, Section 1 in Fire Protection Handbook, 17th Ed., NFPA, Quincy, MA, 1991.

Duong, D. Q., (1990). "The Accuracy of Computer Fire Models: Some Comparisons with Experimental Data from Australia," Fire Safety J., 16(6), 415-431, 1990.

Emmons, H. W., (1985). "The Needed Fire Science," in Fire Safety Science, Proceedings of the First International Symposium, Hemisphere, New York, pp. 33-53, 1985.

Emmons, H. W., (1995). "Vent Flows," The SFPE Handbook of Fire Protection Engineering, 2nd Ed., National Fire Protection Association, Chapter 2-5, Quincy, MA, 1995.

Epstein, M., (1988). "Buoyant Driven Exchange Flow through Small Openings in Horizontal Partitions," Jour. of Heat Transfer, Vol. 110, ASME, 1988.

Fang, J. B. and Breese, J. N., (1980). "Fire Development in Residential Basement Rooms, Interim Report," Natl. Bur. Stand., U.S., NBSIR 80-2120, 1980.

Forney, G. P. and Cooper, L. Y., (1990). "The Consolidated Compartment Fire Model (CCFM) Computer Application CCFM.VENTS-Part II: Software Reference Guid," Nat. Inst. Stand. Technol., NISTIR 90-4343, 1990.

Forney, G. P. and Moss, W. F., (1994). "Analyzing and Exploiting Numerical Characteristics of Zone Fire Models," Fire Science and Technology, 14, No. 1/2, 49-60, 1994.

Friedman, R., (1991). "Survey of Computer Models for Fire and Smoke," 2nd Ed., Factory Mutual Research Corp., Norwood, MA, Dec. 1991.

Gahm, J. B., (1983). "Computer Fire Code VI, Volume I," NBS GCR 83-451, p. 116, 1983.

Heskestad, G., (1991). "Venting Practices," in Fire Protection Handbook, 17th Ed., NFPA, Quincy, MA, 1991.

Hottel, H. C., (1959). "Certain Laws Governing Diffusive Burning of Liquids," F. Res. Abs., and Rev. 1., p. 41, 1959.

Huggett, C., (1980). "Estimation of Rate of Heat Release by Means of Oxygen Consumption Measurement," Fire and Materials, Vol. 4, pp. 61-65, 1980.

Janessens, M. and Parker, W. J., (1992). "Oxygen Consumption Calorimetery," Heat Release in Fires, Babrauskas, V. and Grayson, S. J., eds., Elsevier Applied Science, London, pp. 31-59, 1992.

Jia, F., Galea E. R., and Patel, M. K., (1997). "Modelling of Flashover and Backdraft Using Fire Field Models," Fire Engineers Journal, pp. 12-13, January 1997. (See also the Symposium on Fire Safety Science, Melbourne, March 1997.)

Jones, W. W., (1985). "A Multicompartment Model for the Spread of Fire, Smoke and Toxic Gases," Fire Safety Journal, pp. 55-79, 1985.

Jones, W. W. and Peacock, R. D., (1989). "Technical Reference Guide for FAST Version 18," Natl. Inst. Stand. Techol., Tech. Note 1262, 1989.

Jones, W. W., Forney, G. P., Peacock, R. D., and Reneke, P. A., (2000). "Technical Reference for CFAST: An Engineering Tool for Estimating Fire and Smike Transpoert," NIST Technical Note 1431, March 2000.

Karlsson, B. and Quintiere, J. G., (2000). "Enclosure Fire Dynamics," CRC Press, Boca Raton, FL, 2000.

Kawagoe, K. D., (1958). "Fire Behaviour in Rooms," Report of the Building Research Institute, Japan, No. 27, 1958.

Kawagoe, K. D. and Sekine, T., (1963). "Estimation of Fire Temperature-Time Curve for Rooms," BRI Occasional Report No. 11, Building Research Institute, Ministry of Construction, Japanese Government, 1963.

Kerrison, L., Galea, E. R., Hoffmann, N., and Patel, M. K., (1994). "A Comparison of FLOW3D Based Fire Field Model with Experimental Room Fire Data," Fire Safety Journal 23, Elsevier Science Limited, Northern Ireland, pp. 387-411, 1994.

Kim, H.-J. and Lilley, D. G., (1997). "Flashover: A Study of Parametric Effects on the Time to Reach Flashover Conditions," Proc. of ASME 17th Int. Computers in Engineering Conf./Design Conf. Paper DETC 97/CIE-4427, Sacramento, CA, Sept. 14-17, 1997.

Kim, H.-J. and Lilley, D. G., (1998). "A Comparison of Flashover Theories," Proc. of ASME Int. Computers in Engineering Conf., Atlanta, GA, Sept 13-16, 1998.

Kim, H.-J. and Lilley, D. G., (1999a). "Basic Models in Fire Development," Proc. of ASME Int. Computers in Engineering Cong., Las Vegas, NV, Sept. 12-15, 1999.

Kim, H.-J. and Lilley, D. G., (1999b). "Burning Rates of Typical Items in Fires," Proc. of ASME Int. Computers in Engineering Cong., Las Vegas, NV, Sept. 12-15, 1999.

Kim, H.-J. and Lilley, D. G., (1999c). "Comparison of Theories for Room Flashover," Paper AIAA-99-0343, 37th Aerospace Sciences Meeting, Reno, NV, Jan. 11-14, 1999.

Kim, H.-J. and Lilley, D. G., (1999d). "Fire Growth and Flashover," International Joint Power Generation Conference, San Francisco, CA, July, 25-28, 1999.

Kim, H.-J. and Lilley, D. G., (2000a). "Heat Release Rates of Burning Items in Fires," Paper AIAA-2000-0722, 38th Aerospace Sciences Meeting, Reno, NV, Jan. 1-13, 2000.

Kim, H.-J. and Lilley, D. G., (2000b). "Models of Fire Development: A Review," Paper AIAA-2000-0594, 38th Aerospace Sciences Meeting, Reno, NV, Jan. 1-13, 2000.

Kim, H.-J. and Lilley, D. G., (2000c). "Problems and Sample Calculations Related to Fire Development," Paper DETC2000/CIE-14680, ASME 20th Computers and Information in Engineering Conference, Baltimore, MD, Sept. 10-14, 2000.

Kim, H.-J. and Lilley, D. G., (2000d). "Review of Basic Models in Fire Dynamics," ASME Int. Mechanical Engineering Congress and Exposition, Orlando, FL, Nov. 5-10, 2000.

Kim, H.-J. and Lilley, D. G., (2001). " Temperature and Smoke Prediction in Structrual Fires," Paper DETC01/CIE-21677, Proceedings of ASME 21th International

Computers and Information in Engineering Conference, Pittsburgh, Pennsylvania , September 9-12, 2001.

Klote, J. H., (1994). "Method of Predicting Smoke Movement in Atria With Application to Smoke Management," NISTIR 5516, National Institute of Standards and Technology, p. 94, November 1994.

Klote, J. H. and Forney, G. P., (1993). "Zone Fire Modeling With Natural Building Flows and a Zero Order Shaft Model," NISTIR 5251, p. 42, September 1993.

Krasny, J., Parker, W., and Babrauskas, V., (2001). "Fire Behavior of Upholstered Furniture and Mattresses," William Andrew Publishing, Norwich, NY, 2001.

Lawson, J. R., Walton, W. D., and Twilley, W. H., (1984). "Fire Performance of Furnishings as Measured in the NBS Furniture Calorimeter, Part 1," NBSIR 83-2787, National Bureau of Standards, Gaithersburg, MD, Jan. 1984.

Lawson, J. R. and Quintiere, J. G., (1985). "Slide Rule Estimates of Fire Growth" Fire Technology, Vol. 21, No. 4, pp. 267-291, Nov. 1985, (See also NBSIR 85-3196, National Bureau of Standards, Gaithersburg, MD, 1985).

Lilley, D. G., (1989). "Combustion," Stillwater, OK, 1989.

Lilley, D. G., (1990a). "Fuels, Flammability, Fires and Flames," Applied Engineering, Stillwater, OK 1990.

Lilley, D. G., (1990b). "Prediction of Fire Development in Buildings," Proc. of ASME Int. Computers in Engineering Conf., Boston, MA, Aug. 5-9, 1990.

Lilley, D. G., (1991). "Computerized Reconstruction of Building Fires," Proc. of ASME Int. Computers in Engineering Conf., Santa Clara, CA, Aug. 18-22, 1991.

Lilley, D. G., (1992). "Computational Fluid Dynamics: Course Notes," Applied Engineering, Stillwater, OK, 1992.

Lilley, D. G., (1995a). "Fire Dynamics" Short Course, Stillwater, OK, 1995.

Lilley, D. G., (1995b). "Temperature Measurements in a Small House Fire," Oklahoma Fire & Arson Investigator, Vol. 4 No. 1, pp. 6-8, Fall 1995.

Lilley, D. G., (1995c). "Fire Dynamics," Paper AIAA-95-0894, 33rd Aerospace Sciences Meeting, Reno, NV, Jan. 9-12, 1995.

Lilley, D. G., (1996). "Fire Hazards of Flammable Fuel Release," Paper AIAA-96-0405, 34th Aerospace Sciences Meeting, Reno, NV, Jan. 15-18, 1996.

Lilley, D. G., (1997a). "Structural Fire Development," Paper AIAA-97-0265, 35th Aerospace Sciences Meeting, Reno, NV, Jan. 6-10, 1997.

Lilley, D. G., (1997b). "Estimating Fire Growth and Temperatures in Structural Fires," Paper AIAA-97-0266, 35th Aerospace Sciences Meeting, Reno, NV, Jan. 6-10, 1997.

Lilley, D. G., (1997c). "Temperature Measurements in a Small House Fire," IAAI Fire & Arson Investigator, Vol. 47, No. 3, pp.54-56, March 1997.

Magee, R. S. and McAlevy, R. F., (1971). "The mechanism of flame spread," J. Fire and Flammability, 2, 1971.

McCaffrey, B. J., Quintiere J. G., and Harkleroad, M. F.., (1981). "Estimating Room Temperatures and the likelihood of Flashover Using Fire Data Correlations," Fire Technology, Vol. 17, No. 2, 1981.

Mitler, H. E., (1985). "Comparison of Several Compartment Fire Models: An Interim Report," NBSIR 85-3233, NIST, Gaithersburg, MD, 1985.

Mitler, H. E. and Emmons, H. W., (1981). "Documentation for CFCV, the Fifth HARVARD Computer Fire Code," NBSGCR 81-344, Natl. Bur. Stand., p. 187, 1981.

Mitler, H. E. and Rockett, J., (1987). "A User's Guide for FIRST, a Comprehensive Single Room Fire Model," NBSGCR 87-2529, Natl. Bur. Stand., 1987.

Modak, A.T., (1977). "Thermal Radiation from Pool Fires," Combustion and Flame, Vol. 29, p. 177, 1977.

NBFU, (1956). "Fire Resistance Ratings of Less Than One Hour," National Board of Fire Underwriters, New York, NY, 1956.

Nelson, H. E., (1989). "An Engineering View of the Fire of May 4, 1988 in the First Interstate Bank Building, Los Angeles, California," Natl. Inst. Stand. Technol. NISTIR 89-4061, 39 p, 1989.

Nelson, H. E., (1990). "FPETOOL: Fire Protection Engineering Tools for Hazard Estimation," *Natl. Inst. Stand. Technol., NISTIR 438*0, 120 p., October 21-24, 1990.

NFPA, (1995). "Guide for Fire and Explosion Investigations," NFPA, 921, Quincy, MA, 1995.

NFPA, (1991). "Fire Protection Handbook," 17th Edition (Cote, A. E., and Linvile, J. L., Appy, M. K., and Benedetti, R. P., eds.), NFPA, Quincy, MA, 1991.

Nilsson, L., (1971). "The Effect of Porosity and Air Flow on the Rate of Combustion of Fire in an Enclosed Space," Bulletin 18, Lund Institute of Technology, Lund, 1971.

Patton, A. J., (1994). "Fire Litigation Sourcebook," 2nd Edition, Wiley, NY, 1994.

Peacock, R. D., Forney, G. P., Reneke, P. A., Portier, R. W., and Jones, W. W., (1993a). "CFAST, The Consolidate Model of Fire Growth and Smoke Transport," NIST Technical Note 1299, February 1993.

Peacock, R. D., Jones, W. W., and Bukowski, R. W., (1993b). "Verification of a Model of Fire and Smoke Transport," Fire Safety J. 21, 89-129, 1993.

Peacock, R. D., Jones, W. W., Bukowski, R. W., and Forney, C. L., (1991a). "Software User's Guide for the HAZARD I Fire Hazard Assessment Method Version 1.1.," NIST Handbook 146, Vol. 2, 1991.

Peacock, R. D., Jones, W. W., Bukowski, R. W., and Forney, C. L., (1991b). "Technical Reference Guide for the HAZARD I Fire Hazard Assessment Method Version 1.1.," NIST Handbook 146, Vol. 2, 1991.

Peacock, R. D., Jones, W. W., Forney, G. P., Portier, R. W., Reneke, R. A., Bukowski, R. W., and Klote, J. H., (1994). "An Update Guide for HAZARD 1 Version 1.2," NIST Report NISTIR 5410, May 1994.

Peacock, R. D., Reneke, P. A., Jones, W. W., Bukowski, R. W., and Forney, G. P., (1997). "A User's Guide for FAST, Engineering Tools for Estimating Fire Growth and Smoke Transport," Natl. Inst. Stand. Technol., Special Pub. 921, 180 pp. 1997.

Peacock, R. D., Reneke, P. A., Forney, C. L., and Kostreva, M. M (1998). "Issues in Evaluation of Complex Fire Models," Fire Safety Journal, 30, 103-136, 1998.

Pettersson, O., Magnusson, S. E., and Thor, J., (1976). Fire Engineering Design of Steel Structures, Stalbyggadsinstitutet, Stockholm, 1976.

Portier, R. W., Peacock, R. D., and Reneke, P. A., (1996). "FASTLite: Engineering Tools for Estimating Fire Growth and Smopke Transport," NIST Special Publication 899, Gaithersburg, MD, April 1996.

Purser, D. A., (1988). "Toxicity Assessment of Combustion Products," Chapter 1-14 in The SFPE Handbook of Fire Protection Engineering, 1st Ed., NFPA and SFPE, 1988.

Quintiere, J. G., (1994). "Principles of Fire Behavior," Delmar Publishers, Albany, NY, 1994.

Quintiere, J. G., (1995). "Compartment Fire Modeling," Chapter 3-5 in The SFPE Handbook of Fire Protection Engineering, 2nd Ed., NFPA and SFPE, Quincy, MA, 1995.

Quintiere, J. G., (1995). "Surface Flame Spread," Chapter 2-14 in The SFPE Handbook of Fire Protection Engineering, 2nd Ed., NFPA and SFPE, Quincy, MA, 1995.

Quintiere, J. G. and Harkleroad, M., (1984). "New Concepts for Measuring Flame Spread Properties," Symposium on Application of Fire Science to Fire Engineering, American Society for Testing and Materials and Society of Fire Protection Engineers, Denver, Co, June 27, 1984.

Ramachandran G., (1995). "Stochastic Models of Fire Growth," in The SFPE Handbook of Fire Protection Engineering, 2nd Ed., NFPA and SFPE, Quincy, MA, p. 3-296, 1995.

Reneke, P. A., Peatross, M. J., Jones, W. W., Beyler, C. L., and Richards, R., (2000). "Comparison of CFAST Predcitions to USCG Real-Scale Fire Tests," NISTIR 6446, National Technical Information Service, p. 16, January 2000.

Rockett, J. A., (1976). "Fire Induced Gas Flow in an Enclosure," Comb. Sci., and Tech., 12, 1976.

SFPE, (1995). "The SFPE Handbook of Fire Protection Engineering," 2nd Edition (DiNenno, P. J., Beyler, C. L., Custer, R. L. P., and Walton, W. D., eds.), NFPA and SFPE, Quincy, MA, 1995.

Spearpoint, M. J., Mowrer, F. W., and McGrattan, K. B., (1999). "Simulation of Compartment Flashover Fire Using Hand Calculations, Zone Models and a Field Model," International Conference on Fire Research and Engineering (ICFRE3), 3rd Proceedings Society of Fire Protection Engineers (SFPE), National Institute of Standards and Technology (NIST) and International Association of Fire Safety Science (IAFSS). Oct. 4-8, 1999, Chicago, IL, Society of Fire Protection Engineers, Boston, MA, 3-14 pp, 1999.

Tanaka, T., (1983). "A Model of Multiroom Fire Spread," NBSIR 83-2718, Nat. Bur. Stand., p. 175, 1983.

Tewarson, A., (1995). "Generation of Heat and Chemical Compounds in Fires," in The SFPE Handbook of Fire Protection Engineering, 2nd Ed., NFPA and SFPE, Quincy, MA, 1995.

Thomas, P. H., (1974). "Fires in Enclosures," Paper in Heat Transfer in Fires (P. L. Blackshear, ed.), Halsted-Wiley, New York, pp. 73-94., 1974.

Thomas, P. H., (1981). "Testing Products and Materials for Their Contribution to Flashover in Rooms," Fire and Materials, Vol. 5, No. 3, pp. 103-111, 1981.

Thomas, P. H. and Heselden A. J. M., (1972). "Fully Developed Fires in Single Compartments," Fire Research Note No. 923, Fire Research Station, Borehamwood, 1972.

Thomas, P. H., Bullen, M. L., Quintiere, J. G., and McCaffrey, B. J., (1980). "Flashover and Instabilities in Fire Behavior," Combustion and Flame, Vol. 38, pp. 159-171, 1980.

Thompson, P. and Marchant E., (1995). "A Computer Model for the Evacuation of Large Building Populations," Fire Safety Journal, Vol. 24, No. 2, 1995.

USFA, (1999). "Multimple-Fatality Fires Reported to NFIRS 1994-1996," United States Fire Administration, Oct. 1999.

Walton, W. D., (1985). "ASET-B: A Room Fire Program for Personal Computers," Fire Technology, Vol. 21, No. 4, Nov. 1985, pp. 293-309. See also NBSIR-85-3144, April, 1985.

Walton, W. D. and Thomas P. H., (1995). "Estimating Temperatures in Compartment Fires," Chapter 3-6, Section 3 in The SFPE Handbook of Fire Protection Engineering, 2nd Ed., NFPA and SFPE, Quincy, MA, 1995.

Walton, W. D., Baer, S. R., and Jones, W. W., (1985). "User's Guide for FAST," National Bureau of Standards, NBSIR 85-3284, 1985.

Watts, J. M., (1991). "Probabilistic Fire Models," Fire Protection Handbook, National Fire Protection Association, Quincy, MA, 1991.

Zukoski, E. E., (1985). "Fluid Dynamic Aspects of Room Fires," in Fire Safety Science (Grant, C. E. and Pagni, P. J., eds.), Hemisphere, New York, pp. 1-30, 1985.

VITA

Hyeong-Jin Kim

Candidate for the degree of

Doctor of Philosophy

Thesis: STRUCTURAL FIRE MODELING

Major Field: Mechanical Engineering

Biographical:

Personal Data: Born in Chongju, Korea, on April 14, 1969, the first son of Gyung-Ju Kim and Suk-Hyun Kim.

Education: Graduated from Dong-Am High School, Chonju, Korea in February 1987; received Bachelor of Engineering degree in Mechanical Design from Chonbuk National University, Chonju, Korea in February 1993; received the Master of Engineering degree in Precision Mechanical Engineering from Chonbuk National University, Chonju, Korea in February 1995. Completed the requirements for the Doctor of Philosophy degree with a major in Mechanical Engineering at Oklahoma State University in August 2001.

Experience: Employed as a Lecturer by Iksan National University and Howon University, Chonbuk, Korea at 1996; employed as a graduate teaching assistant in the School of Mechanical and Aerospace Engineering, Oklahoma State University, Stillwater, Oklahoma, USA, from 1996 to 2001; employed as a research associate (part-time) by Lilley & Associates, Stillwater, Oklahoma, USA, from 1996 to 2001.

Professional Membership: American Institute of Aeronautics and Astronautics (AIAA), American Society of Mechanical Engineers (ASME), Fluid Power Society (FPS), and Korean-American Scientists and Engineers Association (KSEA, served as an OK chapter president).